R-7824-5489

PB84-133818

VALIDATION OF PULSE TECHNIQUES FOR THE SIMULATION OF EARTHQUAKE MOTIONS IN CIVIL STRUCTURES

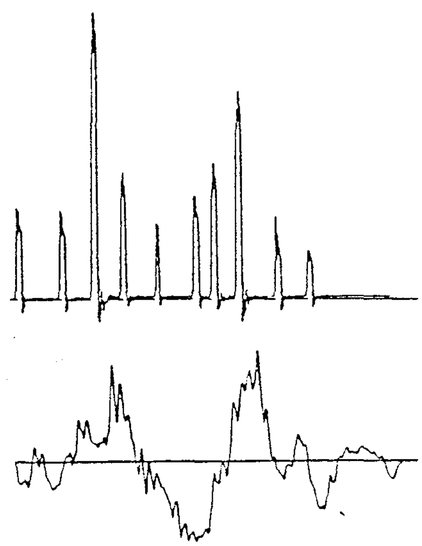

May 1983

Prepared Under

National Science Foundation
Grant No. CEE77-15010

AGBABIAN ASSOCIATES
250 North Nash Street
P.O. Box 956
El Segundo, CA 90245-0956

50272-101

REPORT DOCUMENTATION PAGE	1. REPORT NO. NSF/CEE-83211	2.	3. Recipient's Accession No.

4. Title and Subtitle Validation of Pulse Techniques for the Simulation of Earthquake Motions in Civil Structures	5. Report Date May 1983
	6.
7. Author(s) F.B. Safford, S.F. Masri	8. Performing Organization Rept. No. R-7824-5489
9. Performing Organization Name and Address Agbabian Associates 250 North Nash Street P.O. Box 956 El Segundo, CA 90245-0956	10. Project/Task/Work Unit No. 11. Contract(C) or Grant(G) No. (C) (G) CEE7715010
12. Sponsoring Organization Name and Address Directorate for Engineering (ENG) National Science Foundation 1800 G Street, N.W. Washington, DC 20550	13. Type of Report & Period Covered 14.

15. Supplementary Notes

16. Abstract (Limit: 200 words)

Results are presented of research undertaken to validate the application of pulse techniques for the simulation of earthquake motions in civil structures. A pulse train algorithm was developed and is shown to closely approximate structural motions induced by earthquakes. A simple anti-earthquake algorithm was also developed. This algorithm, when used in conjunction with various types of pulse units, shows promise in the reduction of structural motions at the damage or life-threatening thresholds. The anti-earthquake algorithm is presently limited to preselected fixed amplitude pulses. Two gas pulse generating systems were produced and are said to be in a state of operational readiness. It is suggested that additional calibration tests at low to medium nozzle throat settings be conducted. In addition, surge suppressors should be added to the plenum chambers to improve nozzle efficiencies and to reduce the interaction of pneumatic surges with the plenum chamber balancing piston.

17. Document Analysis a. Descriptors

Earthquakes
Algorithms
Structures
Dynamic structural analysis
Generators
Earthquake resistant structures

b. Identifiers/Open-Ended Terms

Pulse techniques
Ground motion
F.B. Safford, /PI
S.F. Masri, /PI

c. COSATI Field/Group

18. Availability Statement	19. Security Class (This Report)	21. No. of Pages
NTIS	20. Security Class (This Page)	22. Price

(See ANSI-Z39.18) See Instructions on Reverse OPTIONAL FORM 272 (4-77) (Formerly NTIS-35) Department of Commerce

ABSTRACT

This research project was undertaken to validate the application of pulse techniques for the simulation of earthquake motions in civil structures. Major efforts were in the development of algorithms to generate pulse trains and to develop digitally programmable gas pulse thrusters.

An algorithm employing adaptive random search was successfully developed to generate pulse trains which, when applied to a system, will closely approximate structural motions induced by earthquakes. This algorithm permits placement of pulse excitation units in multiple locations of test convenience. Computer studies of several structures yielded information on the performance required for pulse units with respect to optimum exciter locations, phase effects, thrust magnitude, pulse widths, and impulse. A rudimentary anti-earthquake algorithm was also developed which has potential applications at extreme structural motions to reduce severe building damage or life threatening situations.

Two programmable cold gas pulse systems were successfully developed and are available for tests. The gas pulse systems performed reliably and safely. Start-up, shut-down and repeat tests may be performed quickly and efficiently. Changing pulse train commands involves entering only time and amplitudes on the keyboard of the control microcomputer. The system is readily transported to test sites and set-up time is expected to be less than a day. Peak output force is slightly less than 10,000 lbf and minimum pulse width is about 25 ms. Signal monitors provide time history records of input command signals, metering nozzle position, chamber pressure and output force.

Demonstration tests on a single story commercial structure were conducted and the gas pulsers performed as intended. Output forces and pulse durations obtainable with these units make them suitable for use on small buildings, large equipment, piping systems, open frame structures and electric power distribution centers.

Preceding page blank

ACKNOWLEDGEMENTS

The research project has been supported by a National Science Foundation grant to Agbabian Associates (Grant No. CEE 77-15010). This support is gratefully acknowledged.

Principal contributors to this work were F.B. Safford and S.F. Masri. F.B. Safford was responsible for the system development and the gas pulse generator and S.F. Masri was responsible for the pulse train algorithm and for the anti-earthquake algorithm. Significant contributions were made by D.G. Yates in the design of the gas pulser and by B. Barclay in system development, calibration and test. Other contributors to the project were Prof. G.A. Bekey of the University of Southern California, in algorithm development; A.R. Maddox, U.S. Naval Weapons Center for support and guidance on gas flow in supersonic nozzles, and J. Sagherian of Agbabian Associates for reduction of test data.

TABLE OF CONTENTS

TABLE OF CONTENTS (Concluded)

SECTION 1

INTRODUCTION

A research program was undertaken to validate the application of pulse techniques for the simulation of earthquake motions in civil structures. Such a program for on-site excitation of civil structures to earthquake motion can provide for the following needs:

- Adequate experimental justification for complex computer models
- Proof testing of new and rehabilitated structures
- Seismic testing of existing structures

This determination of the behavior of structures subjected to such jolts is accomplished using three-orthogonal-axes earthquake simulation of civil structures.

1.1 BACKGROUND

Previous analytical and experimental work with mechanical (metal-cutting) pulse generation indicated that pulse trains placed at convenient locations on a civil structure could simulate motion closely approximating earthquake-induced motions. The simplicity of the pulses (on, off, and amplitude) suggested that large amounts of power or energy could be reasonably handled in a test situation.

The very low periods of large buildings require long duration pulses and high forces. Military and small space rockets would appear to be an attractive application. Rockets have been used to measure modal properties by Scruton and Harding (UK) on a chimmey in 1957, by Corvin and Steinhilber (W. Gr.) on a nuclear power plant containment structure in 1979, and by Sato and Sawabe (Japan) on microwave communications towers in 1980. Trade-off studies were conducted for adaptability of rockets for pulse train applications. These pulse train studies showed a need for flexibility in thrust magnitude and burn time, both of which required awkward modifications of the rockets at this early stage of investigation.

Alternative studies were conducted on variable throat nozzles and on other forms of propellants such as cold gas, steam, and hydrazine. From these studies, a nozzle with an internal metering plug was chosen, and used with nitrogen at a commercial pressure of 2460 psig as a propellant. This approach provided the flexibility required in pulse programming but the thrust levels would be useful only on small structures and large equipments. The two pulse rockets are pictured in Figure 1-1.

1.2 SCOPE OF WORK

The first major phase of this research program was the development of efficient algorithms for pulse generation for earthquake simulation in civil structures and also for the suppression or reduction of earthquake-induced structural motions by counteracting pulses. The second major phase involved the development of the pulse generating system itself, a system that involved electrical, mechanical, hydraulic and gas dynamic subsystems. The use of a metering nozzle for variable thrust control raised questions of thrust efficiency at the onset. A final phase of the research program included a demonstration test upon a structure.

This report covers the main development phases of the research grant. The first sections describe the gas pulse system (Sec. 2) and the gas pulse generator (Sec. 3). A discussion of motion simulation by pulse trains is given in Section 4. Section 5 presents data from calibration and initial test runs of the pulse generators. A demonstration of motion reduction by pulses (Sec. 6) and a demonstration test upon a structure (Sec. 7) completes the technical sections of the report. The final sections discuss a utilization plan and conclusions.

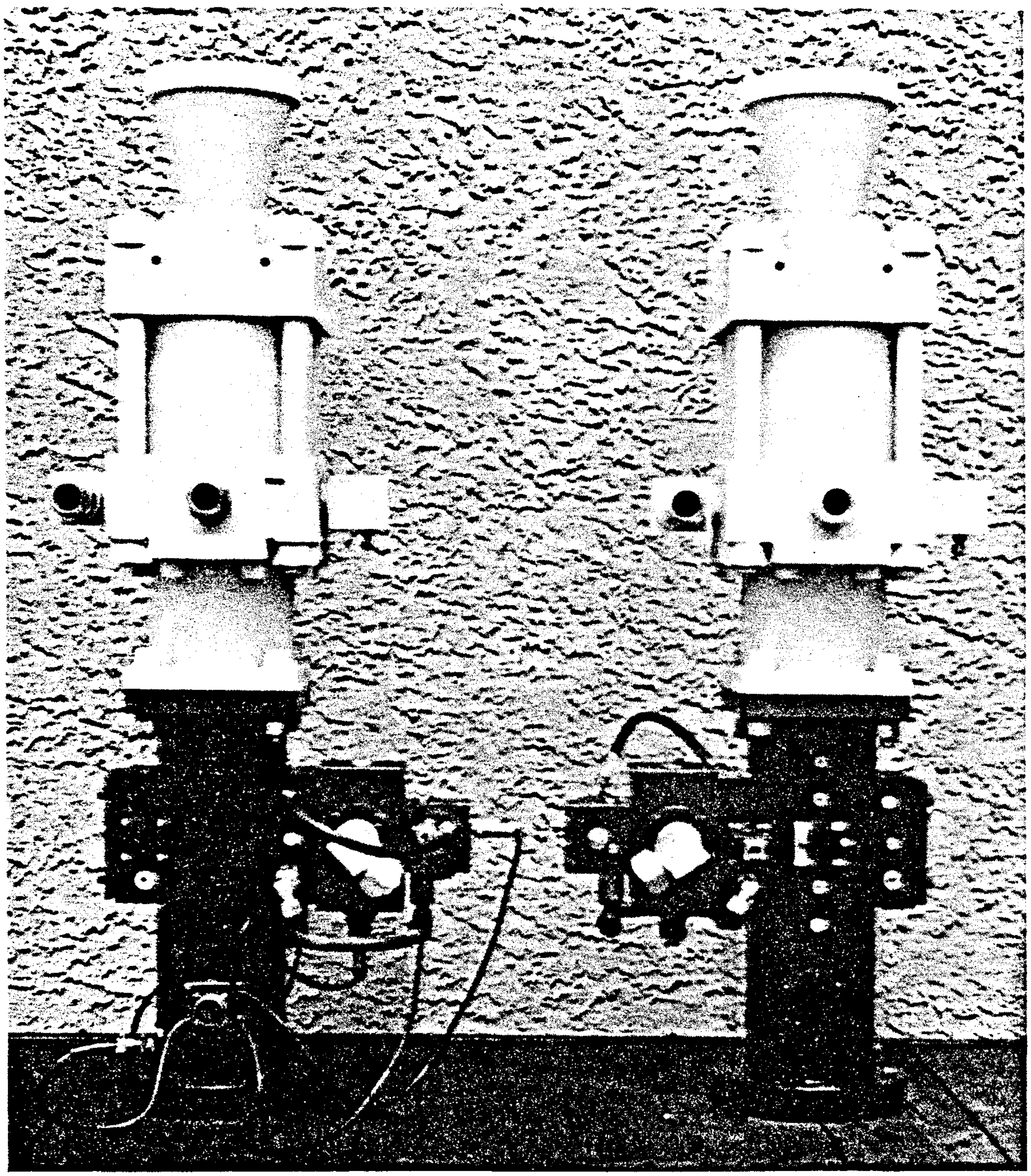

FIGURE 1-1. TWO PULSE THRUSTER UNITS DEVELOPED FOR THIS PROJECT

SECTION 2

GAS PULSE SYSTEM

2.1 GAS PULSE SYSTEM

Two gas pulse systems have been developed and are schematically illustrated in Figure 2-1. Two independent systems were produced so as to place each system in opposing directions for tests of structures or large equipments. This "opposed positioning" permits the sense of positive and negative force pulses. The operations of the two systems are controlled by a common microcomputer. Each gas pulse system is composed of the following subsystems:

- Pulse Rocket
- Hydraulic subsystem
- High pressure gas supply
- Control microcomputer

In addition, signal monitors and data recordings are provided for. Signal monitoring is particularly critical when the gas pulse system is used in the anti-earthquake mode (rocket thrusts to counter structural motions). Monitor signals of supply pressure and stroke position requirements of the metering nozzle of the pulse rockets are used as feedback signals.

2.2 PULSE ROCKET

The pulse rocket is pictured in Figures 2-2 and 2-3, and schematically shown in Figure 2-4. The pulse unit mounted upon a hydraulic actuator is 55 in. in length and weighs 500 lb. Thrust amplitudes are controlled in the on-state by positioning the metering plug for the required throat area in the nozzle for flow control. The off-state for the pulse occurs by signaling the hydraulic actuator to move the metering plug to seal off gas flow at the nozzle.

Nominal thrust or output force with gas supply at initial pressure is 10,000 lbf. The convergent-divergent nozzle is the

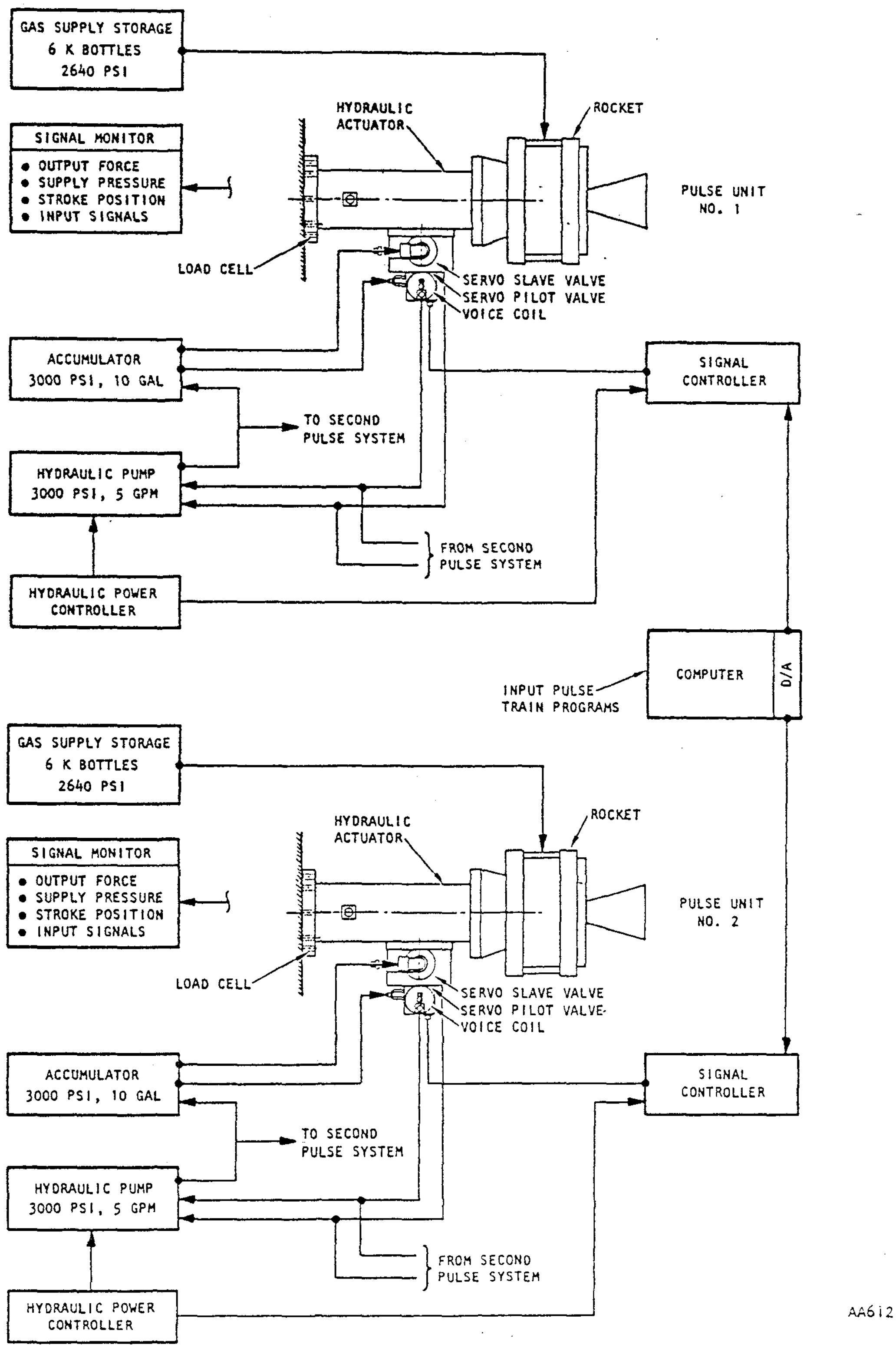

FIGURE 2-1. SCHEMATIC OF TWO GAS REACTION PULSE-GENERATING SYSTEMS CONTROLLED BY CENTRAL MICROCOMPUTER

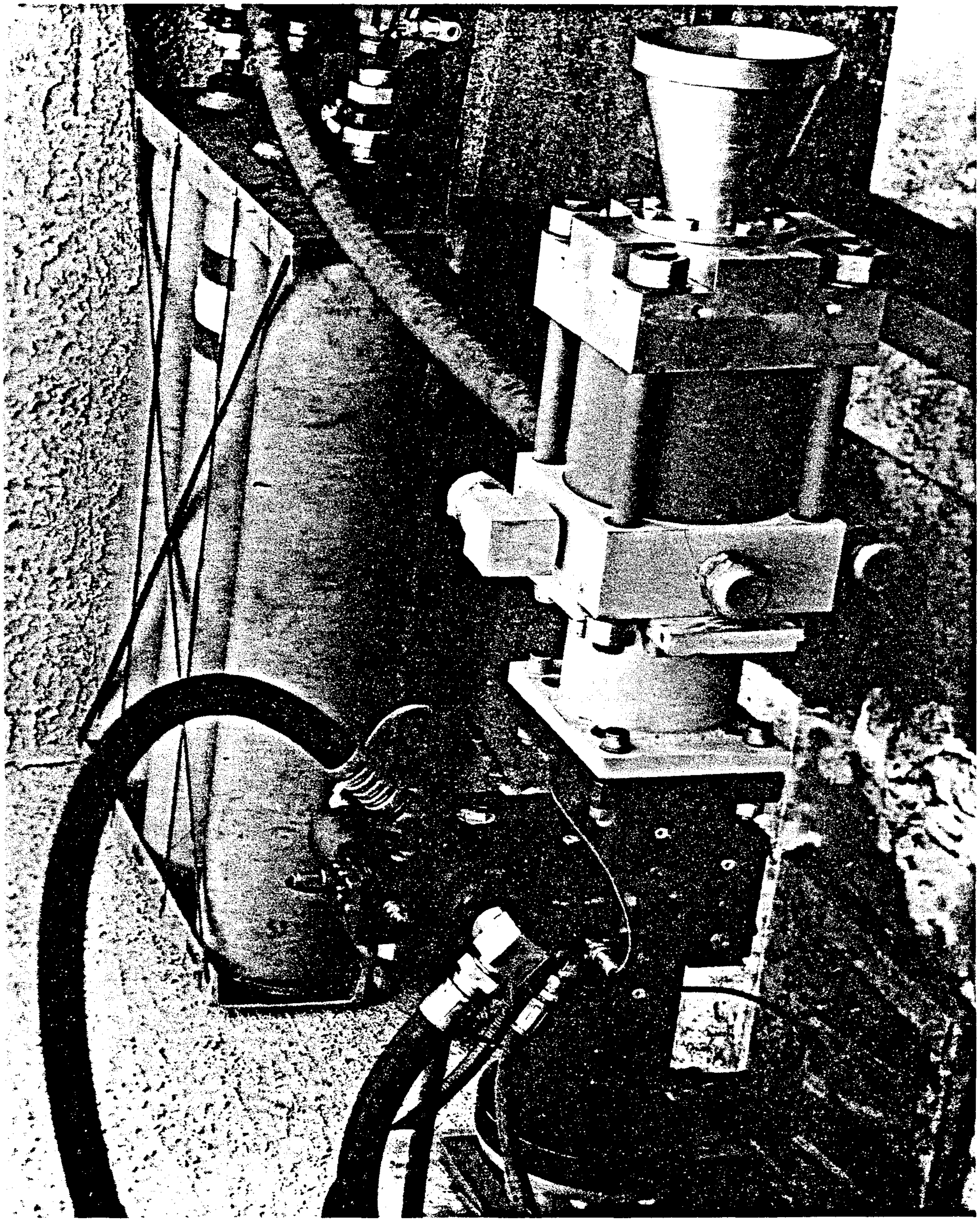

FIGURE 2-2. GAS PULSE GENERATOR ON TEST STAND

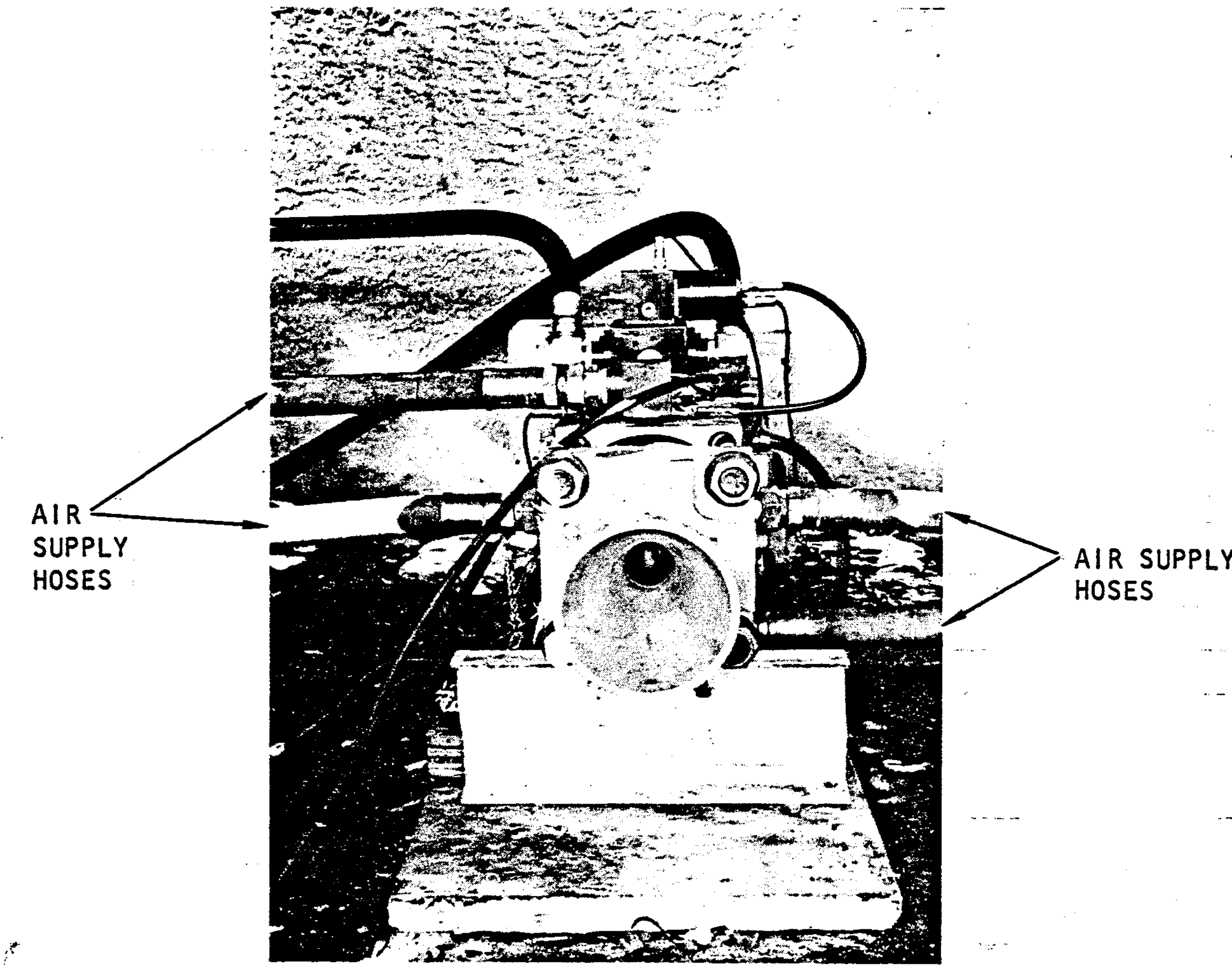

FIGURE 2-3. FRONT VIEW OF GAS PULSE GENERATOR

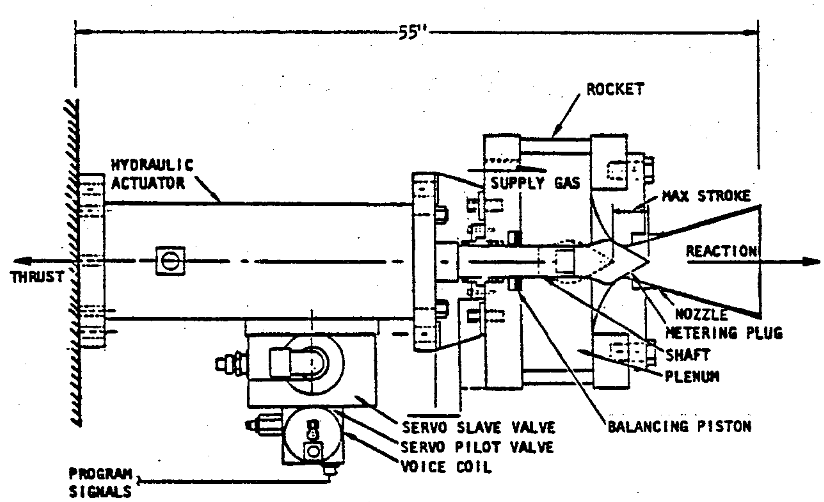

FIGURE 2-4. GAS REACTION FORCE PULSE GENERATOR EQUIPPED WITH A 90-GPM SLAVE VALVE AND A 5-GPM PILOT VALVE

De Laval type and is 8.2 in. in length, with a 2-in.-dia. throat and a 6.78-in. exit diameter. This configuration gives a cone angle of 32.5 deg and an efficient flow of 98% (2% loss by divergence). The plenum chamber behind the nozzle houses the metering shaft, gas seals, and air supply hose connections. The chamber is 9 in. long and 8 in. ID.

2.3 HYDRAULIC SUBSYSTEM

The function of the hydraulic subsystem, upon command from a microcomputer, is to position the metering plug in the gas rocket. This subsystem consists of a hydraulic actuator, hydraulic power supply, power control panel and signal controller.

The hydraulic actuator is pictured in Figure 2-2 and schematically in Figures 2-1 and 2-4. This actuator has an output force of 6,600 lbf and a stroke of 2 in. Overall dimensions are 24 in. in length and 6.3 in. body diameter. Two units were acquired from Ling Electronics.

The force output rating of the actuator was selected on the basis of the total mass to be moved (metering plug, shaft, and hydraulic piston) and the gas pressures in the plenum chamber of the rocket. High output force is required for rapid opening and closing of the metering plug. To improve rise times, oversized hydraulic pilot valves (5 gpm) and slave valves (90 gpm) are used. Rise times less than 13 msec have been achieved.

The hydraulic power supply is given in the schematic of Figure 2-5. The principal energy source is the 10 gal accumulator which is used to drive the actuators. The accumulator has sufficient capacity for most earthquake applications and thereby eliminates the need for a high cost hydraulic pump. A small hydraulic pump (5 gpm) proved adequate to bring the subsystem up to operating pressure (3000 psi) and sustain the leakage flow in the actuator because actuator leakage occurs in both slave and pilotvalves and in the hydrostatic bearings. One of the 10 gal accumulators is pictured in Figure 2-6.

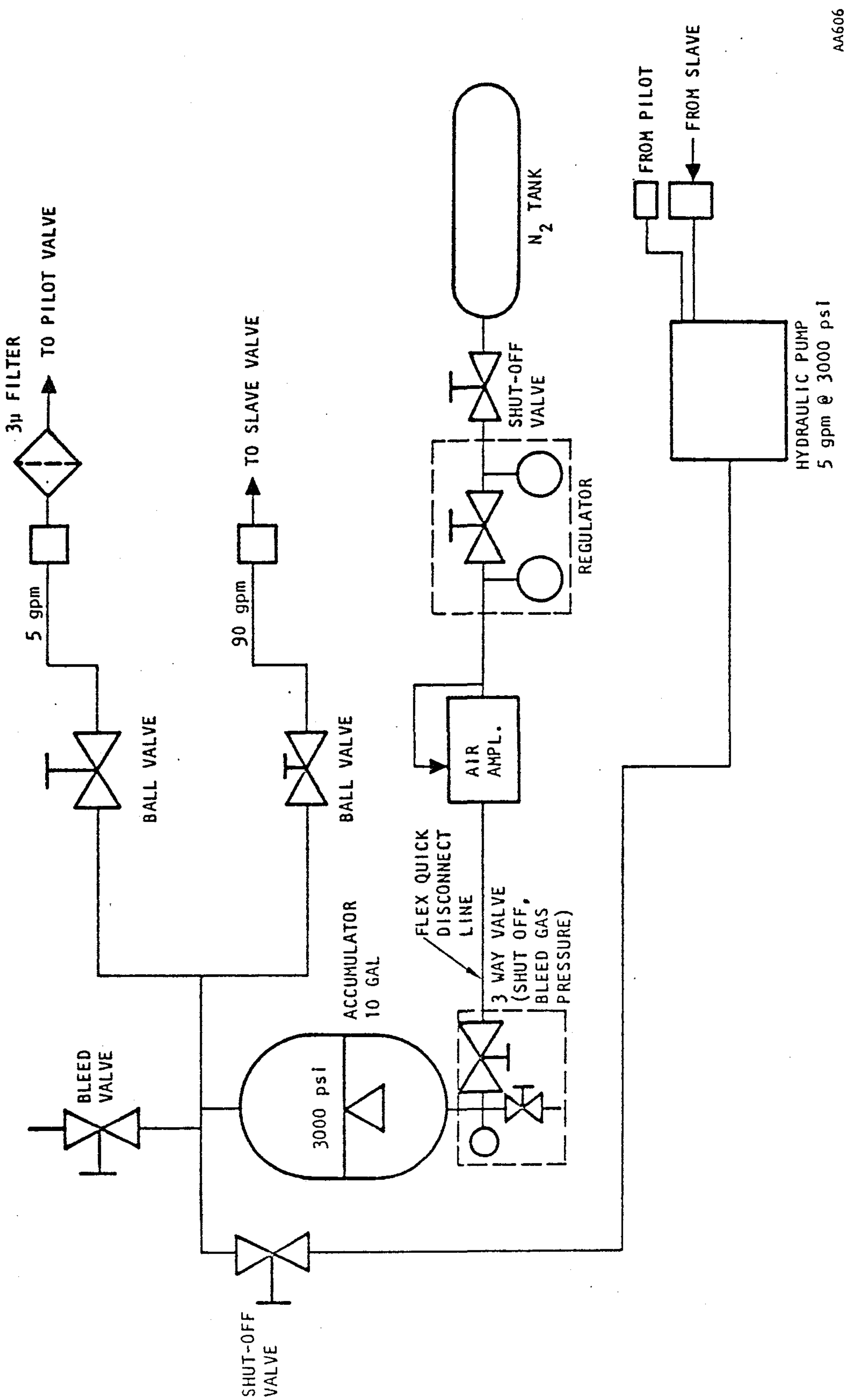

FIGURE 2-5. HYDRAULIC POWER SUPPLY AND CHARGING SYSTEM, PLUG NOZZLE ACTUATOR

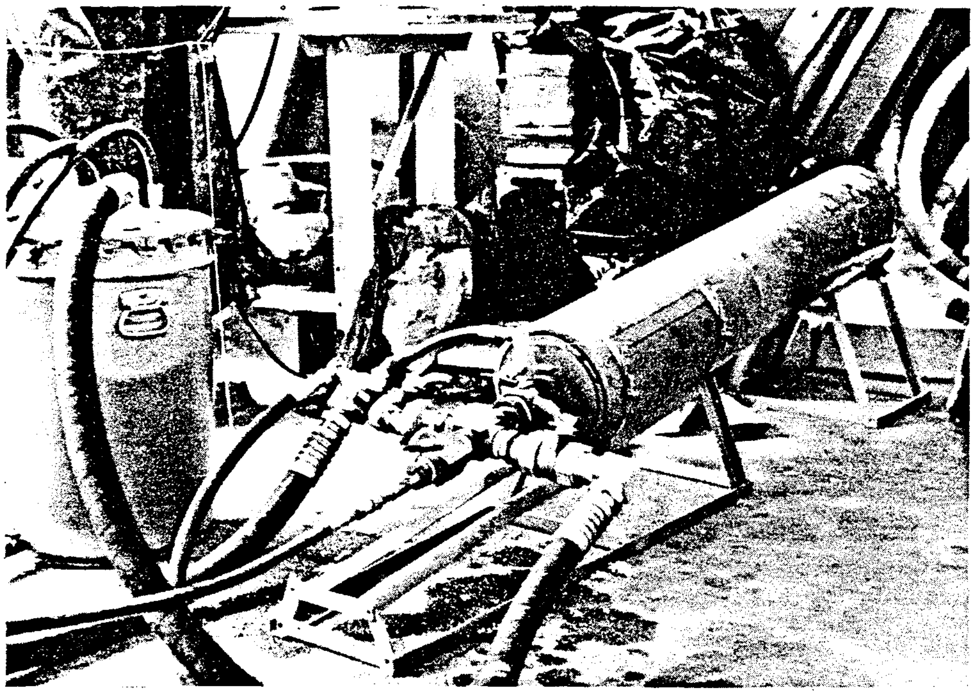

FIGURE 2-6. 3000 PSI HYDRAULIC ACCUMULATOR USED AS POWER SOURCE FOR HYDRAULIC ACTUATOR

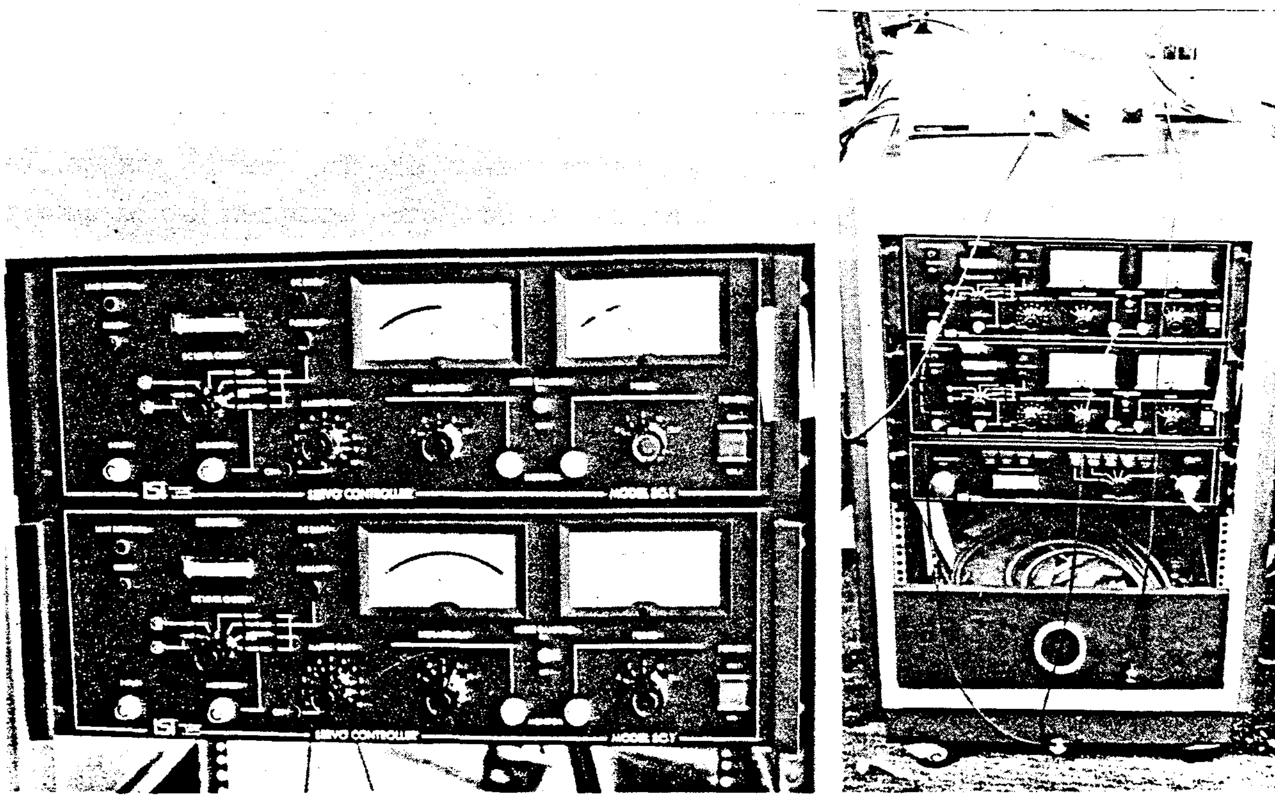

FIGURE 2-7. CONTROL CONSOLE FOR TWO HYDRAULIC ACTUATOR SYSTEMS. TOP TWO PANELS ARE SERVOCONTROLLERS FOR EACH ACTUATOR. BOTTOM PANEL IS HYDRAULIC PUMP CONTROL.

Operation of the hydraulic power supply is performed by control electronics to power up the system to pressure and includes override and interlocks for temperature and fluid levels. Command of the hydraulic actuator is through the servo controller. Two of these units are pictured in Figure 2-7. These units receive input commands from the microcomputer by which each servo controller operates an actuator. Feedback signals from pressure differentials, servo valve position and actuator position provide accurate response to the input signals. Schematics of the hydraulic servo and servo controller are given in Figures 2-8 and 2-9.

To assure safety, all pipe fittings, valves, and hoses are rated at 12,000 psi burst pressure. The hydraulic system operates under pressure at 3000 psi.

2.4 GAS STORAGE SUBSYSTEM

Gas supply storage for nitrogen gas consists of six standard industrial high pressure tanks, four 10 ft long 1-1/4 in. dia. flexible hoses and the plenum chamber for each gas pulse generator system. Three pressure tanks are mounted as a group with each tank equipped with a valve and a manifold. A typical unit is pictured in Figure 2-10. Gas capacity for each pulse unit is as follows:

Element	No.	Unit Volume	Volume
Tanks	6	2,661	15,966
Hoses	4	212	848
Manifolds	2	105	210
Plenum	1	511	511
			17,535 in^3
			(10.2 ft^3)

For each unit, this amounts to 134 lb of nitrogen compressed at 2640 psig.

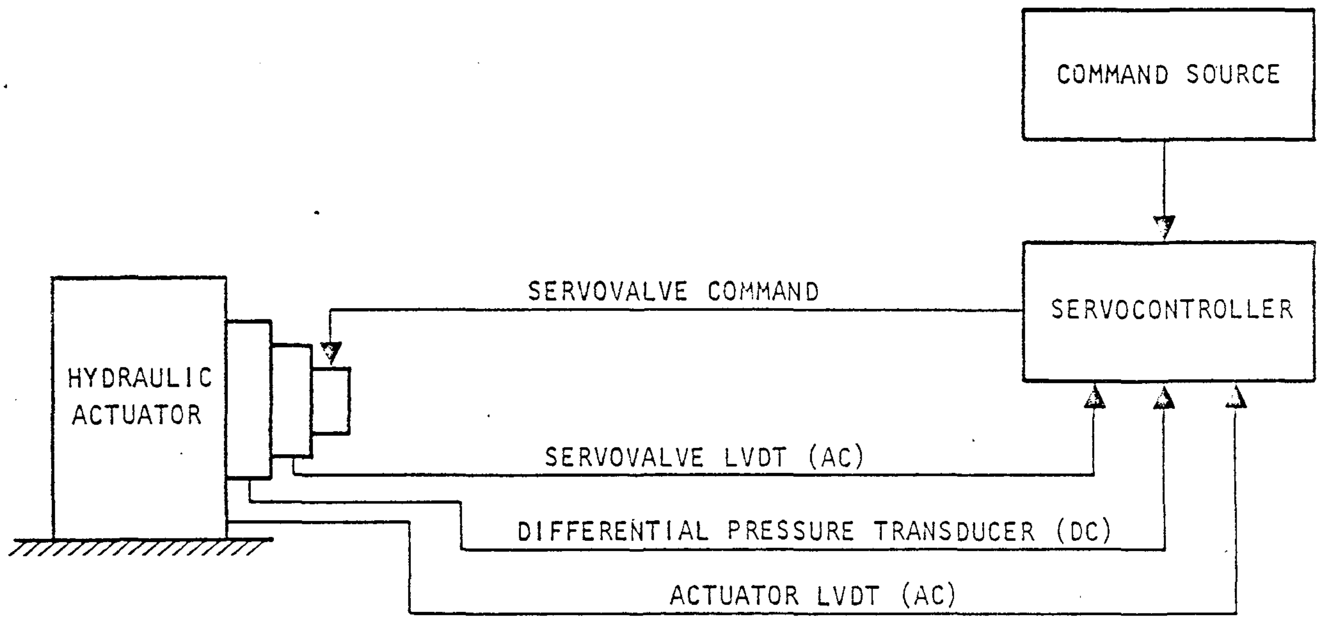

FIGURE 2-8. HYDRAULIC SERVOCONTROL BLOCK DIAGRAM FOR HYDRAULIC ACTUATOR

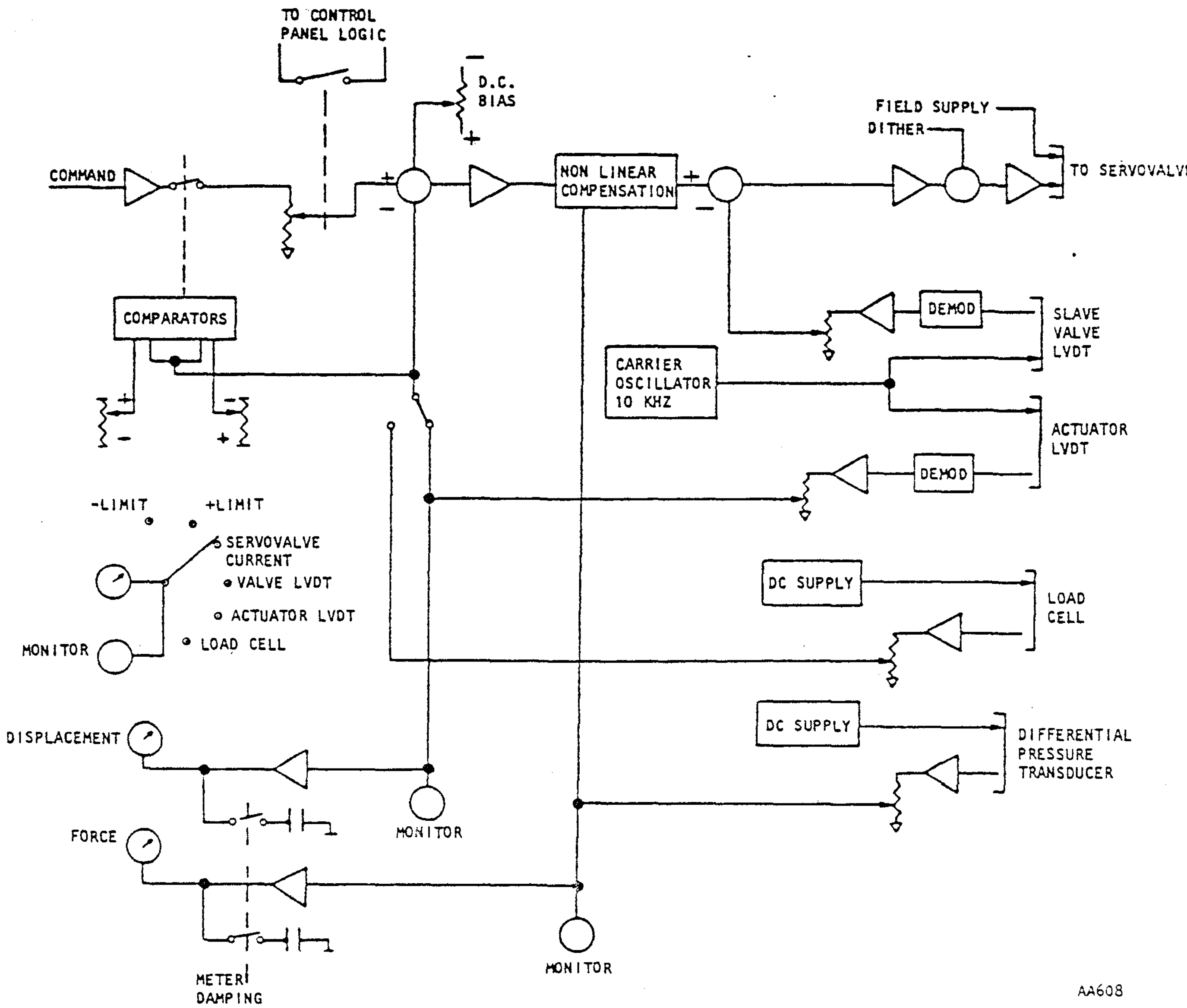

FIGURE 2-9. SERVOCONTROLLER BLOCK DIAGRAM FOR HYDRAULIC ACTUATOR

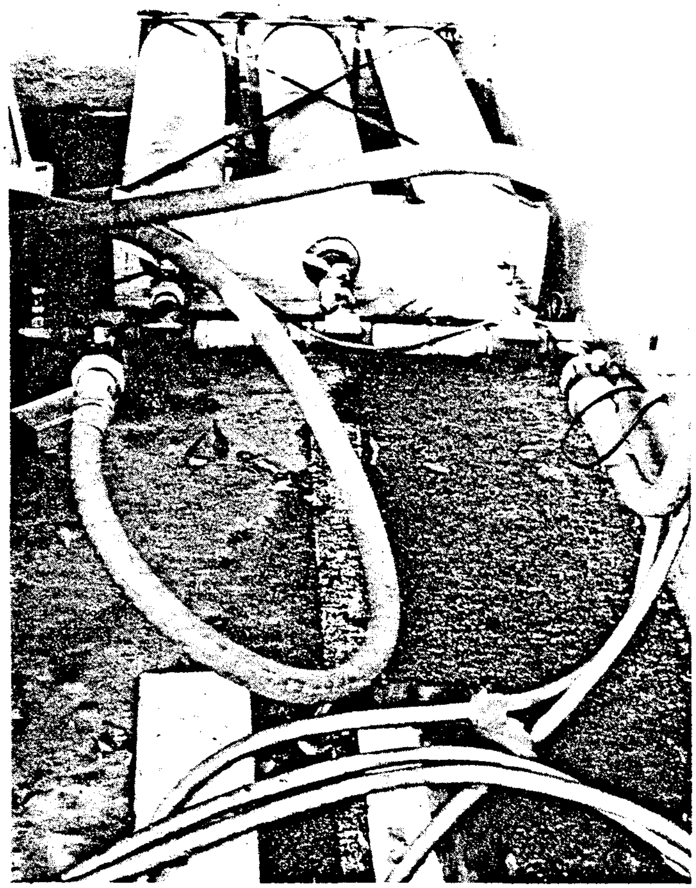

FIGURE 2-10. HIGH PRESSURE GAS STORAGE UNITS (ONE SET OF FOUR) USED TO SUPPLY PULSER

2.5 CONTROL MICROCOMPUTER

The microcomputer controls the firing pulses for both pulse generating systems. This computer, a PDP 11V03L, manufactured by the Digital Equipment Corp., is pictured in Figure 2-11, and its main features are diagrammed in Figure 2-12. Operation of the pulse generator requires that both pulse generating and counter-motion algorithms be programmed in machine language (real time).

Four channels are available for output via a D/A converter, and these are used in channel pairs for valve position and time commands to each pulse generator (hydraulic servo controller). Sixteen system channels are available for input via A/D converter to receive input signals of dynamic response of structures. These input or feedback signals are used by the anti-earthquake algorithm to initiate pulses at appropriate time durations and amplitudes to reduce structural motions that would be caused by an earthquake.

Programming for earthquake testing is straightforward. A test program is initiated and the valve position (amplitude) and the on/off times are entered for each pulse unit from the keyboard. The desired pulse program is stored in memory and upon call-up will initiate the pulse firing sequence.

2.6 SIGNAL MONITORING AND DATA PROCESSING

Performance of the gas pulses is monitored and recorded as functions of time by the following:

- Metering nozzle position – Hydraulic actuator LVDT.
- Plenum chamber pressure – Pressure transducer Teledyne model 206AGX, 0-3000 psig.
- Thrust – Load cell Interface model 1220AF, 0-25,000 lbf.
- Command pulse train – Direct recording signals.

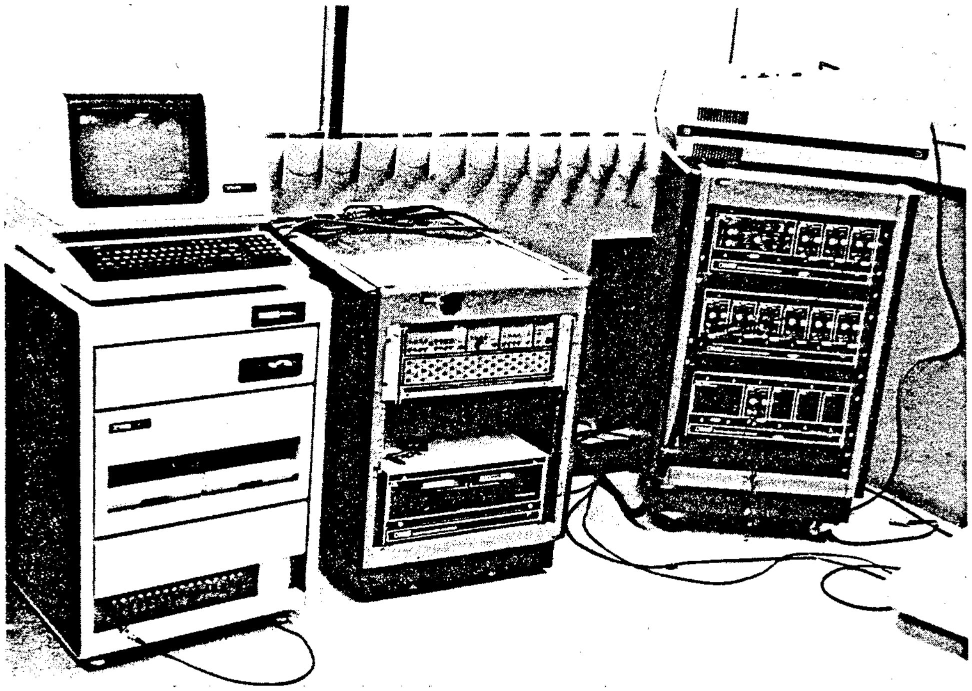

FIGURE 2-11. CONTROL MICROCOMPUTER (LEFT) AND DATA RECORDING AND PROCESSING SYSTEM (CENTER AND RIGHT)

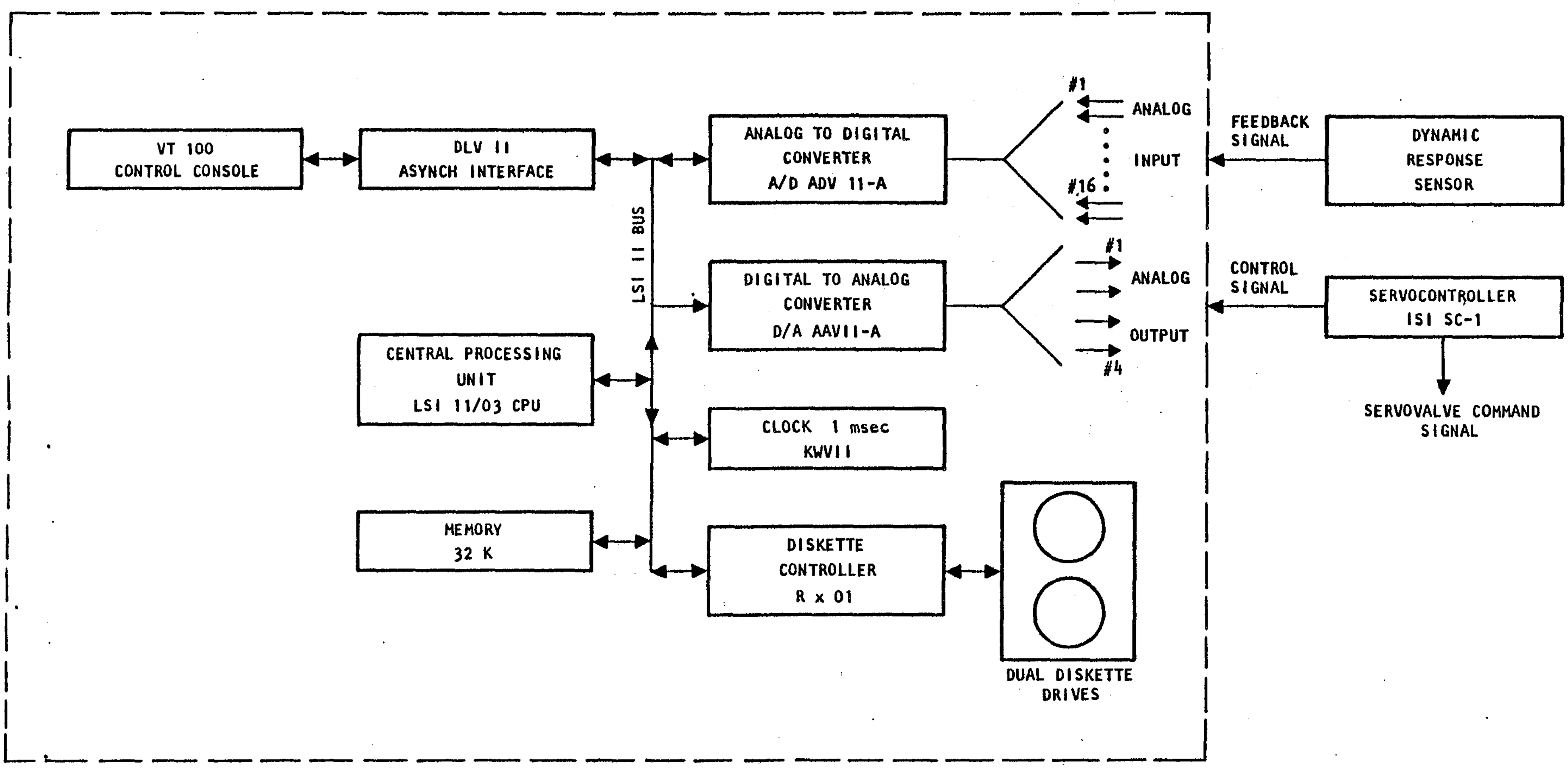

AA607

FIGURE 2-12. MICROCOMPUTER SYSTEM USED TO CONTROL PULSE GENERATOR SYSTEM

These recorded signals permit a quick assessment of performance and a means of determining the nozzle coefficient from

$$C_{FX} = \frac{F}{A_t\ P_c}$$

where

C_{FX} = Nozzle coefficient

F = Rocket thrust, lbf

A_t = Throat area, in^2

P_c = Chamber pressure, psia

Several methods are available for recording test results. The method used in this report is by signal capture via an A/D converter into circulating registers. Subsequent processing on digital data acquisition/processing equipment is performed within a few minutes after testing; the Zonic equipment used for this procedure is pictured in Figure 2-11. Data displays are in time histories and Fourier spectra. Eventually, data is transferred to a main-frame computer for time series analysis.

SECTION 3

GAS PULSE GENERATOR

The design of the cold gas generator involved not only its performance but safety as well, especially in view of the high pressure storage capacity, flexible hose links, pipe fittings, and the pulse rocket. Pictures of the two pulse rockets mounted on their hydraulic actuators are shown in Figure 1-1.

3.1 DESIGN CONSTRAINTS

A major constraint in the design of the gas pulse generator was the selection of the internal gas pressure. The setting of maximum pressure levels was determined by safety considerations and the availability of standard pipe fittings and hoses and commercially available high pressure nitrogen tanks. These considerations set the nominal operating gas pressure of the system at 2640 psig (standard commercial K size gas storage bottle 1.54 ft^3). Commercial pipe fittings and hoses have burst pressures of 12,000 psig. With 2640 psig as nominal, a maximum value of 3000 psig can be used when high thrusts are required.

A secondary design constraint was the internal pressures upon the metering plug. As can be observed in Figure 3-1, when the plug is in the closed position (no flow) the projected flat plate area times the internal chamber pressure (P_c) presents an initial force which must be overcome by the hydraulic actuator. This force, plus the reaction forces of the masses of the metering plug, shaft, and actuator piston, controls the opening time of the pulser. Closing, as from a full open position, also includes a side-on gas pressure at the front of the metering plug, but this is a lesser force than above. A pressure balancing piston was added to compensate for the pressure forces on the rear of the metering nozzle. This device promotes a more rapid opening. The piston, as can be seen in the sketch of Figure 3-1, is actuated by a step in the shaft for nozzle position of 0 to 0.25 in.

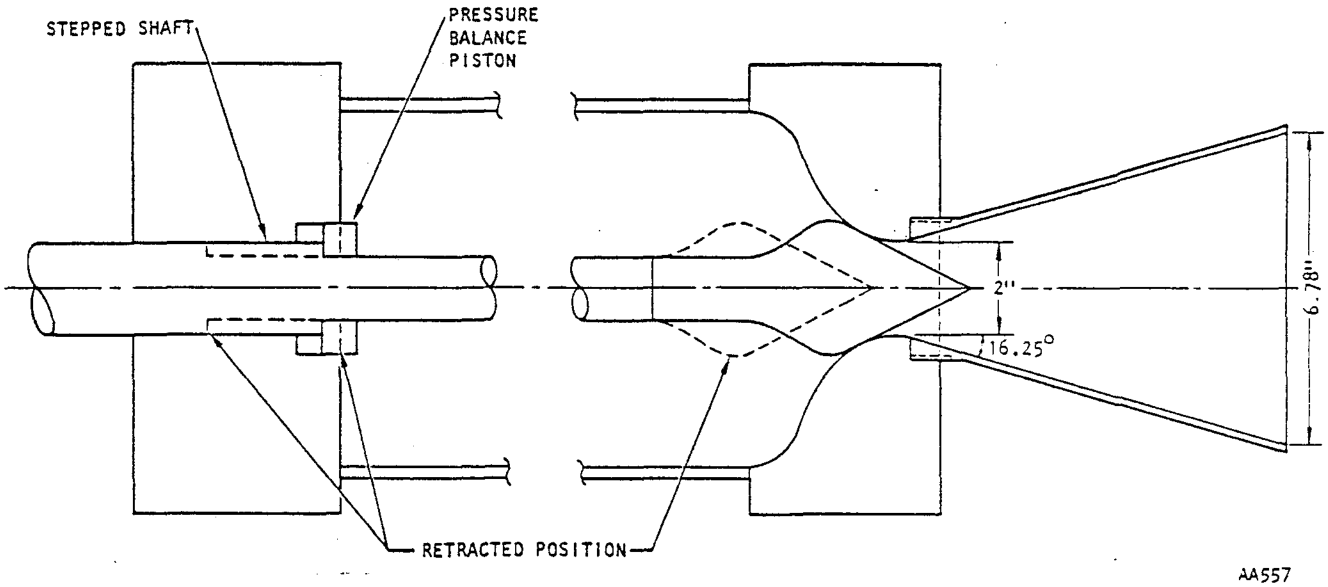

(a) Metering nozzle and pressure balance piston configuration

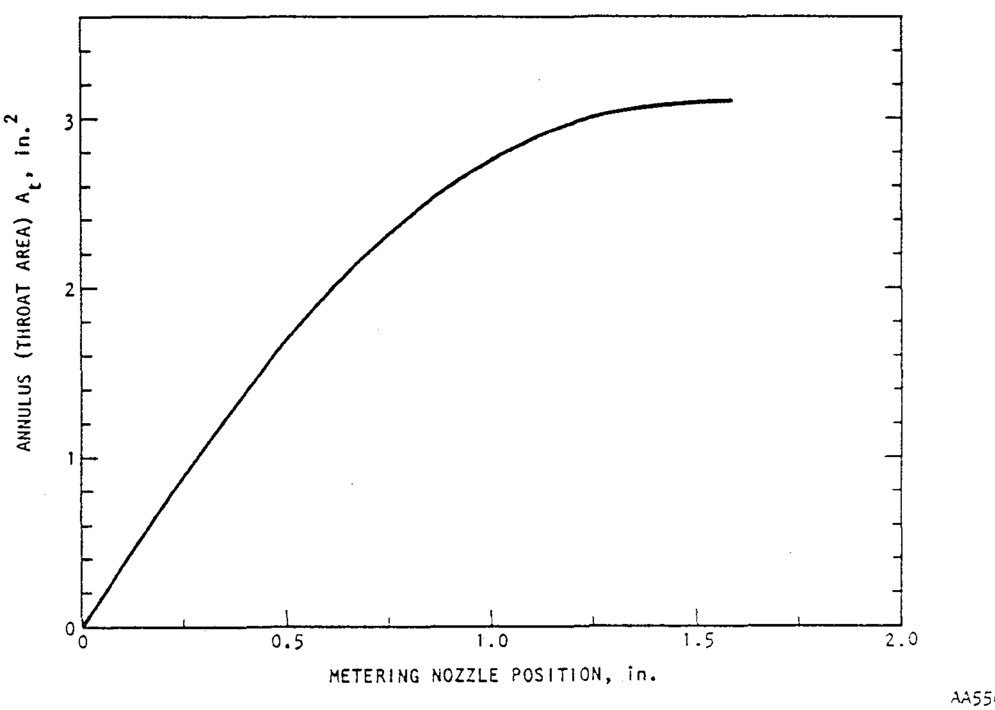

(b) Calibration curve

FIGURE 3-1. THROAT AREA (ANNULUS) AS A FUNCTION OF METERING NOZZLE POSITION

These design limits set the requirements of the hydraulic actuator at 6,600 lb output force and the throat diameter (d_t) of the De Laval nozzle at 2 in. (A_t = 3.14 in^2).

3.2 SELECTION OF ROCKET THRUST

The maximum thrust of the rocket (metering plug in fully retracted position) can be established by the following:

$$F = C_{FX} P_c A_t$$

where

F = Rocket thrust, lbf

P_c = Chamber pressure, psia = 2143 + 14.7 = 2157.7 psia

A_t = Throat area, in^2 = 3.14 in^2

C_{FX} = Nozzle coefficient = $\lambda\eta C_F$

where

λ = Flow divergence factor in supersonic section = 0.98

η = Friction loss factor = 0.95

C_F = Lossless nozzle coefficient

Hence, $F = 6300\ C_F$.

Flow divergence in the supersonic section of a nozzle is related to the cone angle by

$$\lambda = \frac{1}{2}(1 + \cos\alpha)$$

where

α = 1/2 nozzle exit cone

Good design sets λ at 0.98, and this results in an exit cone angle of 32.5 deg (hence, α = 16.25°) such that the exit area of the cone is A_e = 36.1 in^2 (d_e = 6.78 in.).

Friction loss factor η = 0.95 is empirical. The lossless nozzle coefficient is found from the following:

$$C_F = \left[\gamma \left(\frac{2}{\gamma + 1} \right)^{\frac{\gamma + 1}{2(\gamma - 1)}} \right] \left\{ \frac{2}{\gamma - 1} \left[1 - \left(\frac{P_e}{P_c} \right)^{\frac{\gamma - 1}{\gamma}} \right] \right\}^{1/2} + \left(\frac{P_e - P_o}{P_c} \right) \frac{A_e}{A_t}$$

where

γ = Ratio of coefficients of specific heat, for N_2 = 1.41

P_e = Pressure at exit plane of nozzle

P_c = Chamber pressure

P_o = Atmospheric pressure

A_e = Area at exit plane of nozzle

A_t = Throat area

For full expansion at the nozzle exit plane, $P_e = P_o$ and maximum thrust occurs for the design chamber pressure

$$C_F = 1.577$$

and

$$C_{FX} = \lambda \eta \; C_F = 1.47$$

design thrust

F = 10,000 lbf for 2460 psig static storage pressure

3.3 VARIABLE THRUST

Thrust may be varied by commanding the position of the metering plug from the closed (no flow) position to the full open (maximum flow). On command from a signal programmed in the microcomputer, the metering plug retracts to a specified position, at which point the throat area is an annulus between the conic surface of the metering plug and the wall of the convergent section of the nozzle. Figure 3-1 shows the functional relation between the retracted position of the metering plug and the throat area, A_t.

Loss in thrust efficiency will occur with small throat areas due to over-expansion of the flow at the exit plane of the nozzle. Additionally, secondary shocks at the apex of the metering plug, compression shock, and turbulence will combine to reduce efficiency. For practical applications, the nozzle coefficient C_{FX} must be calibrated for a range of chamber pressure, throat area, and thrust, using the relation

$$C_{FX_i} = \frac{F_i}{A_{t_i} P_{c_i}}$$

3.4 THRUST PREDICTION (PROGRAMMING)

The present gas storage capacity for each pulse generator consists of six gas bottles, four 10 ft long hoses, and the plenum chamber of the gas rocket. This storage capacity amounts to 10.2 ft^3, and 134 lb of nitrogen compressed at 2640 psig. After each pulse, the stored gas is reduced in pressure, and hence, less potential energy. Thus, to program a pulse train, a series of incremental solutions to the gas equations are required. For example, chamber pressure of 2640 psig can reduce to 400 psig and internal energy would reduce thereby from 134 Btu/lb to 119 Btu/lb after the last pulse. At the beginning of each pulse, the state of the pressure, internal energy, temperature, and weight of gas (reservoir) must be known in order to program the next pulse for thrust, by the throat area and the calibrated nozzle coefficient. An example of these calculations is given in Table 3-1.

Thrust is given by

$$F = - \dot{m} V_{xe} + A_e (P_e - P_o)$$

where

F = Thrust, lbf

$\dot{m}$ = Mass rate of flow, lb-sec/ft

A_e = Exit area of nozzle, in^2

P_e = Exit pressure, psia

P_o = Ambient pressure, psia

TABLE 3-1. EXAMPLE OF INCREMENTAL CALCULATIONS NEEDED TO ESTABLISH VALVE POSITION FOR THRUST REQUIREMENTS

				Plenum Chamber			Storage Capacity			Weight Rate of Flow	Jet Velocity	Density
				Static		Transient						
Pulse No.	Req'd Force	Valve Position		P_{start} (psig)	P_{end} (psig)	P_c (psig)	Start W (lb)	Stop W (lb)	Diff. ΔW (lb)	$\dot{w}$ lb/sec	V_{ex} ft/sec	ω lbs/ft^3
		in.	in^2									
1	1,230	0.12	0.44	2,200	2,157	2,145	111.87	110.32	1.55	18.3	2,161	10.97
2	847	0.10	0.34	2,157	2,127	2,099	110.32	109.3	1.07	12.68	2,149	10.86
3	4,332	0.46	1.63	2,127	1,985	1,812	109.3	104.1	5.2	66.1	2,109	10.13
4	2,742	0.30	1.12	1,985	1,896	1,793	104.1	100.8	3.3	41.63	2,119	9.71
5	1,105	0.13	0.51	1,896	1,876	1,828	100.8	100.15	0.75	16.7	2,124	9.53
6	2,078	0.23	0.88	1,876	1,810	1,716	100.05	97.54	2.51	31.52	2,121	9.17
7	2,348	0.29	1.08	1,810	1,735	1,658	97.54	94.68	2.86	35.63	2,120	8.81
8	3,554	0.45	1.60	1,735	1,625	1,542	94.68	90.45	4.23	54.13	2,112	8.45
9	1,400	0.2	0.75	1,625	1,583	1,537	90.45	88.8	1.65	21.53	2,092	8.27
10	302	0.05	0.18	1,583	1,574	1,556	88.8	88.43	0.375	4.64	2,093	8.20

For these calculations $P_e = P_o$ was assumed, with subsequent correction made using the calibrated nozzle coefficient C_{FX}.

For the jet velocity,

$$V_{xe} = \lambda V_e$$

where

λ = Nozzle divergence factor = 0.98

V_e = Jet velocity, ft/sec

$$V_e = \left\{\left(\frac{2\gamma}{\gamma - 1}\right)\left(\frac{P_c}{\rho_c}\right)\left[1 - \left(\frac{P_o}{P_c}\right)^{\frac{\gamma-1}{\gamma}}\right]\right\}^{1/2}$$

where

ρ_c = Gas density in chamber, lb-sec^2/ft^4

Other parameters as given before.

The mass flow through nozzle is

$$\dot{m} = \left[\gamma\left(\frac{2}{\gamma + 1}\right)^{\frac{\gamma + 1}{2(\gamma-1)}}\right]\frac{P_c A_t}{A_c}$$

where A_c is the acoustic velocity (ft/sec) in the chamber and is given by:

$$A_c = \sqrt{\gamma \frac{P_c}{\rho_c}} \quad \text{plus temperature correction}$$

Other parameters have been defined previously.

From the general flow equation and for the condition of no flow, the chamber pressure is given by:

$$\frac{P_c v_c}{J} + U_c = \text{constant}$$

where

ν_c = Specific volume, ft^3/lb

U_c = Internal energy, Btu/lb

J = Heat equivalent of work, 778 ft-lb/BTU

Flow occurs upon retraction of the metering plug, which results in a drop in chamber pressure (P_c). This quantity is required to predict thrust:

$$\frac{P_c \nu_c - 0.53 P_c \nu_t}{J} + (U_c - U_t) = \frac{V_t^2}{2gJ}$$

and

$$P_t = \left(\frac{2}{\gamma + 1}\right)^{\frac{\gamma}{\gamma-1}} P_c = 0.53 P_c$$

$$V_t \approx \sqrt{\gamma \frac{0.53 P_c}{\rho_t}}$$

where

ν_c, ν_t = Specific volumes at chamber and throat, ft^3/lb

ρ_t = Density at throat, $lb\text{-}sec^2/ft^4$

P_t = Pressure at throat, psia

V_t = Velocity in throat, ft/sec

3.5 SAFETY FEATURES

The structure of the pulse rocket was designed with safety as a principal consideration. Major elements were the end caps, cylinder, and tie rods.

- End Caps. Stress including preload from the 4 tie rods was less than 20,000 psi.
- Tie-rods. 1-1/4 in. diameter, AISI 1045 cold drawn steel, 100,000 psi yield strength. Stressed to 41,000 psi.

- Cylinder (Plenum Chamber). 8 in. ID, 3/8 in. thick wall, 9 in. long. Material AISI 1026 heat treated to 118,000 psi tensile stress. Worse case hoop stress 45,000 psi.

SECTION 4

MOTION SIMULATION BY PULSE TRAINS

4.1 BACKGROUND

Simulation of structural motions by a series of pulses in order to match motions induced by man-made or natural events was undertaken in 1973. The motivation for this effort was the need for test and experimental information, particularly about motion-time histories of large and massive structures as they can be expected to react to future catastrophic events.

These studies demonstrated that the pulse trains could be all in one direction of a single axis if desired or necessary, or could be in either direction. A pulser performs only three functions: on, off, and magnitude. This simplicity is essential for controlling large amounts of energy.

4.2 PULSE TRAIN DEVELOPMENT

The development of a pulse train to replace an earthquake or other events for testing or experiment is illustrated in Figure 4-1 below:

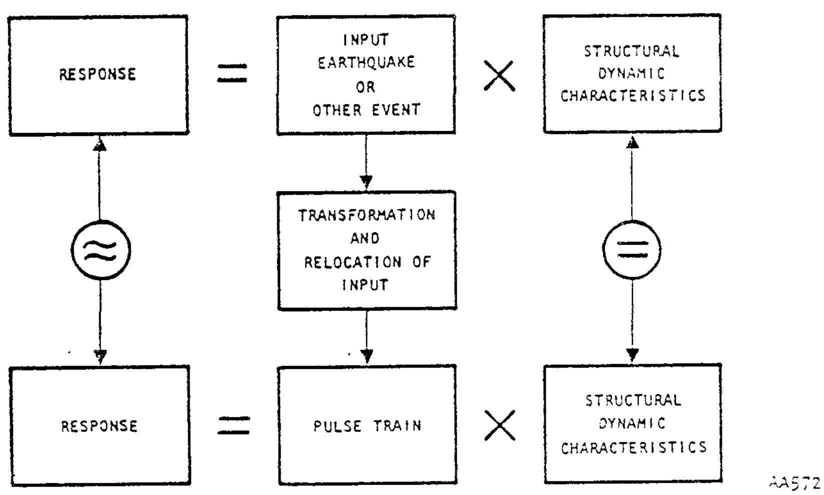

FIGURE 4-1. USE OF PULSE TRAINS TO OBTAIN EQUIVALENT STRUCTURAL RESPONSES TO EARTHQUAKE OR OTHER EVENTS

The transformation and relocation function in Figure 4-1 changes the continuous ground motion of an earthquake, to a series of discrete pulses placed on a structure or building at locations of test convenience. The response due to pulses is approximate to the criteria or objective response. Computer studies have shown this approximation can easily be held to about a 5% error level over the motion-time history. This error can change in actual tests due to the dependence on the performance of pulse excitation devices.

The determination of pulse trains is made by successive iterations using a general purpose computer. The algorithm developed for this research project is described and detailed by Masri and Safford in "Optimization Procedure for Pulse-Simulated Response," which is reprinted in the Appendix. The three parameters for each pulse (on, off, and magnitude) and for each pulse train location, potentially require an extremely large number of iterations for convergence to a global minimum. Algorithms using conventional convergence methods require excessively long run times. The difficulties encountered in obtaining convergence required the development of an algorithm which employed random search techniques.

4.3 RANDOM SEARCH

A new random-search global optimization algorithm was developed in which the variance of the step-size distribution is periodically optimized. By searching over a variance range of 8 to 10 decades, the algorithm finds the step-size distribution that yields the best local improvement in the criterion function. The variance search is then followed by a specified number of iterations of local random search where the step-size variance remains fixed. Periodic wide-range searches are introduced to ensure that the process does not stop at a local minimum. This algorithm is the basic building block for the specialized pulse algorithm presented in the appendix and is listed in the bibliography by Masri et al., "A Global Optimization Algorithm Using Adaptive Random Search."

4.4 SIMULATION OF MOTIONS USEFUL FOR STRUCTURAL INVESTIGATIONS

Emphasis in simulation has been placed upon simulating earthquake motions in structures. However, the pulse method is sufficiently versatile for the inducement of other types of motion. As can be seen in Figure 4-2, sinusoidal motion can be developed. Other studies have shown that random vibrations can also be generated. Housner in 1946 (see Bibliography) showed that base motion input of pulses with random amplitude could represent the effects of earthquakes on dynamic systems. Single pulse or multi-pulse tests can also be used to obtain transfer functions of structures and for extraction of modes.

4.5 PERFORMANCE CHARACTERISTICS

Studies of the ratio of the time duration of dynamic motion of a structure to the sum of the pulse times varies from 3 to 1 to 5 to 1 for each point of input. A pulse train developed for a specific structure is not unique, for a generally appearing different pulse train will produce the same result. This non-uniqueness permits development of pulses more compatible to the performance of excitation devices. Experience has also shown that the structural response is somewhat insensitive to errors in the pulse train amplitudes.

4.6 IMPULSE AND FORCE REQUIREMENTS

Operations with the algorithm for pulse generation have also disclosed a need for secondary optimization for minimization of impulse and force requirements. Table 4-1 covers average requirements for a pulse train as well as total impulse required for application to a 25-story building. Applications of pulse excitation on the 33rd floor requires average forces for 18 pulses of 1.9 million lb and a total impulse of 23 million lb-sec. This study on the 25-story building was one of the first made and very little interactive effort was employed.

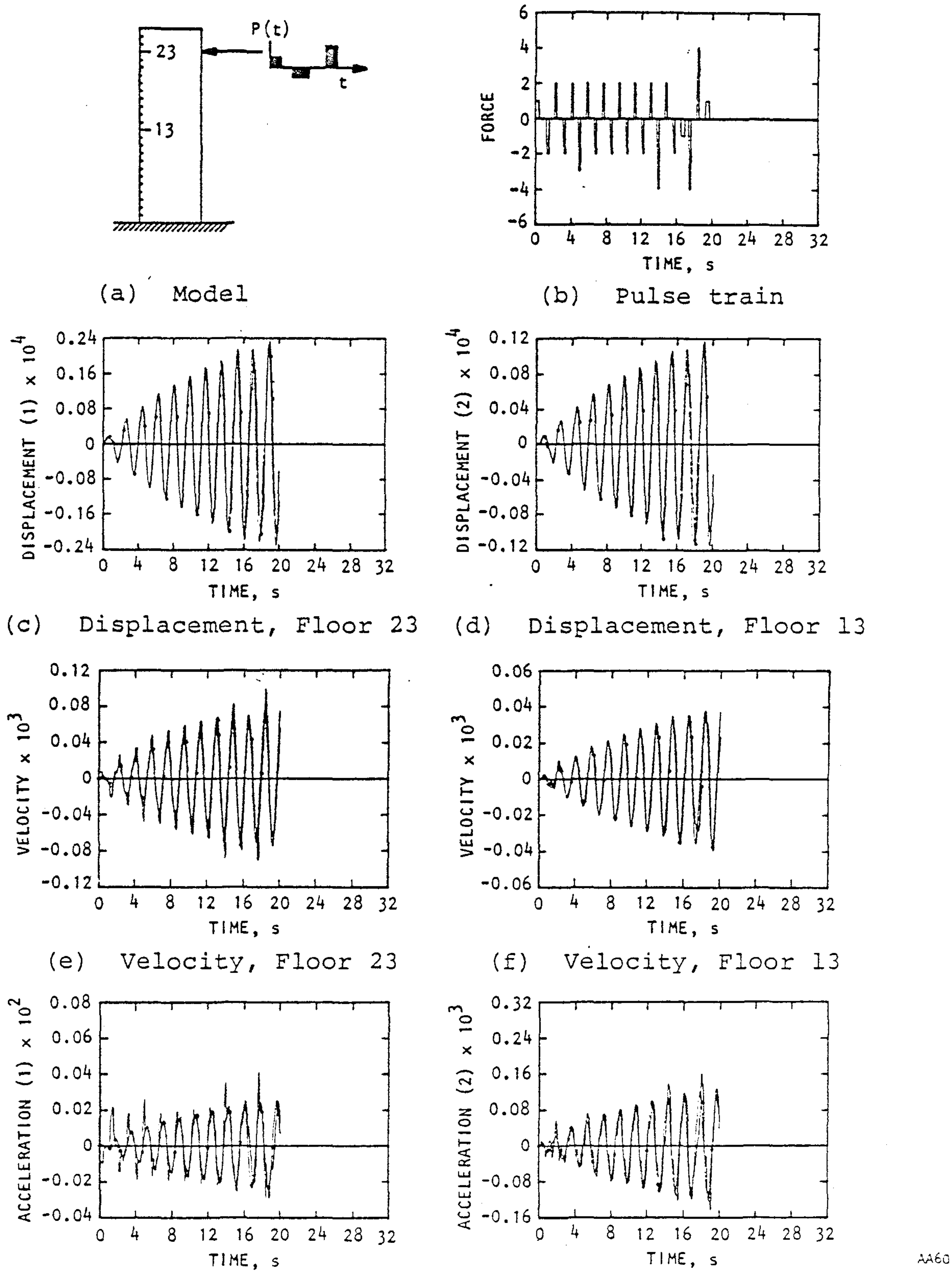

(a) Model (b) Pulse train

(c) Displacement, Floor 23 (d) Displacement, Floor 13

(e) Velocity, Floor 23 (f) Velocity, Floor 13

(g) Acceleration, Floor 23 (h) Acceleration, Floor 13

FIGURE 4-2. COMPARISON OF EXACT ——— AND PULSE SIMULATED -o-o- MOTIONS OF 25-DOF BUILDING. CRITERIA INPUT IS SINUSOIDAL EXCITATION OF FLOOR 23. PULSE TRAIN ALSO APPLIED TO FLOOR 23.

By placing the pulse units at four different floors, average force dropped to 470,000 lb and total impulse to 8.8 million lb-sec.

TABLE 4-1. PULSE TRAIN REQUIREMENTS TO EXCITE 25-STORY OFFICE BUILDING TO EL CENTRO 1940 EARTHQUAKE

Pulse Unit Location	No. of Pulses Req'd	Average Pulse Duration, Sec	Average Force, lbf	Total Impulse, lb-sec
23rd floor only	18	0.784	1.91×10^6	23.44×10^6
23rd, 18th, 13th and 8th floors	52 (13 per floor)	0.41	0.47×10^6	8.849×10^6

Table 4-2 covers the pulse train requirements for a 3-story test structure located at the Earthquake Engineering Research Center, University of California, Berkeley. This table is useful in comparing force and impulse requirements for various placements of pulse units. This latter application resulted from improvements to the algorithm and from more interactive efforts.

TABLE 4-2. PULSE TRAIN REQUIREMENTS TO EXCITE 3-STORY UCB TEST STRUCTURE TO EL CENTRO 1940 EARTHQUAKE

Pulse Unit Location	No. of Pulses Req'd	Average Pulse Duration, Sec	Average Force, lbf	Total Impulse, lb-sec
3rd floor only	23	0.100	1,882	4,324
2nd floor only	23	0.083	4,076	6,906
1st floor only	24	0.077	6,387	10,704
All floors	75 (25 per floor)	0.048	4,507	9,545

4.7 ANTI-EARTHQUAKE APPLICATIONS OF PULSES

It is possible, using the information from the above discussion, to show that a pulse generating system could be used to reduce structural dynamic motions by firing the pulses to oppose the earthquake motions of a building. An array of transducers would be required in the building to sense acceleration, velocity, displacements, and/or strain. An on-line computer to receive and process these feedback signals in real time would be used to counterfire the pulse units at the proper time phasing, time duration, and amplitude.

An on-line pulse control algorithm was developed for use with distributed parameter structures and for arbitrary disturbances. This effort was part of the research grant. This algorithm was programmed in machine language for the DEC PDP 11VO3-L microcomputer (described earlier in Sec. 2). This computer is equipped with 16 signal channels via A/D conversion for transducer feedback and 4 command channels from the computer via D/A conversion to control the pulses. A more complete description of this anti-earthquake system is in the reprint of the paper given in Appendix A.

This anti-earthquake study must be viewed at this time as an exploratory study. Eventual applications to large buildings will require a careful evaluation of pulse system reliability and pulse forces required. The high reliability and low costs of integrated circuits permit large redundancy for the processed sensor data, readiness status checks, and voting logic. In addition, redundant motion sensors would be used. Pulses would be sized for force output and pulse durations to operate only when the building motion exceeds potentially damaging or life threatening thresholds (i.e., motions beyond the seismic resistance of the building). Force-time requirements would require pulses to be in the form of solid propellant rockets.

SECTION 5

CALIBRATION

Calibration and initial test runs were performed to establish nozzle coefficients and operating characteristics of the pulse generators. A complete matrix of tests was not performed for the full range of chamber pressures and metering nozzle positions due to program limitations.

5.1 MACHINE OPERATIONS

Numerous tests were made upon the hydraulic actuator to optimize feedback for maximum rise time of the hydraulic piston to step and pulse function commands. A series of calibrations was also performed on the LVDT of the piston shaft for use in establishing metering nozzle position (throat area).

During these operations, the only major failure of the system occurred with the galling of the aluminum shaft of the metering nozzle. Galling occurred between the shaft and its housing in the base block of the plenum chamber. Shafts from each unit were re-machined and shrink-fitted with 0.10 in. thick wall steel tubing. Grease fittings were also added to each unit.

5.2 CALIBRATIONS

The following four signals were used for calibration and measurement of pulse performance:

- Input signal from computer (in./volt)
- Metering plug position LVDT (in./volt) for throat area
- Chamber pressure (psig)
- Output thrust (lbf)

The phase relationships between these several signals are displayed in the overlay plot of Figure 5-1. Studies were made for

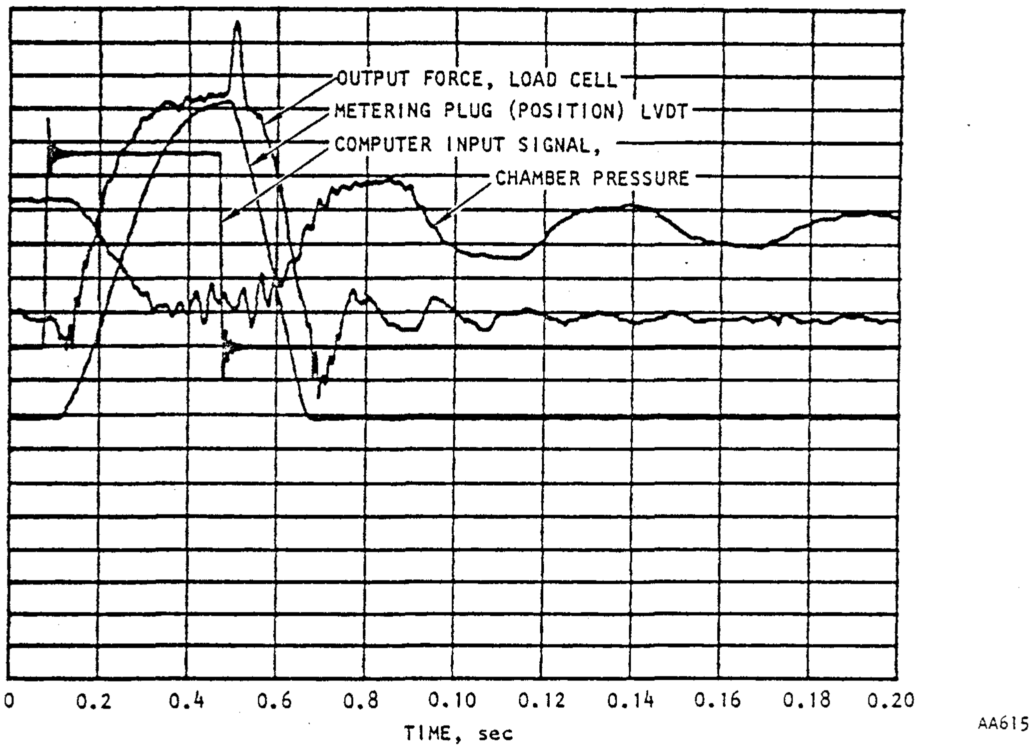

FIGURE 5-1. OVERLAY OF TIME HISTORY DATA MEASURING PERFORMANCE OF A PULSE UNIT AND SHOWING PHASE RELATIONSHIPS

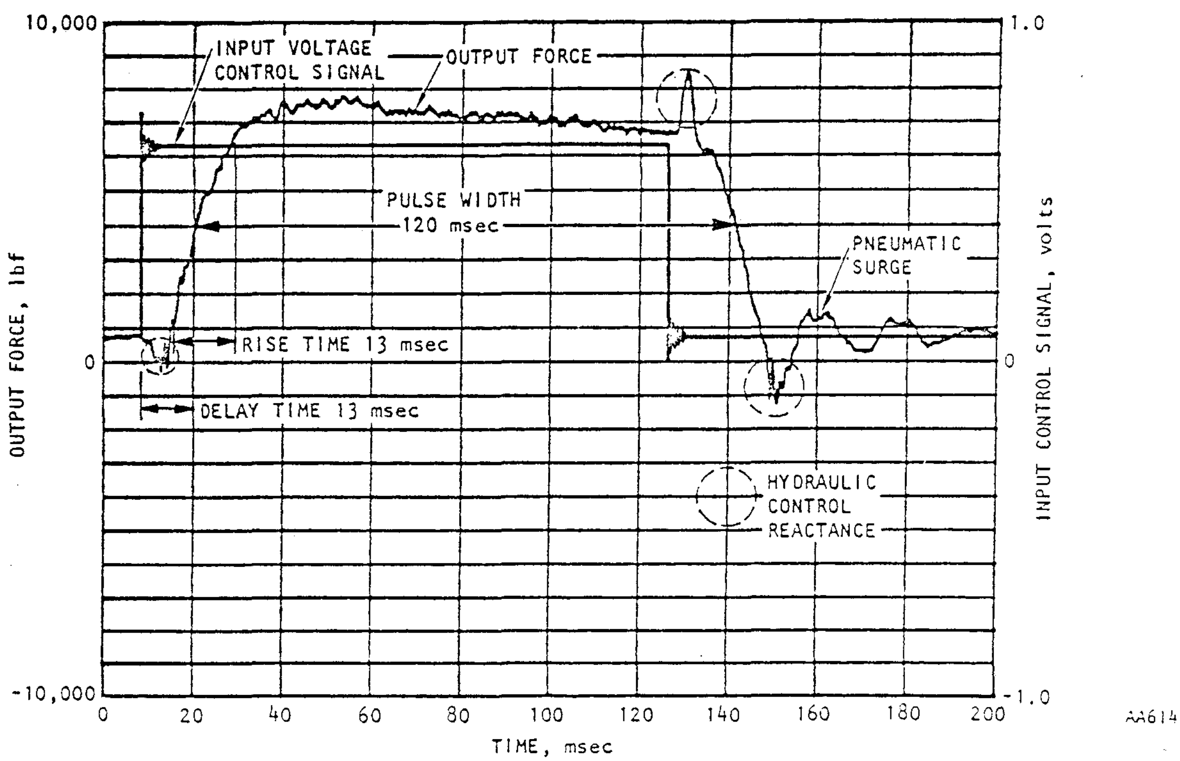

FIGURE 5-2. PHASE RELATIONSHIP INPUT SIGNAL FROM MICROCOMPUTER AND OUTPUT FORCE

the phase relationship between input voltage signal and output thrust as shown in Figure 5-2. Delay time between the onset of the input signal and 50% level of maximum for the thrust was 13 msec. Rise time of thrust from 10% to 90% of maximum was also 13 msec.

5.3 NOZZLE COEFFICIENTS

Nozzle coefficients were determined from the following relation:

$$C_{FX} = \frac{F}{A_t P_c}$$

where

F = Thrust, lbf

A_t = Throat area, in.^{2}

P_c = Chamber pressure, psia

The predicted nozzel coefficient, which includes the exit velocity divergence factor and a function loss factor, was given as 1.47 (see Sec. 3). Data from tests showed a variation in nozzle coefficients, which were somewhat independent of chamber pressures but were directly affected by pneumatic surges in the plenum chamber, hoses, and storage tanks. This surging may be observed in Figure 5-3, which plots both thrust and chamber pressure as a function of time. Surge periods are a function of chamber pressure, ranging from 51 msec (19.6 Hz) at 2500 psig to 62 msec (16.1 Hz) at 1000 psig. Evaluation of data showed a relation of the nozzle coefficient to the ratio of pulse duration to surge period. For pulse duration longer than the surge period, unstable flow results with a consequential reduction in thrust. Table 5-1 lists the effects of pneumatic surge upon nozzle coefficients.

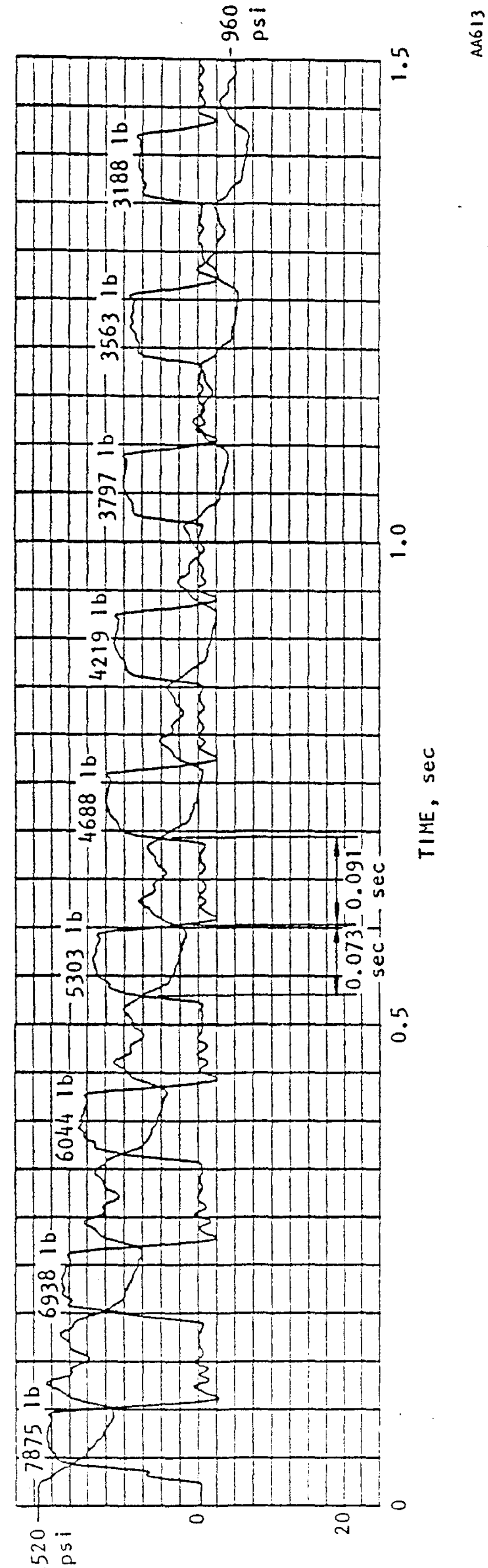

FIGURE 5-3. OVERLAY OF CHAMBER PRESSURE AND OUTPUT FORCE TIME HISTORIES (100 Hz LOW PASS FILTER)

TABLE 5-1. EFFECT OF PNEUMATIC SURGE ON NOZZLE COEFFICIENTS

Pulse Duration, msec	Pneumatic Surge Period, msec	Ratio: Pulse Duration / Surge Period	Nozzle Coefficient, C_{FX}
46	56	0.8	1.50
55	56	1.0	1.37
73	56	1.3	1.36
89	56	1.6	1.18

5.4 THRUST PREDICTION AND TEST

Prediction of thrust is given by

$$F = \beta \frac{\dot{W}}{g} \lambda V_e$$

where

F = Rocket thrust, lbf

$\dot{W}$ = Flow rate, lb/sec

V_e = Jet velocity, ft/sec

λ = Nozzle divergence factor, 0.98

β = Pneumatic surge factor

Except for the pneumatic surge factor, the above parameters are covered in more detail in Section 3. The pneumatic surge factor is the ratio of the empirical nozzle coefficient (when surging is present) and the calculated nozzle coefficient. For the test data for the 9-pulse test shown in Figure 5-3,

$$\beta = \frac{C_{FX(exp)}}{C_{FX(calc)}} = \frac{1.36}{1.47} = 0.925$$

and

$$F = 0.907 \frac{\dot{W}}{g} V_e$$

Calculations and test data are shown in Table 5-2. The average difference between predictions and test data for thrust is 1.8%.

TABLE 5-2. COMPARISON OF CALCULATED THRUST TO THRUST TEST DATA FOR 9-PULSE TEST OF FIGURE 5-3.

Pulse No.	Calculation			Test	Difference, %
	Flow Rate $\dot{W}$, lb/sec	Exit Velocity F_e, ft/sec	Thrust F, lbf	Thrust F, lbf	
1	138.0	2066	8035	7875	2.0
2	124.0	2018	7052	6938	1.6
3	110.0	1964	6089	6094	0.1
4	100.0	1921	5414	5303	2.1
5	91.0	1877	4814	4688	2.7
6	83.6	1837	4328	4219	2.6
7	77.3	1807	3937	3797	3.7
8	71.1	1772	3551	3563	0.4
9	65.5	1736	3205	3188	0.5

SECTION 6

DEMONSTRATION OF MOTION REDUCTION BY PULSES

A demonstration of motion reduction by pulsers was accomplished using an analog computer to model a three-story moment-resisting frame structure (test structure at the University of California, Berkeley). Base motion to this structure employed a random noise generator for the analog computer. The algorithm developed for motion reduction was employed with the DEC PDP 11VO3L microcomputer shown in Figures 2-1 and 2-11. The analog computer used in this study is shown in Figure 6-1. This demonstration was accomplished on-line in real time.

The effect of anti-earthquake pulse control on the 3rd floor velocity and displcement of the UCB test structure is shown in the analog data traces of Figure 6-2. In this figure, the effect on motions of the structure with or without pulse control can be observed in the data records. The counteracting pulses may be triggered at crossings of specified thresholds. Figure 6-3 illustrates the rms velocity levels attained for two different thresholds with respect to "no pulse" control. A more elaborate data display of acceleration, velocity and displacement for the 3rd floor of the analog of the UCB structure with respect to the countering pulse train is presented by the data of Figure 6-4. Demonstrations using the gas pulsers for motion suppression on a structure were not made due to funding limitations.

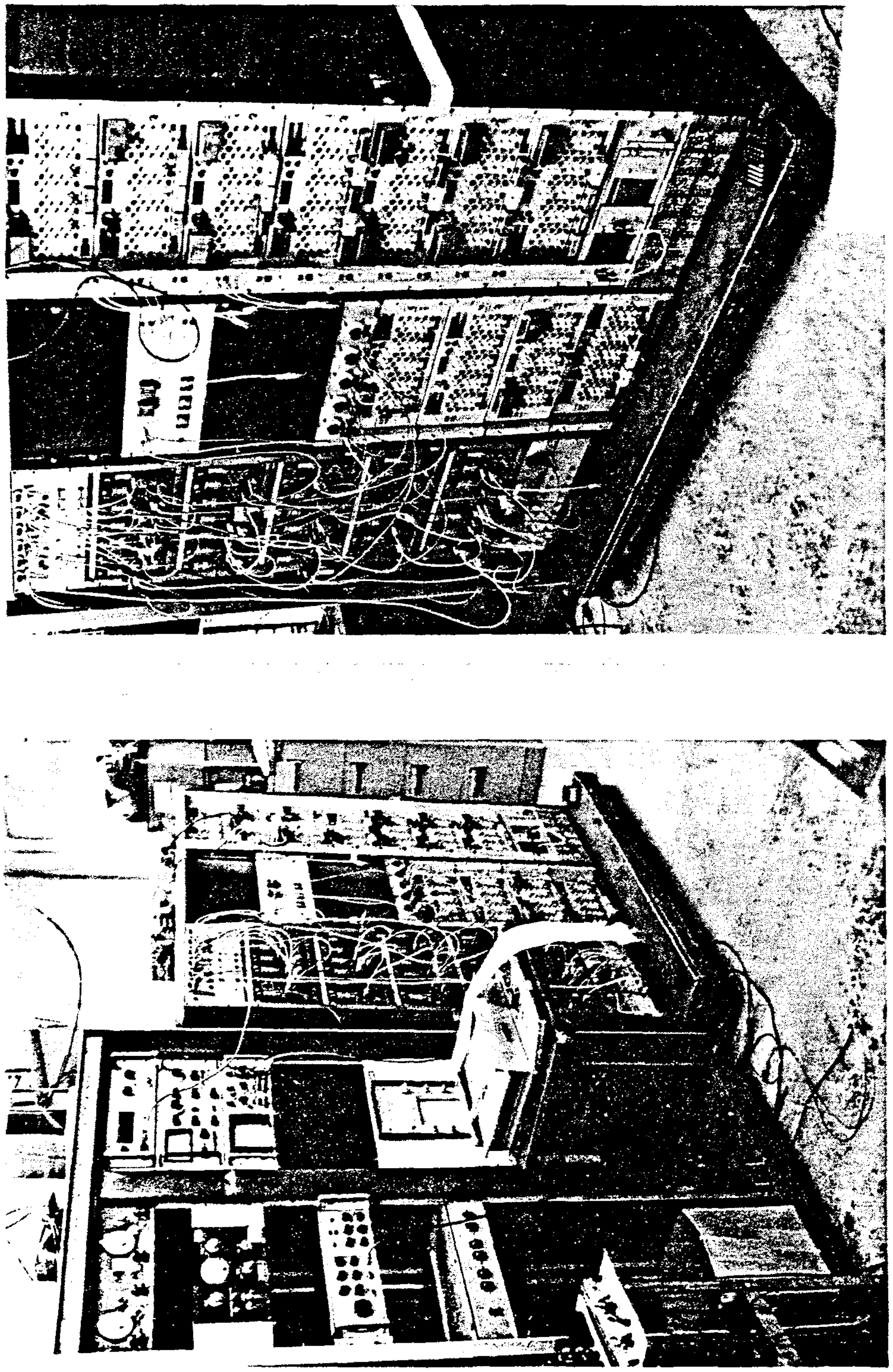

FIGURE 6-1. ANALOG COMPUTER USED FOR REAL TIME SIMULATION OF 3-STORY STRUCTURE FOR INVESTIGATION OF ANTIEARTHQUAKE APPLICATIONS OF PULSE GENERATORS

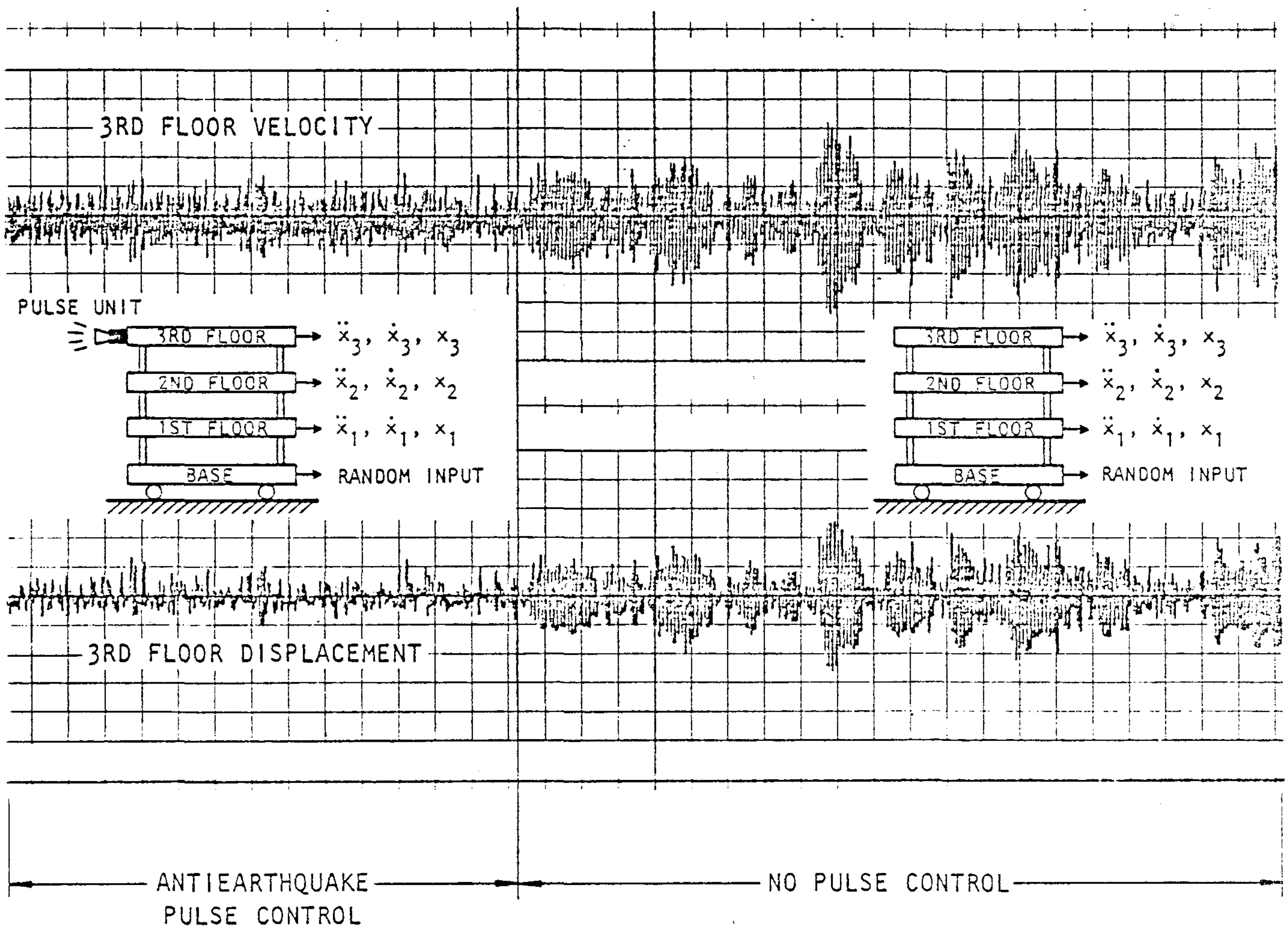

FIGURE 6-2. EFFECT OF ANTIEARTHQUAKE PULSE CONTROL ON THIRD FLOOR VELOCITY AND DISPLACEMENT OF UCB TEST STRUCTURE TO RANDOM BASE MOTION INPUT

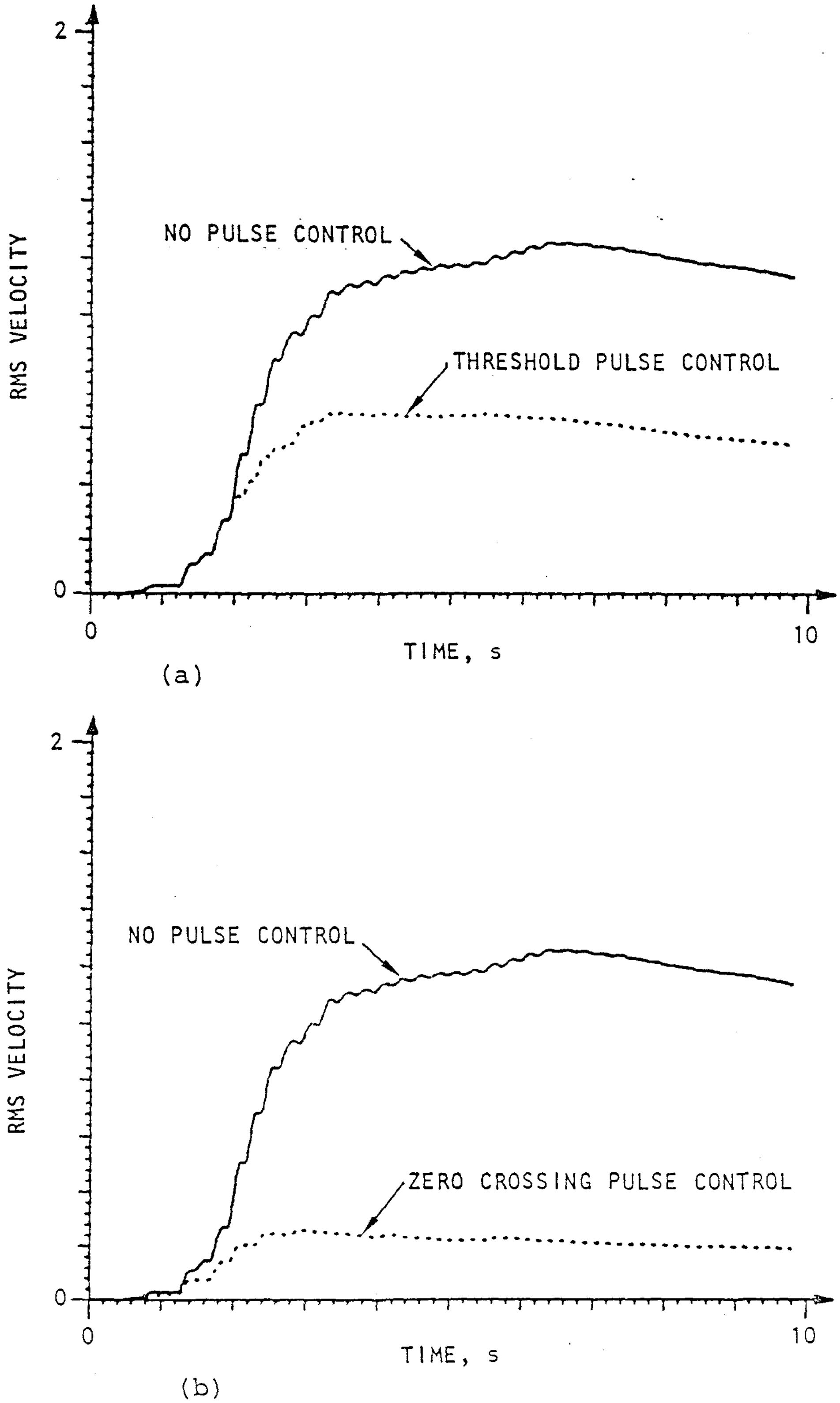

FIGURE 6-3. RMS VELOCITY RESPONSE OF UCB STRUCTURE WITHOUT PULSE CONTROL AND WITH PULSE CONTROL SET FOR SPECIFIED THRESHOLD AND FOR ZERO CROSSING

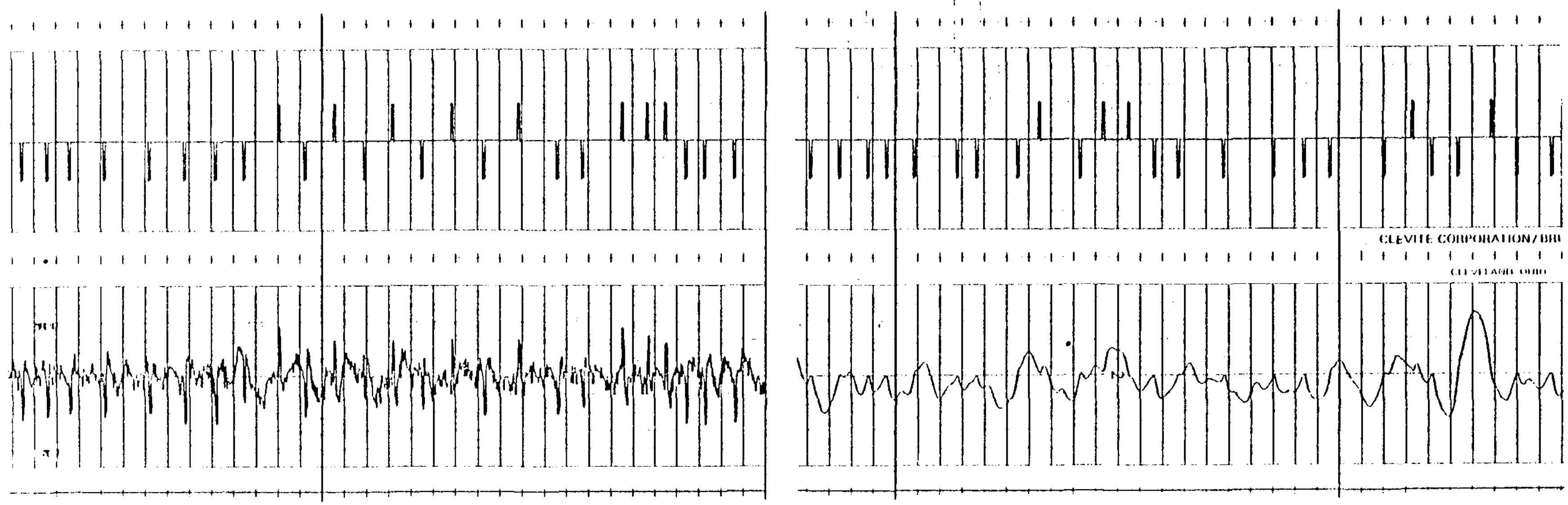

(a) 3rd floor acceleration and pulse control

(b) 3rd floor velocity and pulse control

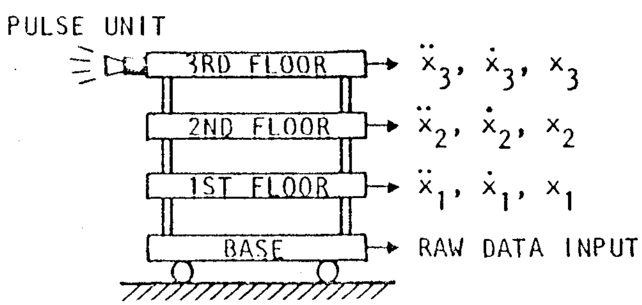

(c) UCB test structure

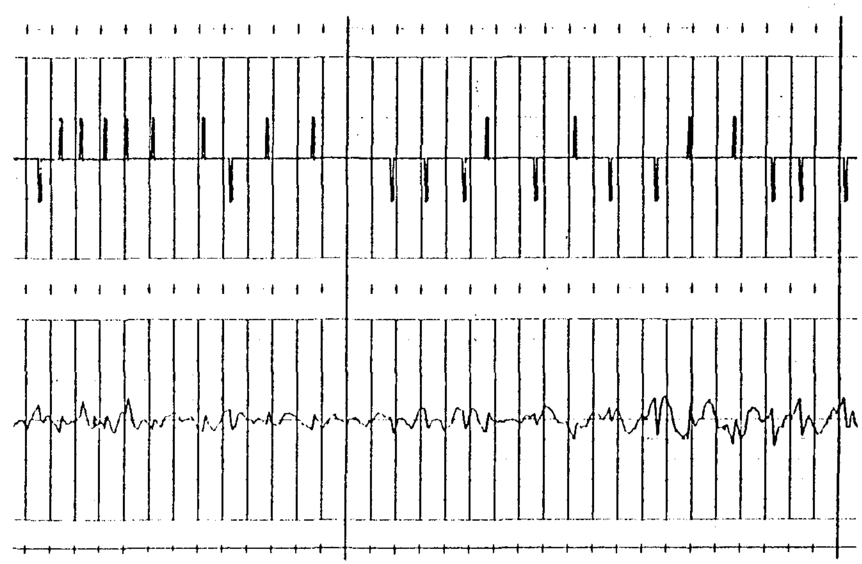

(d) Third Floor displacement and pulse control

FIGURE 6-4. EFFECT OF PULSE CONTROL ON ACCELERATION, VELOCITY, AND DISPLACEMENT OF THIRD FLOOR UCB TEST STRUCTURE

SECTION 7

DEMONSTRATION TESTS ON A BUILDING

7.1 OBJECTIVES

The objectives of the Demonstration Test were to specify a pulse train and compare it to the test pulse train achieved. Originally, a more complete demonstration was planned for the moment resisting steel frame structure at the University of California, Berkeley, project (see Appendix) but development efforts and teething problems were of such magnitude as to restrict any extensive calibration and demonstration tests.

7.2 DEMONSTRATION CONFIGURATION

A demonstration test was conducted upon a one-story office building. This building is a wood frame-stucco structure on a concrete floor slab foundation. Test configuration is illustrated in Figure 7-1, where one gas pulse unit is mounted against the concrete slab and an accelerometer is mounted on the roof. This configuration was necessitated by program limitation. Normal procedure would be to mount both pulse units on the roof.

7.3 SPECIFIED PULSE TRAIN

The specified pulse train is presented in Figure 7-2a and its Fourier transform magnitude in Figure 7-3a. This pulse train was adapted from pulse trains used to study the UCB steel frame structure for a modified El Centro 1940 earthquake (details in Appendix). Figure 7-3a shows the major portions of the force content below 7 Hz.

7.4 TESTS

Tests were performed on the demonstration building. The pulse train measured during this test is plotted in Figure 7-2b

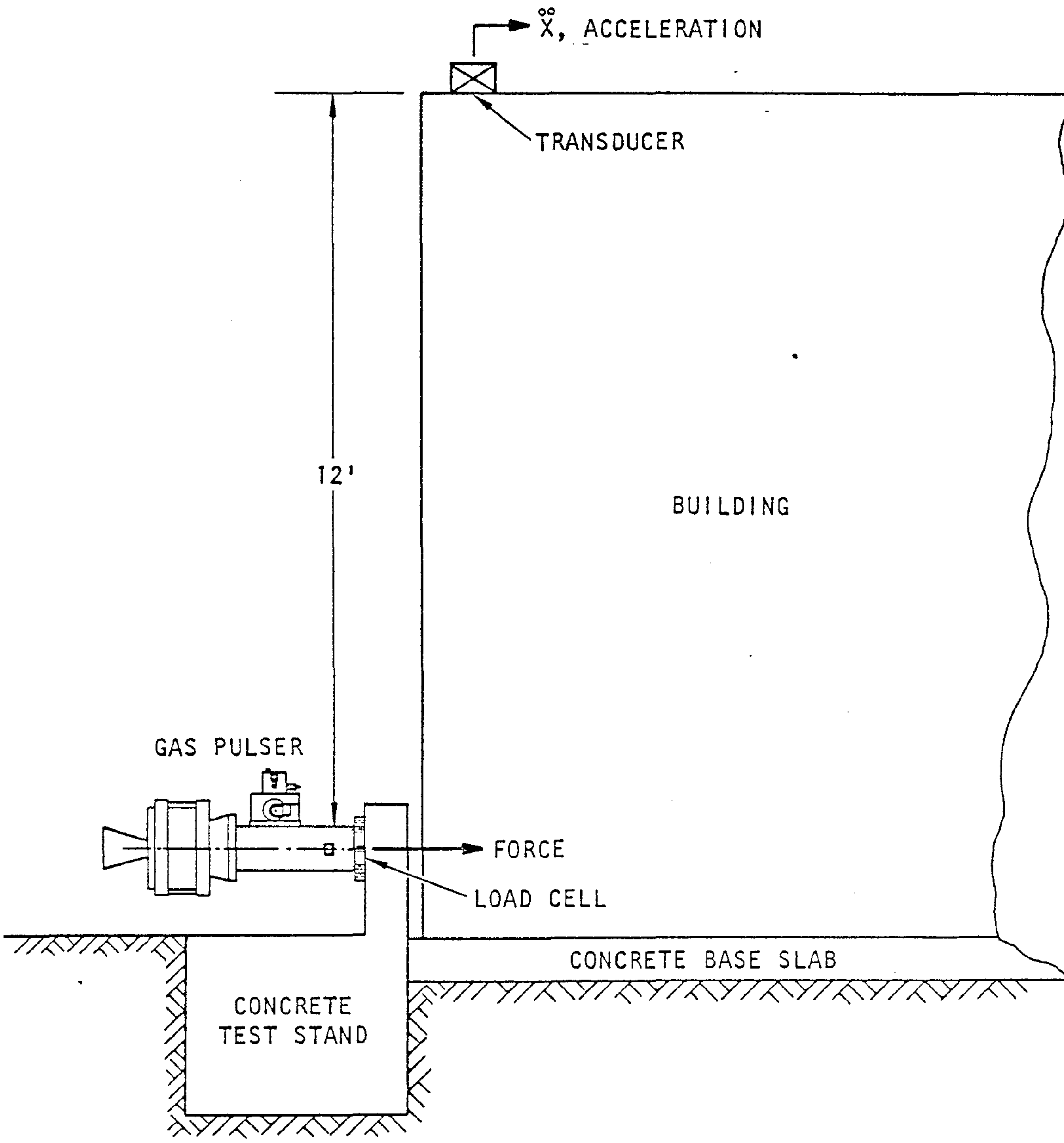

FIGURE 7-1. BUILDING DEMONSTRATION TEST, GAS PULSER INPUT IS INTO CONCRETE BUILDING SLAB; BUILDING IS WOOD-FRAME AND STUCCO CONSTRUCTION

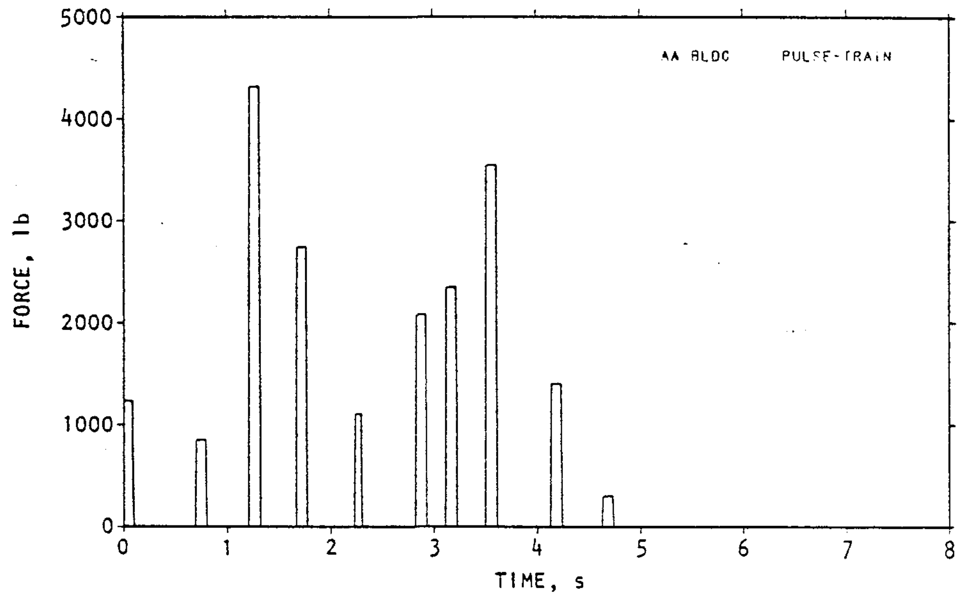

(a) Specified pulse train

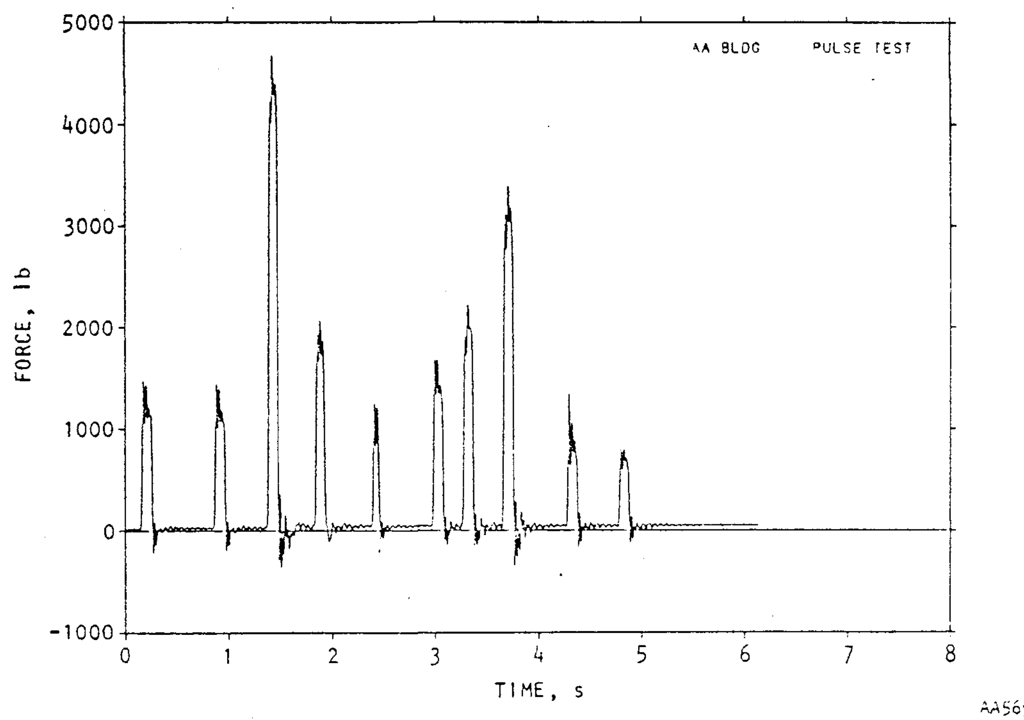

(b) Pulse train obtained from test

FIGURE 7-2. SPECIFIED INPUT PULSE TRAIN AND PULSE TRAIN OBTAINED FROM TEST ON DEMONSTRATION BUILDING

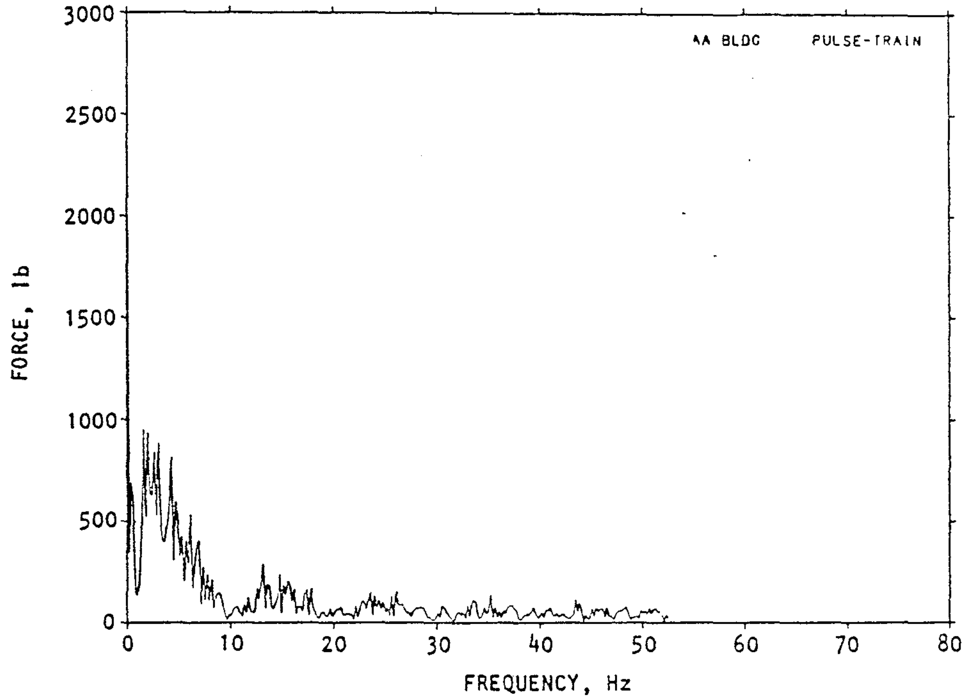

(a) Specified input pulse train

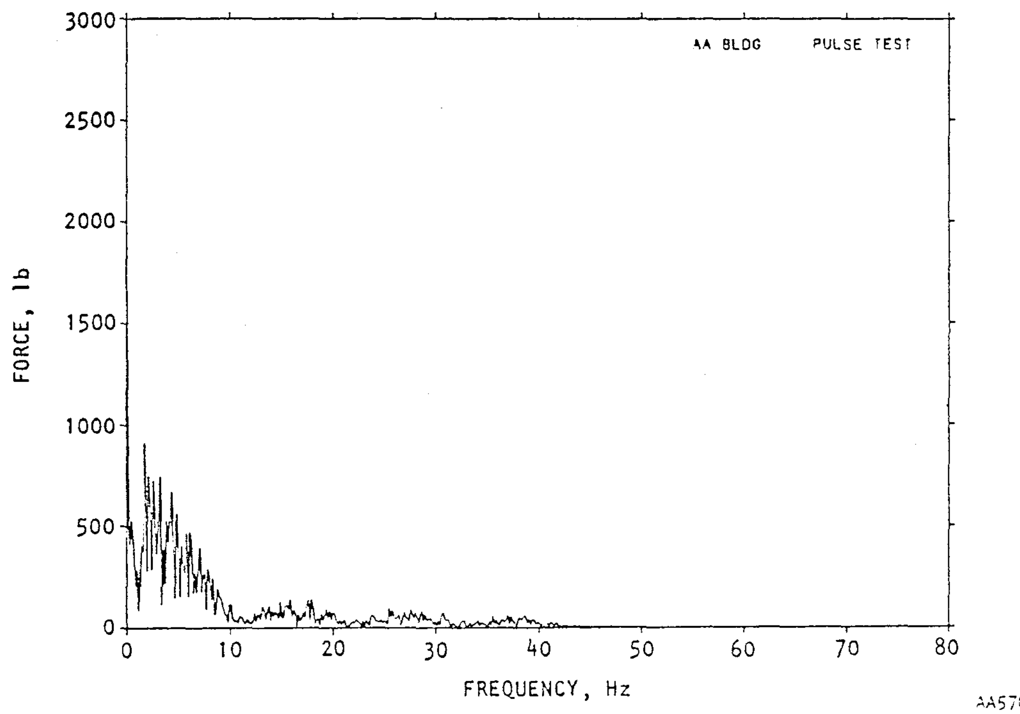

(b) Pulse train obtained from test

FIGURE 7-3. FOURIER MAGNITUDES OF SPECIFIED AND ACTUAL PULSE TRAINS and its Fourier transform magnitude given in Figure 7-3b. Motions of the test building are given in Figure 7-4a for acceleration, in Figure 7-4b for velocity, and in Figure 7-4c for displacement.

7.5 SYSTEM PERFORMANCE

Examination of the pulse trains in Figure 7-3 show quite accurate timing of the test pulse train with respect to the specified pulses. However, deviations occurred with respect to test thrust amplitudes achieved. These variations are summarized in Table 7-1 where the overall impulse was 12 percent below specified requirements.

Average variation in thrust is 20 percent of specified excluding the anomaly of the last pulse. Previous analytic studies have noted that nominal force variations have small effects upon induced structural motions.

Investigation of the test pulses was made and plots of the positions of the metering nozzle are shown in Figure 7-5. Prior to test, an unpressurized pulse test was performed to verify correct command signal coding on the computer. This trace is compared to the nozzle position trace under transient pressures of the test. Under pressure, the test position corresponded to the thrust delivered. Table 7-2 lists the positions and areas of the nozzle. Additional information is provided in Figure 7-6, covering chamber pressure-time history for the test. This figure discloses pneumatic surges described in Section 5 on calibration. It has been concluded that these pressure surges interact with a balancing piston (Fig. 3-1a) in the plenum chamber and affect the servo position control, particularly for the small to moderate throat areas.

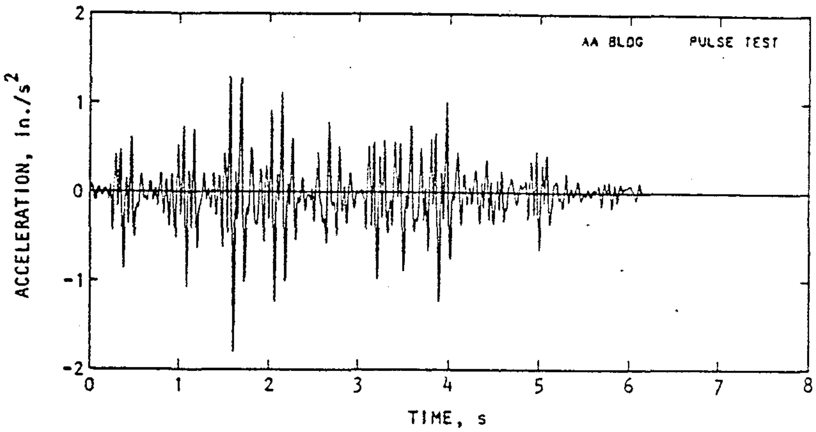

(a) Measured acceleration time history

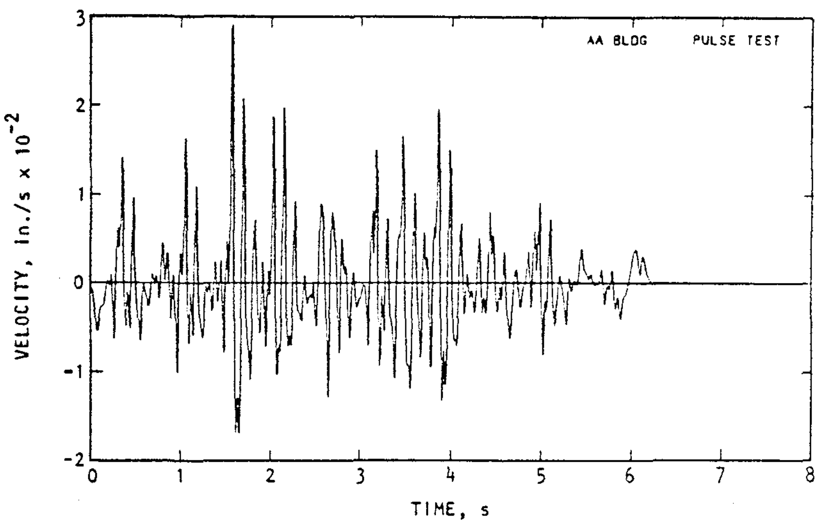

(b) Velocity-time history (integrated)

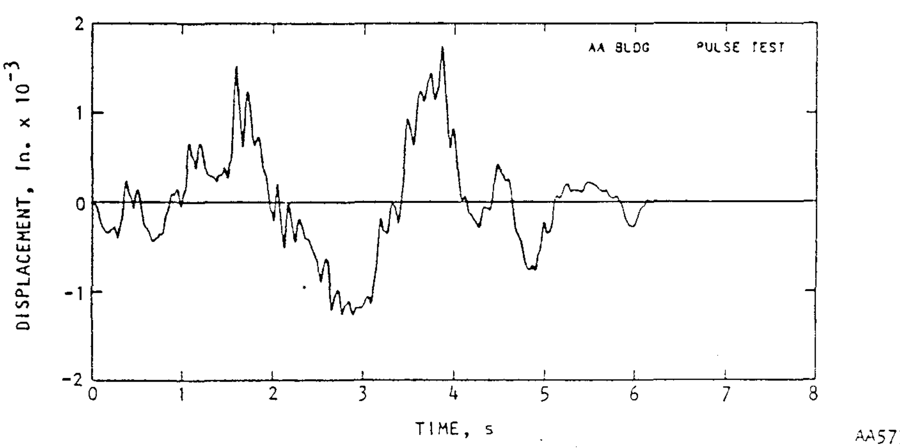

(c) Displacement-time history (integrated)

FIGURE 7-4. MOTION-TIME HISTORIES FROM ROOF OF DEMONSTRATION BUILDING INDUCED BY PULSE TRAIN (Fig. 7-2)

TABLE 7-1. COMPARISON OF PROGRAMMED AND TEST THRUST AND IMPULSE

Pulse No.	Pulse Duration (sec)	Force			Impulse		
		Program (lbf)	Test (lbf)	Error %	Program (lb-sec)	Test (lb-sec)	Error %
1	0.0948	1230	1250	1.6	116.6	118.5	1.6
2	0.0948	846	1100	30	80.2	104.3	30
3	0.0948	4322	4250	-1.7	409.7	402.9	-1.7
4	0.076	2742	1850	-33	208.4	140.6	-33
5	0.057	1105	1000	-9.5	63.0	57.0	-9.5
6	0.096	2078	1500	-28	199.5	144.0	-28
7	0.0948	2348	1900	-19	222.6	180.1	-19
8	0.096	3554	3100	-13	341.6	297.6	-13
9	0.095	1400	900	-36	133.0	85.5	-36
10	0.094	302	650	115	28.4	61.6	115
Total	0.893				1803	1592	-12

TABLE 7-2. METERING NOZZLE, POSITION AND THRUST AREA, FOR NO GAS PRESSURE AND FOR OPERATING PRESSURE

Pulse No.	Dry Run No Gas Pressure		Demonstration Test Operating Pressure		Comparison	
	Nozzle Position (in.)	Throat Area (in.^{2})	Nozzle Position (in.)	Throat Area (in.^{2})	Nozzle Position % Error	Throat Area % Error
1	0.16	0.63	0.13	0.51	-19	-19
2	0.08	0.35	0.12	0.47	50	34
3	0.65	2.12	0.63	2.09	-3	-1.4
4	0.33	1.22	0.25	0.95	-24	-22
5	0.12	0.48	0.13	0.51	8	6.3
6	0.28	1.05	0.21	0.82	-25	-22
7	0.37	1.33	0.32	1.20	-13.5	-9.8
8	0.58	1.95	0.57	1.80	-1.7	-7.7
9	0.18	0.9	0.13	0.51	-28	-43
10	0.038	0.18	0.11	0.45	189	309

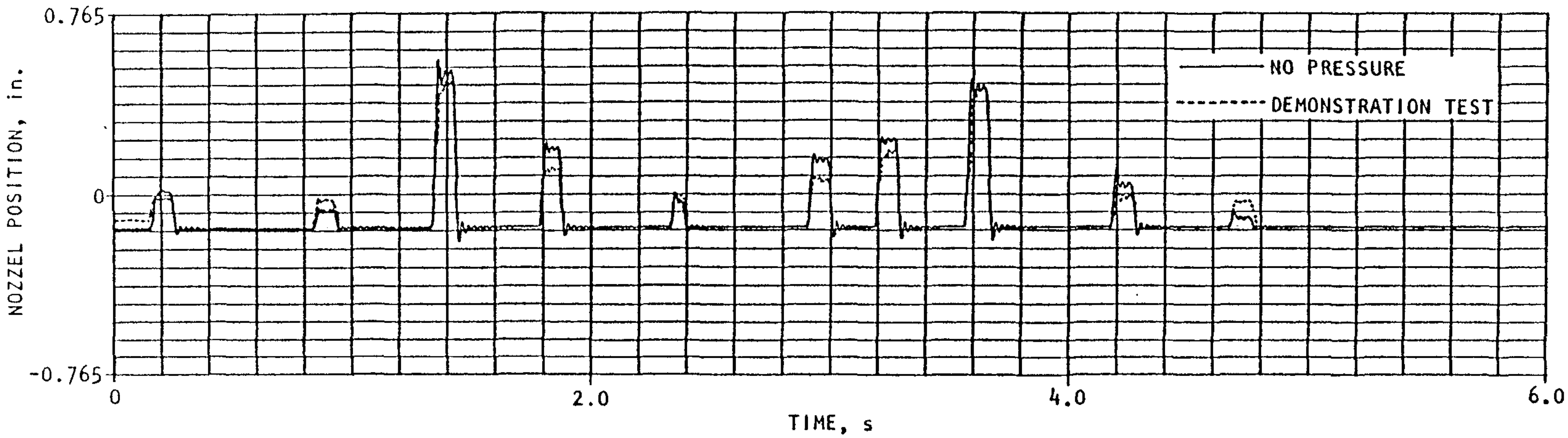

FIGURE 7-8. NOZZLE POSITION DURING DEMONSTRATION TEST: NO GAS PRESSURE (SOLID LINE) AND OPERATING PRESSURE (DOTTED LINE)

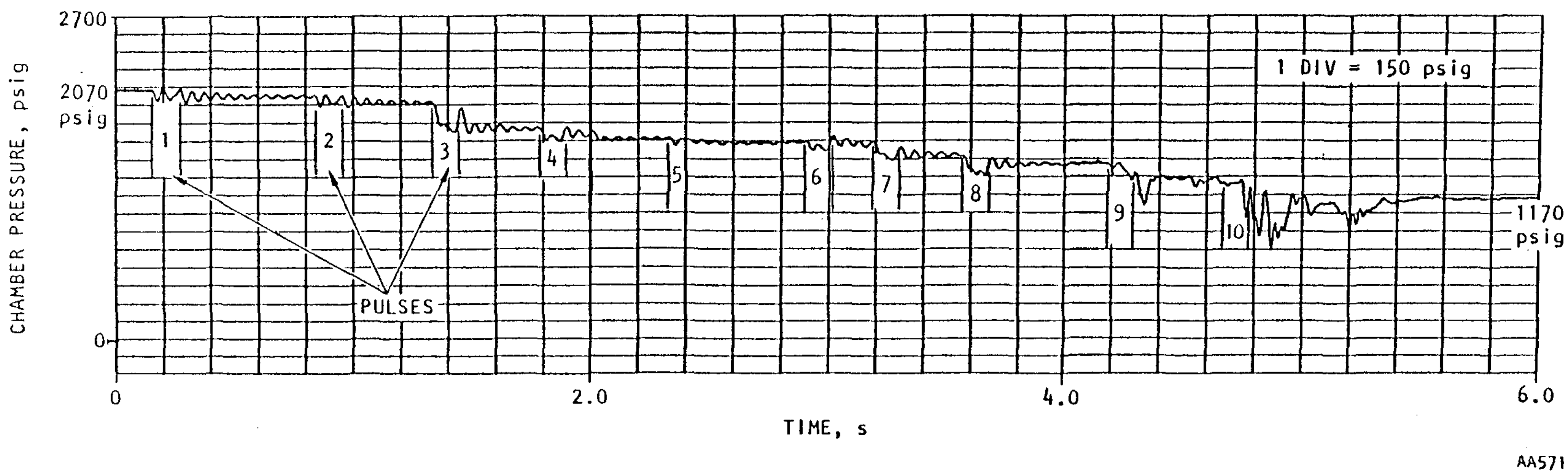

FIGURE 7-5. CHAMBER PRESSURE DURING DEMONSTRATION TEST

SECTION 8

UTILIZATION

8.1 TECHNICAL PAPERS

In fulfillment of the utilization plan covered by this grant, five technical papers which resulted from this research have been presented at symposiums and conferences. These papers received peer review and have been published. A sixth paper has been submitted for publication. Reprints of the following listed papers are provided in the Appendix of this report.

"Earthquake Environment Simulation by Pulse Generation," *Proc. 7th World Conf. on Earthquake Engineering* , Geoscience Aspects, Pt. II, pp 73-80, Istanbul, Turkey, Sep 1980.

"An Optimization Procedure for Pulse-Simulated Dynamic Response," ASCE Nat'l. Conv., *Jnl. Struct. Div. ASCE*, 107:ST9, Sep 1981, pp 1745-1761.

"Development and Use of Force Pulse Train Generators," ASCE/EMD Specialty Conference, Proceedings on Dynamic Respone of Structures, Experimentation, Observation, Prediction and Control, G. Hart, Ed., Atlanta, Jan 1981.

"Anti-Earthquake Application of Pulse Generators," ASCE/EMD Specialty Conference, Proceedings on Dynamic Response of Structures, Experimentation, Observation, Prediction and Control, G. Hart, ed., Atlanta, Jan 1981.

"Pulse Excitation Techniques," Society of Automotive Engineers, Aerospace Congress & Exposition, Anaheim, CA, Oct 25-28, 1982, Pub. "Advances in Dynamic Analysis and Testing," SP-529 and the 1982 Transactions of the SAE, Sep 1983.

"Development of a Pulse Rocket for Earthquake Excitation of Structures," submitted for publication.

8.2 DISSEMINATION

Dissemination of this report has been accomplished with copies sent to the following academic, professional organizations, government agencies, and private corporatons.

Academic Institutions:

- California Institute of Technology
- California State University, Los Angeles
- Columbia University
- Georgia Institute of Technology
- Kansas State University
- Massachusetts Institute of Technology
- Princeton University
- Rice University
- Stanford University
- University of California, Berkeley
- University of California, Irvine
- University of California, Lawrence Livermore National Laboratory
- University of California, Los Angeles
- University of Illinois
- University of Michigan
- University of Minnesota
- University of Missouri, Rolla
- University of Nevada, Reno
- University of Southern California
- University of Texas

Professional Societies:

- American Technology Council, Affiliated with Structural Engineers Association of California
- Earthquake Engineering Research Institute

Federal Government Organizations:

- Dept. of the Army
  - Corps of Engineers, Huntsville Div.
  - Construction Engineering Research Laboratory
  - Office of the Chief of Engineers
  - Waterways Experiment Station
  - Harry Diamond Laboratories

- Dept. of the Navy
  - Naval Civil Engineering Laboratory (now CEL)
  - Naval Facilities Engineering Command
  - Naval Research Laboratory
  - Naval Ship Systems Command
- Nuclear Regulatory Commission
- Tennessee Valley Authority
- Veterans Administration
- Dept. of Energy, Division of Reactor Design and Development
- Dept. of Transportation, FHWA
- NASA, Langley
- Defense Nuclear Agency
- Dept. of Defense Explosives Safety Board
- Federal Emergency Management Agency
- National Technical Information Service
- Dept. of the Air Force, Weapons Laboratory

Industrial Organizations

- Portland Cement Association
- Electric Power Research Institute
- Southwest Research Institute

State Government Organizations:

- California Dept. of Transportation
- California State Office of Architecture and Construction in the Department of General Services
- California Legislature Joint Committee on Seismic Safety
- California State Building Standards Commission

Private Corporations

- The Aerospace Corporation
- Rockwell International
- Hughes, Fullerton, CA
- Computex, Inc.

SECTION 9

RESULTS

The gas pulse system performed reliably and safely. Start-up, shut-down and repeat tests may be performed quickly and efficiently. Repeat tests depend upon charging time of the high pressure supply tanks. In general, this recharging time amounted to one hour. Changing pulse train commands involves entering only time and amplitudes on the keyboard of the control microcomputer. The system is readily transported to test sites, and set-up time is expected to be less than a day for two technicians.

Output force at 2640 psig chamber pressure is 9,600 lbf and minimum pulse width is 26 msec. Delay time from input command signal to the 50 percent rise time of the pulse is 13 msec. Each pulse unit has a gas storage capacity of 10.2 ft^3 for 134 lbs of gas at 2640 psig. Gas storage units may be connected to one pulser unit if desired for extended tests. Signal monitors provide time-history records of input command signals, metering nozzle position, chamber pressure and output force.

Design of the gas pulse generator employed conventional one-dimensional gas flow equations. Comparisons of calculated to test results were satisfactory. Programming of pulse trains is performed at this time from the one-dimensional flow equation. With more test runs, calibration curves will be used.

In the early design stages, there was concern about thrust efficiency due to the potential rise of compression shocks at the tip of the nozzle in the supersonic diffuser and the effects of water vapor in the storage gas. In addition, the increase in the ratio of specific heats with pressure and at low temperature, was expected to reduce thrust. None of the foregoing effects appears to be significant, at least from the measurements and tests made to date.

Rapid opening of the metering nozzle induced pressure oscillation in the plenum chamber and supply hose systems. Pulse duration at or longer than the pneumatic surge period, reduced nozzle efficiencies by as much as 21 percent. At small to moderate nozzle openings, these pressure surges acted upon a balancing piston in the plenum chamber. These surges limited the ability of the servo control to compensate, with the result that nozzle openings can fall short of commanded positions up to 25 percent for moderate openings, and to exceed commanded position for small openings by up to 200 percent.

An algorithm employing adaptive random search was successfully developed to generate pulse trains which will closely approximate structural motions induced by earthquakes. This algorithm permits placement of pulse excitation units in multiple locations of test convenience. Computer studies of several structures yielded information on the performance required for pulse units with respect to thrust, pulse widths, and impulse. A counter-earthquake algorithm was also developed to reduce structural motions induced by earthquakes. Several computer studies were made, and demonstration tests using an analog computer were successfully accomplished. This algorithm is currently limited to fixed amplitude pulses.

Demonstration tests on a single-story structure were successful. One pulse unit was fixed to the building concrete base slab and the induced motion was recorded from a roof accelerometer. Program restraints and building safety permitted the use of only one pulse unit, and this unit was attached to the concrete floor slab of the building. Normally both pulse units would be placed on the roof and expected building motions would be at least 3 orders of magnitude greater than was obtained in the demonstration test. Total test input impulse was 12 percent below specified due to the pneumatic surges discussed above.

The research work produced as a result of this grant has been utilized through the publication of five technical papers. A sixth paper has been submitted for publication. Distribution of this report has been made in accordance with the utilization plan.

SECTION 10

CONCLUSIONS

Two gas pulse generating systems were produced and are in a state of operational readiness. These systems are suited for earthquake testing of small buildings, large industrial equipment and frame structures such as microwave and power transmission towers.

An efficient pulse train algorithm was developed for use in programming the gas pulse system for motion simulation. A simple anti-earthquake algorithm was also developed. This algorithm when used in conjunction with various types of pulse units shows promise in the reduction of structural motions at the damage or life threatening thresholds. In its present form, the anti-earthquake algorithm is limited to preselected fixed amplitude pulses. Further development work is required to improve the algorithm.

Additional calibration tests at low to medium nozzle throat settings are required. These data will permit improvements and ease in programming pulse trains with respect to the gas supply. Surge suppressors need to be added to the plenum chambers to improve nozzle efficiencies and to reduce the interaction of pneumatic surges with the plenum chamber balancing piston.

REFERENCES

Bekey, G.A. and Ung, M.T. "A Comparative Evaluation of Two Global Search Algorithms," *IEEE Trans. Systems, Man, and Cybernet*, SMC-4:1, 1974, pp 112-116.

Binder, R.C. *Advanced Fluid Dynamics and Fluid Machinery*. New York: Prentice Hall, 1951.

Corvin, P. and Steinhilber, H. "Seismic Tests at the HDR Facility Using Explosives and Solid Propellant Rockets," *Trans. 6th Int. Conf. on Struct. Mech. and Reactor Tech.*, paper K14-3, Paris, 1981.

Ellenwood, F.O.; Kulik, N.; Gray, N.R. *Specific Heats of Certain Gases Over Wide Ranges of Pressures and Temperatures*, Cornell Univ. Bull. 30, Oct 1947.

Gurin, L.S. and Rastrigin, L.A. "Convergence of the Random Search Method in the Presence of Noise," *Automation and Remote Control*, 26:9, 1965, pp 1505-1511.

Housner, G.W. "Characteristics of Strong-Motion Earthquakes," *Bull. Seismol. Soc. Amer.*, 37:1, Jan 1947, pp 19-27.

Hudson, D.E. "Some Problems in the Application of Spectrum Techniques to Strong-Motion Earthquake Analysis," *Bull. Seismol. Soc. Amer.*, 52:2, Apr 1962, pp 417-430.

Jeans, J. *Kinetic Theory of Gases*. New York: Dover.

Masri, S.F.; Bekey, G.A.; and Safford, F.B. "Optimum Response Simulation of Multidegree Systems by Pulse Excitation," *Jnl. Dyn. Systems, Measurement and Control, ASME*, 97:1, Mar 1975.

----. "An Adaptive Random Search Method for Identification of Large-Scale Nonlinear Systems," 4th Symp. for Identification and System Parameter Estimation, Int. Federation of Automatic Control, Tbilisi, USSR, Sep 1976.

----. "A Global Optimization Algorithm Using Adaptive Random Search," *Applied Mathematics and Computation*, 7, 1980, pp 353-375.

Masri, S.F. and Safford, F.B. "Dynamic Environment Simulation by Pulse Techniques," *Proc. ASCE Eng. Mech. Div.*, 101:EMI, Feb 1976, pp 151, 170.

Rastrigin, L.A. "The Convergence of the Random Search Method in the Extremal Control of a Many Parameter System," *Automation and Remote Control*, 24:11, 1963, pp 1337-1342.

Safford, F.B. and Masri, S.F. "Analytical and Experimental Studies of a Mechanical Pulse Generator," *Jnl. Eng. for Industry Trans., ASME*, Series B., 96:2, May 1974.

Sato, Y. and Sawabe, Y. "Vibration Tests on Reinforced Concrete Towers for Microwave Telecommunication," *Proc. 7th World Conf. on Earthquake Eng.*, Istanbul, Turkey, Sep 1980.

Schumer, M.A. and Steiglitz, K. "Adaptive Step Size Random Search," *IEEE Trans. Automatic Control*, AC-13:3, 1968, pp 270-276.

Scruton, C. and Harding, D.A. *Measurement of Structural Damping of a Reinforced Concrete Chimney Stack at Ferrybridge "B" Power Station*, NPL/AERO/323, Wallingsford, England, 1957.

Seifert, H.S. and Brown, K. *Ballistic Missile and Space Vehicle Systems*. New York: John Wiley and Sons, 1961.

Sutton, G.P. *Rocket Propulsion Elements*. New York: John Wiley and Sons, 1956.

Zucrow, M.J. *Aircraft and Missile Propulsion*, 2 Vols. New York: John Wiley and Sons, 1964.

APPENDIX

PAPERS PUBLISHED AS A DIRECT RESULT OF THIS RESEARCH GRANT

- Optimization Procedure for Pulse-Simulated Response
- Earthquake Environment Simulation by Pulse Generators
- Development and Use of Force Pulse Train Generators
- Anti-earthquake Applications of Pulse Generators
- Pulse Excitation Techniques

Pages A-2 through A-21 have been removed.

Due to copyright restrictions, the paper, "Optimization Procedure for Pulse-Simulated Response," by Sami F. Masri and Frederick B. Safford, has been omitted.

Journal of the Structural Division, ASCE, Vol. 107, No. ST9, Proc. Paper 16521, September 1981, pp. 1743-1761.

NSF Grant CEE-7715010

PROCEEDINGS OF THE SEVENTH WORLD CONFERENCE ON EARTHQUAKE ENGINEERING

September 8-13, 1980
Istanbul, Turkey

7th WCEE
ISTANBUL 1980

VOLUME 2

GEOSCIENCE ASPECTS, PART II

STRONG MOTION INSTRUMENTATION AND DATA COLLECTION

INFLUENCE OF LOCAL CONDITIONS ON GROUND MOTION

SIMULATED AND ARTIFICIALLY GENERATED GROUND MOTIONS

SPECTRAL ANALYSIS AND INTERPRETATION OF GROUND MOTION

EARTHQUAKE ENVIRONMENT SIMULATION BY PULSE GENERATORS

by

S.F. Masri[I] and F.B. Safford[II]

SUMMARY

Simple mechanical pulse-generating devices of fairly recent development are capable of producing short duration forces of large magnitudes over a wide frequency range that can be controlled to satisfy multimode system response. This paper is concerned with the simulation of the motion of typical structural systems subjected to earthquake environments by using suitable pulse trains applied at various locations on the structure. The pulses are selected in such a way that the resulting vibration of the structure matches closely the response that would be produced by the earthquake excitation, as determined by an appropriate error criterion. A suitable optimization algorithm is presented and applied to two realistic example structural systems. It is shown that pulse-excitation techniques offer a viable alternative to conventional testing approaches.

INTRODUCTION

The capability for simulating the response of structures to transient dynamic loadings, such as earthquakes and blast loads, is useful for testing structural adequacy, for improving mathematical models, and for investigating the response of equipment in a structure [1]. In addition to various types of vibration generators that are appropriate for certain classes of structural systems, large testing facilities (which have limited availability) and ground-explosion approaches (which are economically prohibitive) can be used for dynamic tests on equipment and structural systems [2,3].

Housner [4] demonstrated the feasibility of using a sequence of discrete pulses with random amplitude to represent the effects of earthquakes on dynamic systems. Scruton and Harding [5] used a crude explosive charge to excite a tall chimney in order to determine its damping characteristics.

A simple mechanical pulse-generating device of fairly recent development [6] is capable of producing short duration forces of large magnitudes over a wide frequency range that can be controlled to satisfy multimode system response. Such force pulse generators have been successfully used to simulate the in-place motions of up to 500 Hz in equipment weighing up to 200,000 lb and in also measuring system impedance functions [7,8].

[I] Professor, Civil Engineering Department, University of Southern California, Los Angeles, CA 90007, U.S.A.

[II] Principal Engineer, Agbabian Associates, El Segundo, CA 90245, U.S.A.

This paper is concerned with the simulation of the motion of typical structural systems subjected to earthquake environments, by using suitable pulse trains applied at various locations on the structure. Since a discrete number of pulses superficially presents an appearance quite different from a continuous earthquake ground motion, it becomes necessary to select the pulses on the structure in such a way that the resulting vibration matches as closely as possible the response produced by the earthquake ground motion as determined by an appropriate error criterion.

OPTIMIZATION TECHNIQUE

Statement of the Problem

Note that the method of Fig. 1 requires that the criterion response to the continuous input be known, which would generally not be true in practice. To accomplish this objective, the approach proposed here assumes that: (1) a mathematical model of the system under study is known and (2) the inputs of interest (e.g., earthquake or nuclear blast) are given. Under these conditions, the "criterion response" can be calculated and subsequently used to obtain the pulse trains for the simulated test.

The basic criterion used in this study is the integral squared error between the reference and simulated response, evaluated at a sufficient number of locations within the multiple degree-of-freedom system to characterize it as completely as possible. Given the error criterion, then the pulse occurrence times, pulse widths, and the pulse amplitudes are selected by a systematic search algorithm such that the error is minimized.

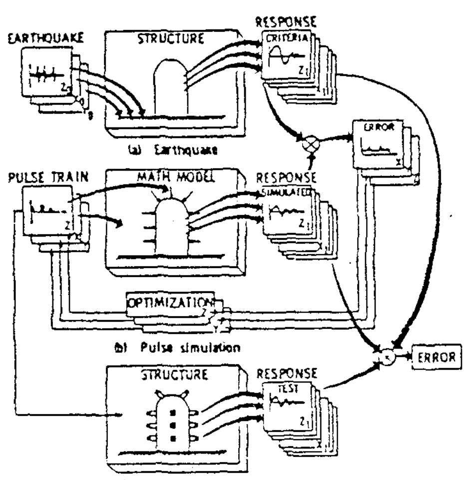

FIGURE 1. PROCEDURE FOR PULSE SIMULATION/ TEST OF A STRUCTURE TO SIMULATE EARTHQUAKE RESPONSE

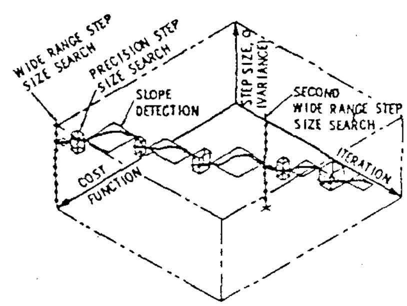

FIGURE 2. ADAPTIVE RANDOM SEARCH, WIDE RANGE AND PRECISION STEP SIZE

Formulation

Consider an n-degree-of-freedom system governed by m nonlinear first-order differential equations of the form

$$\dot{z}_i = Z\,(z_1, z_2, \ldots, z_m, t), \qquad i = 1,2,\ldots,m \tag{1}$$

where $m = 2n$, and the system is subjected to an excitation force vector $\underset{\sim}{G}(t)$. Let the response of the system to this force (the criterion response) at location i in the structure be denoted $\hat{x}_i(t)$, $i = 1,2,\ldots,k$, where k is the number of locations whose motion is to be monitored.

In order to compare the response of the system model, $\underset{\sim}{x}(t)$, to the criterion response $\hat{\underset{\sim}{x}}(t)$, we select the displacements and velocities at k locations. We now define a nonnegative error criterion

$$J = \int_{t_o}^{t_f} \sum_{i=1}^{k} \left\{ C_{1_i}\left[x_i(t) - \hat{x}_i(t)\right]^2 + C_{2_i}\left[\dot{x}_i(t) - \dot{\hat{x}}_i(t)\right]^2 \right\} dt \tag{2}$$

which measures the "goodness of fit" of the system response variables $\underset{\sim}{x}(t)$ to the specified response $\hat{\underset{\sim}{x}}(t)$. The k constants C_{1_i} and C_{2_i} are weighting factors that can be adjusted to emphasize or de-emphasize the significance of the fit at different points in a structure, since a good fit at some points may be much more important for simulating damage and malfunctions.

The specified or criterion responses $\hat{x}_i(t)$ are those recorded in the structure (as during an earthquake) or obtained from applying known excitation forces to the model of Eq. 1. Since our objective is to find a pulse excitation $\underset{\sim}{F}(t)$ that produces a response $\underset{\sim}{x}(t)$ as close as possible to $\hat{\underset{\sim}{x}}(t)$, we restrict each component of $\underset{\sim}{F}(t)$ to the form

$$F_i(t) = \sum_{j=1}^{N} A_j\left[u(t - t_j) - u(t - t_j - W_j)\right] \tag{3}$$

where

A_j = Amplitude of the jth pulse

W_j = Width of the jth pulse

t_j = Initiation time of the jth pulse

and

$u(t)$ = Unit step function

The problem may now be stated precisely as follows:

Given a system that is described by Eq. 1 and a desired time history vector $\hat{\underset{\sim}{x}}(t)$, find the set of numbers $\{t_j, A_j, W_j\}$, $j = 1,2,\ldots N$, which describes each component of the excitation vector such that the error criterion of Eq. 2 is minimized.

Algorithm

The optimization problem consists of selecting the triplet of numbers (t_j, A_j, W_j), which characterizes each input pulse at various system excitation points. In principle, a large number of optimization procedures for such problems are available [9]. However, in view of the large number of parameters possible in this system, the set of feasible optimization procedures is quite limited. Consequently, an adaptive random search algorithm [10] was selected to determine the optimum parameter values for the pulse trains.

The algorithm for the adaptive random search consists of alternating sequences of a global random search with a fixed value for the step-size variance σ^2 followed by searches for the locally optimal σ^2. Fig. 2 illustrates the adaptive algorithm whereby a very wide-range search selects the best standard deviation of step size σ for the coarseness of the increments used, followed by a sequential precision search of finer increments. As the rate of convergence decreases, a new precision search is made, but is directed toward a smaller step size. At selected iteration intervals, the wide-range search is reintroduced to prevent convergence to local minima. The complete algorithm is described in [10].

APPLICATIONS

The optimization procedure was then applied to two test structures: (1) a typical 25-story building model and (2) a 3-story building frame model that has been extensively tested at the University of California at Berkeley (UCB) shaking table facilities. In each case, the mathematical models of the structures were subjected to a ground motion corresponding to El Centro earthquake record to generate the criteria response. Then for each structure, an appropriate selection of pulse trains was determined in order to minimize the mean-square deviation between the criterion response and the simulated response. The pulse characteristics are, at the same time, constrained to realizable physical values for the test.

Model of 25-Story Building

The system shown in Fig. 3 is a 25-story office building designed in accordance with applicable building code provisions for recommended lateral force requirements [11]. Modal analysis of this building, treated as a linear elastic structure, yields the mode shapes and natural frequencies shown in Fig. 4.

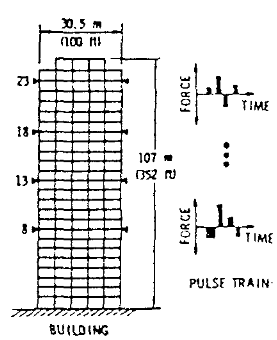

FIGURE 3. GAS PULSERS ARRAYED FOR EARTHQUAKE SIMULATION TEST OF A MULTISTORY BUILDING

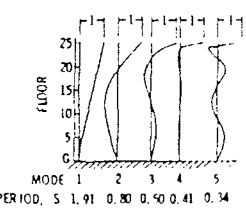

FIGURE 4. BUILDING NATURAL MODES OF VIBRATION

To illustrate the simulation procedure outlined above, it was decided to use four pulse-excitation locations at modal antinodes (Floors 8, 13, 18, and 23) and to attempt to match the response of two locations (Floors 13 and 23). Due to the linearity of the system, its transient response to pulse trains could be determined by using the convolution integral approach. The necessary impulse response functions were determined and are illustrated in Fig. 5 where $h_i^{(j)}(t)$ denotes the response of location i due to a unit impulse applied at location j.

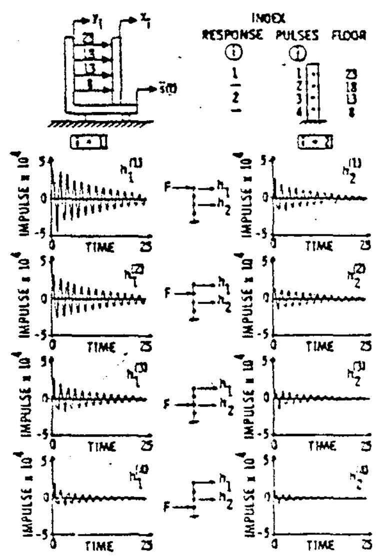

FIGURE 5. IMPULSIVE DISPLACEMENT RESPONSE TO 25 DOF SYSTEM

The El Centro 1940 earthquake ground motion was used as specified base input, and it is resulted in the criteria response shown in Figs. 6a and 6b as solid lines. The earthquake criteria response was simulated by four suitable pulse trains using the optimization algorithim outlined above. The simulated response is superposed on top of the criteria response in Fig. 6, and the time histories of the four required pulse trains are shown in Fig. 7. The ordinates of the response and excitation time histories shown in Figs. 6 and 7 are expressed in terms of dimensionless units.

It is clear from the comparison shown in Fig. 6 that a good match is obtained between the criterion and simulated response. Note that this simulation of the motion over a period of ≈20 sec required ≈13 pulses in each of the four pulse trains.

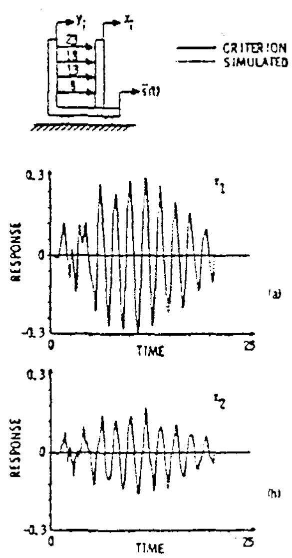

FIGURE 6. COMPARISON OF CRITERION AND SIMULATED RESPONSE OF 25 DOF SYSTEM

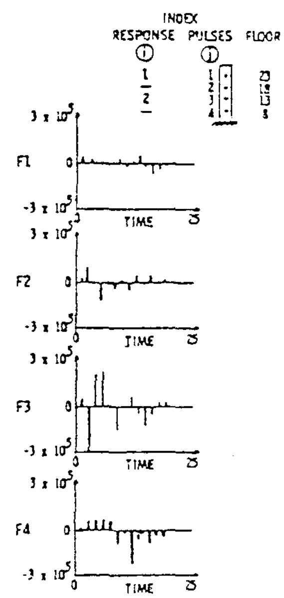

FIGURE 7. OPTIMUM PULSE TRAINS FOR 25 DOF SYSTEM

Model of UCB Frame

The test structure shown in Fig. 8 has been extensively investigated, both experimentally [12] and analytically [13] at the University of California, Berkeley. In the present study, the computer program SAP6 [14] was used to determine the mode shapes and frequencies of a linear model of this structure, and these dynamic characteristics are shown in Fig. 9.

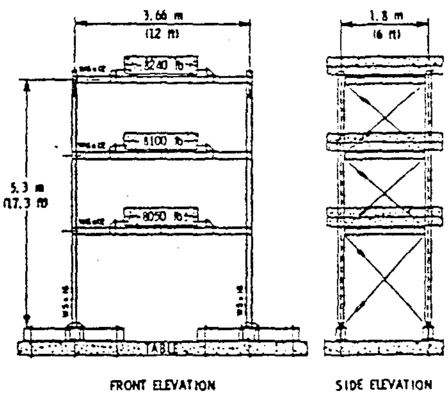

FIGURE 8. UCB TEST STRUCTURE [13]

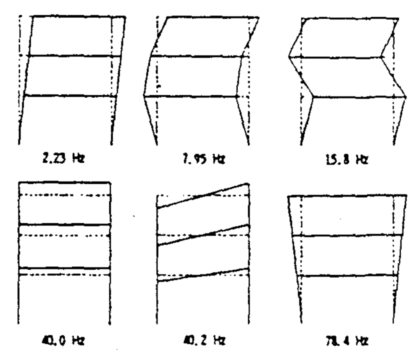

FIGURE 9. MODE SHAPES OF UCB FRAME DETERMINED BY SAP6

Pulse trains were to be applied at the three floor locations. The needed impulsive response functions were analytically determined and are shown in Fig. 10. The criteria response to El Centro 1940 earthquake was likewise analytically determined by using SAP6, and the results are shown as solid lines in response time history of Fig. 11. The adaptive random research optimization procedure was again used to determine the required pulse trains. The resulting simulated motion and the three required pulse trains are shown in Figs. 11 and 12.

This example again results in excellent agreement between the criterion and simulated response. In addition, the response spectra of various locations satisfactorily matched the criterion spectra at corresponding locations.

CONCLUSIONS

On the basis of the investigation reported herein, it is concluded that pulse-excitation techniques offer a viable alternative to large testing facilities (which have limited availability) and ground-explosion approaches (which are economically prohibitive) in simulating earthquake effects on structures, particularly when multiaxis excitation capability is needed.

ACKNOWLEDGMENT

This study was supported by the United States National Science Foundation under Grant No. PFR77-15010. The assistance and guidance provided by Dr. John B. Scalzi is greatly appreciated.

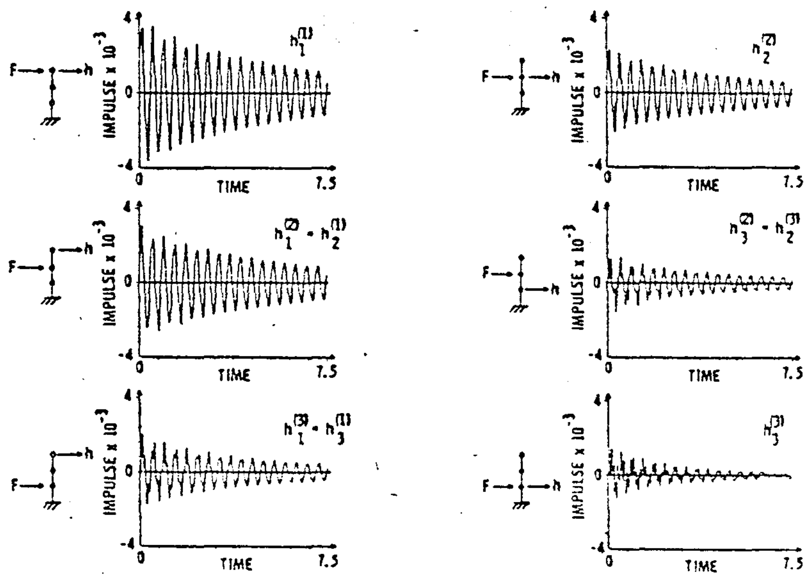

FIGURE 10. IMPULSE FUNCTIONS FOR UCB FRAME

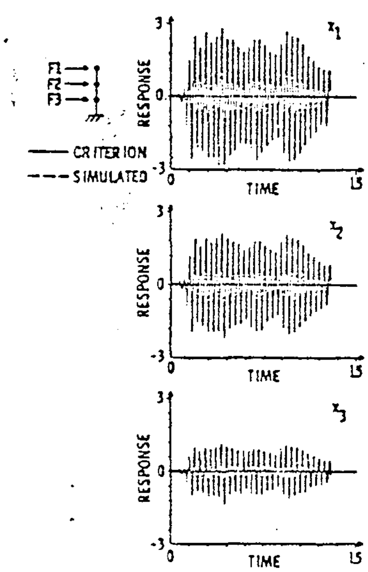

FIGURE 11. COMPARISON OF CRITERION AND SIMULATED RESPONSE OF UCB FRAME

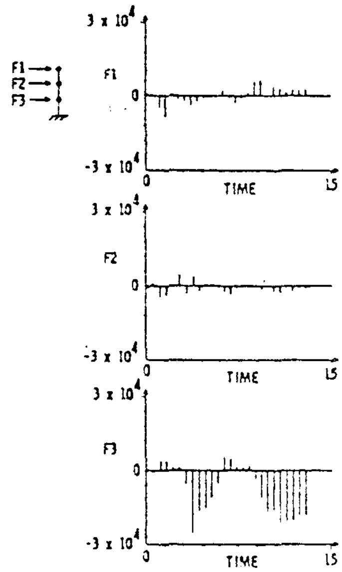

FIGURE 12. OPTIMUM PULSE TRAINS FOR UCB FRAME

REFERENCES

1. Housner, G.W. "Earthquake Environment Testing," Proc. of a Workshop on Simulation of Earthquake Effects on Structures, San Francisco, Sept. 7-9, 1973. Washington, DC: National Academy of Engineering, 1974.

2. Hudson, D.E. "Dynamic Tests of Full-Scale Structures," Proc. Dynamic Response of Structures, Instrumentation, Testing Methods, and System Identification, Univ. of Calif. Los Angeles, Mar 30-31, 1976.

3. Bouwkamp, J.G. "Dynamics of Full-Scale Structures," in Applied Mechanics in Earthquake Engineering, New York: ASME, 1974.

4. Housner, G.G. "Characteristics of Strong-Motion Earthquakes," Bull. Seismol. of Amer., 37:1, Jan 1947, pp. 19-27.

5. Scruton, C. and Harding, D.A. Measurement of the Structural Damping of a Reinforced Concrete Chimney Stack at Ferrybridge "B" Power Station. Wallingsford, England: NPL/Aero/323, 1957.

6. Safford, F.B. and Masri, S.F. "Analytical and Experimental Studies of a Mechanical Pulse Generator," J. of Engineering for Industry, ASME, Series B, 96:2, May 1974, pp. 459-470.

7. Safford, F.B. et al. "Air-Blast and Ground-Shock Simulation Testing of Massive Equipment by Pulse Techniques," 5th Int. Symp. on Military Application of Blast Simulation, Fortifikationsförvaltningen, Stockholm, Sweden, May 23-26, 1977.

8. Yates, D.G. and Safford, F.B. "Measurement of Dynamic Structural Characteristics of Massive Buildings by High-Level Multiple Techniques," Shock & Vibration Bull., 50, SVIC. Washington, DC: Naval Res. Lab, 1980.

9. Himmelblau, David M. Applied Nonlinear Programming. New York: McGraw-Hill, 1972.

10. Masri, S.F.; Bekey, G.A.; and Safford, F.B. "An Adaptive Random Search Method for Identification of Large-Scale Nonlinear Systems," 4th Symp. for Identification and System Parameter Estimation, Int. Federation of Automatic Control, Tbilisi, USSR, Sep 1976.

11. Blume, J.A.; Newmark, N.M.; and Corning, L.H. Design of Multistory Reinforced Concrete Buildings for Earthquake Motions. Skokie, IL: Portland Cement Association, 1961.

12. Clough, R.W. and Tang, D.T. Earthquake Simulator Study of a Steel Frame Structure, Experimental Results, Vol. 1, EERC 75-6. Berkeley, CA: Univ. of Calif. Earthquake Engineering Center, 1975.

13. Tang, D.T. Earthquake Simulator Study of a Steel Frame Structure, Analytical Results, Vol. 2, EERC 75-36. Berkeley, CA: Univ. of Calif. Earthquake Engineering Center, 1975.

14. SAP 6 Computer Program Manual. Civil Eng. Dept., Univ. of Southern California, 1978.

NSF Grant CEE-7715010

Proceedings of the Second

Specialty Conference
on

Dynamic Response of Structures: Experimentation, Observation, Prediction and Control

Organized by the Engineering
Mechanics Division of the
American Society of Civil Engineers

CO-SPONSORED BY:
ASCE/EMD Technical Committee on Experimental
Analysis and Instrumentation
ASCE/EMD Technical Committee on Dynamics
ASCE/STD Technical Committee on Dynamic Effects
Earthquake Engineering Research Institute
National Science Foundation
Structural Engineers Association of California
Wind Engineering Research Council
Georgia Institute of Technology, School of Civil Engineering

Gary Hart, Editor

JANUARY 15-16, 1981
Sheraton, Atlanta
ATLANTA, GEORGIA

Published by the
American Society of Civil Engineers
345 East 47th Street
New York, New York 10017

DEVELOPMENT AND USE OF FORCE PULSE TRAIN GENERATORS

By

Frederick B. Safford[1] and Sami F. Masri[2], M.ASCE

ABSTRACT

The study and investigation of the dynamic response of large structures to levels induced by natural or man-made events require excitation sources which possess large amounts of energy. Additionally, these energy sources must provide: Control of the excitation; portability to the site; ease of attachment to the structure; multiaxial excitation of the structure; and the ability to excite structures from simple harmonic motions to expected multifrequency response-time history motions. The development of force pulse train generators exhibits considerable promise to meet the foregoing for the study of linear and nonlinear dynamic responses of large structures.

INTRODUCTION

Recent analytical and experimental studies[1] indicate that a rudimentary series of rectangular or other simple pulses could be convolved with the impulse functions of a structure to induce motions closely approximating those caused by natural and man-made events. This result greatly simplified the control of high energy devices as the problem is reduced to three functions of on, off, and amplitude control. It was further determined that the excitation could also be placed directly on structures at one location or at multiple locations of test convenience and in single or multiple axes. When the structural excitation is caused by base motion, pulse simulation with generators attached to the same structure can duplicate the natural or man-made event with the exception of the rigid body modes.

Several large energy devices may be adapted for pulse train excitation. These include point source explosives, chemical rockets, metal cutting, and reactance by gas, water, or projectiles. The development and applications of several metal cutting systems are discussed together with a pulse modulated gas reactance system.

Interesting observations can be made through experiments and examinations of pulse trains in both the time and frequency domains. A single pulse is displayed in Figure 1 for both domains. However, a

[1]Associate, Agbabian Associates, El Segundo, California 90245
[2]Professor, School of Engineering, University of Southern California, Los Angeles, California 90007

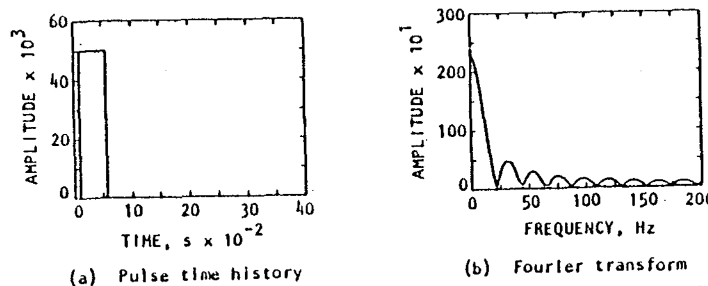

FIGURE 1. SINGLE PULSE TIME HISTORY WITH ASSOCIATED FOURIER TRANSFORM

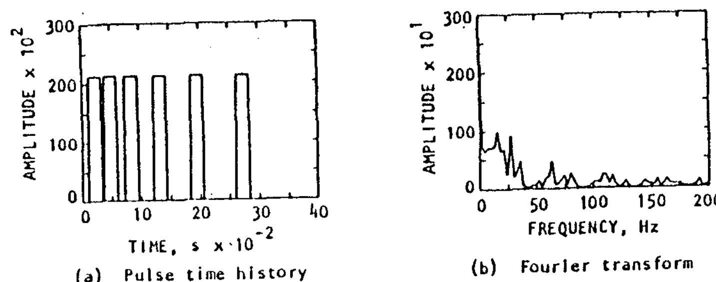

FIGURE 2. MULTIPULSE TIME HISTORY AND ASSOCIATED FOURIER TRANSFORM ROUGHLY DESIGNED TO POPULATE SPECTRAL ENERGY FROM 0 TO 40 Hz

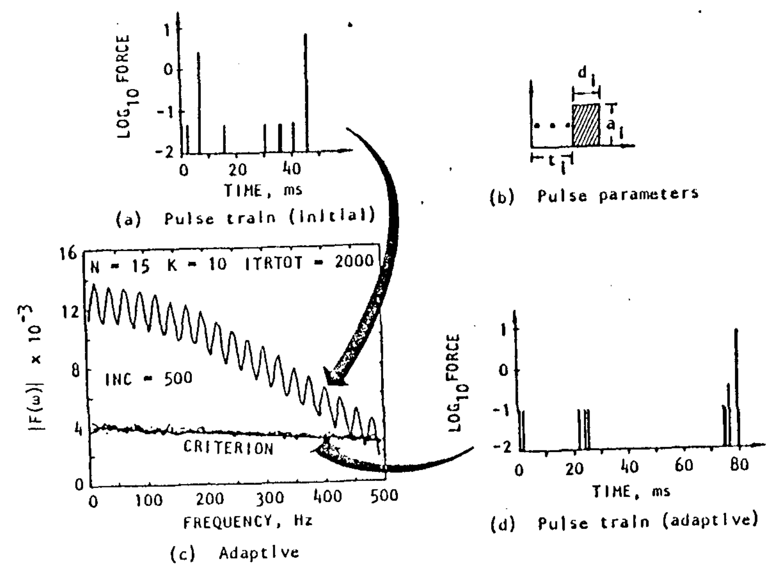

FIGURE 3. GENERATION OF PULSE TRAIN TO MATCH CRITERION FREQUENCY SPECTRUM, ADAPTIVE RANDOM SEARCH

collection of six pulses all of identical amplitudes and durations but spaced at different intervals generates a considerably different spectrum, as shown in Figure 2. Allowing pulse amplitudes, pulse durations, and pulse spacings to be variable parameters permits considerable leeway in shaping the frequency spectrum. Figure 3 illustrates a method of selecting a pulse train to produce a criterion spectrum where the parameters of amplitude, pulse width, and pulse spacings are specified by an iterative optimization algorithm[2]. Additional flexibility can be achieved by permitting the pulse shapes to be such as half-sine, saw tooth, or exponential and in various combinations.

MOTION SIMULATION OF STRUCTURES

Large and massive structures and equipments are largely subjected to (1) base motion excitation as from earthquakes and from ground shocks induced by conventional explosives or nuclear weapons and (2) distributed air loads as from tornadoes, high winds, and weapon blasts. Where the response of these systems is predicted and the dynamic characteristics are known by analysis or test (mode shapes, damping, and transfer functions), tests of these systems require an inverse solution to determine excitation functions. For the base motion problem, test excitation must be determined for one or more locations of convenience upon the structure; for distributed air loads, a few equivalent point locations of convenience must be found. It is required that an identical response (within an acceptable error) to the predicted response (criterion) caused by natural or man-made hazards be obtained. These new excitation functions can usually be found; however, the energy and waveforms required often make testing impractical due to the limitations of conventional shakers and/or costs.

The central issue in testing is to induce multiaxial *motion-time* histories on a structure comparable to those caused by natural or man-made hazards, since failures and malfunctions are essentially nonlinear. Force pulse trains provide practical methods in many applications to test structures and equipments to the thresholds of damage and malfunction by inducing realistic response wave forms. Computational methods to develop the required pulse trains are illustrated in Figures 4 and 5 with an application to a nuclear power containment structure shown in Figure 6. The computational methods are iterative to obtain the pulse train, and the procedure may be used for either linear[3] or nonlinear systems[4]. Various iteration methods may be used; the optimization algorithm[2] of Figure 5 using a spherical random search with a partially automatic control of the variance has proved to be quite efficient. It has been found that the variance can range over ten orders of magnitude, which permits rapid convergence and avoidance of local minima.

APPLICATIONS

A 25-story building (Fig. 7), modeled as a linear system, has the mode shapes of Figure 8, and under base excitation by the El Centro Earthquake yields the motion time histories plotted in Figure 11 for the 13th and 23rd floors[5]. Figure 10 shows the driving point impulse functions for Floors 8, 13, 18, and 23 as well as the transfer impulse functions between floors and each excitation location. Using the procedures of Figures 4, 5, and 6, the force pulse trains of Figure 9 were

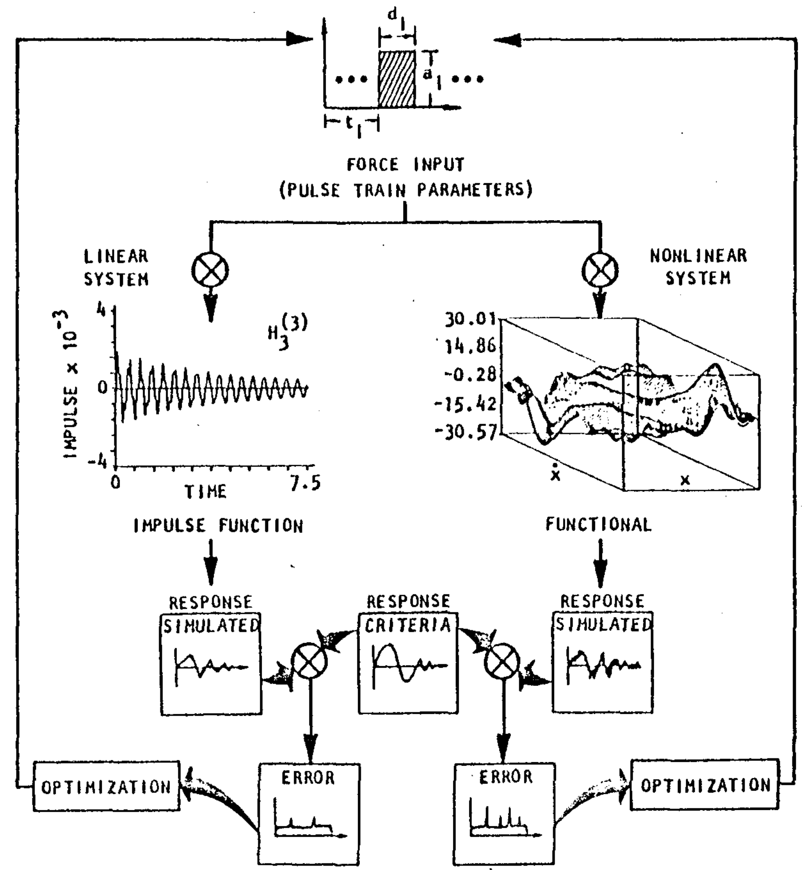

FIGURE 4. COMPUTATIONAL METHOD FOR PULSE TRAIN GENERATION

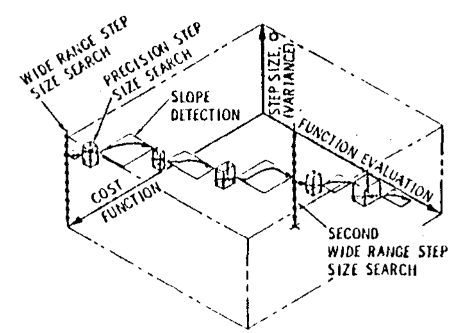

FIGURE 5. OPTIMIZATION ADAPTIVE RANDOM SEARCH ALGORITHM WITH RANGE AND PRECISION STEP SIZE

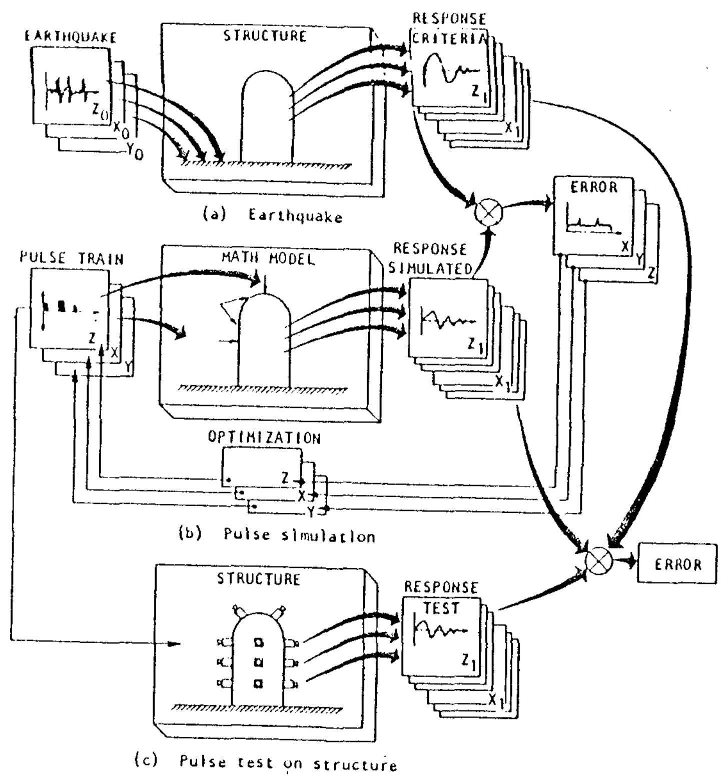

FIGURE 6. PROCEDURE FOR PULSE SIMULATION/TEST OF A STRUCTURE TO SIMULATE EARTHQUAKE RESPONSE

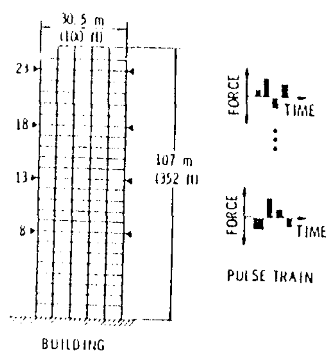

FIGURE 7. GAS PULSERS ARRAYED FOR EARTHQUAKE SIMULATION TEST OF A MULTISTORY BUILDING

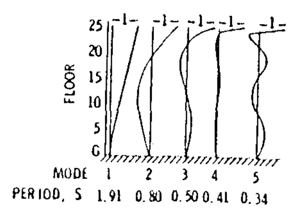

FIGURE 8. BUILDING NATURAL MODES OF VIBRATION

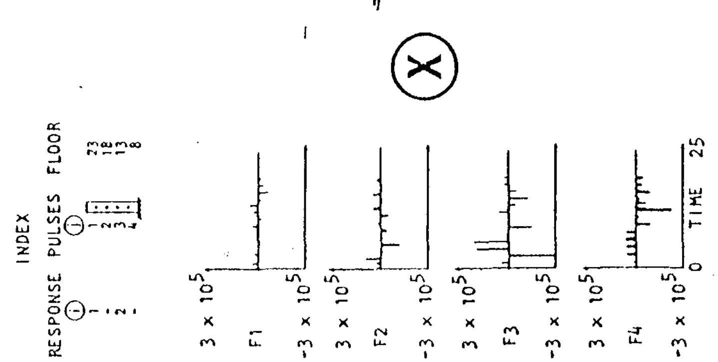

FIGURE 9. OPTIMUM PULSE TRAINS FOR 25 DOF SYSTEM

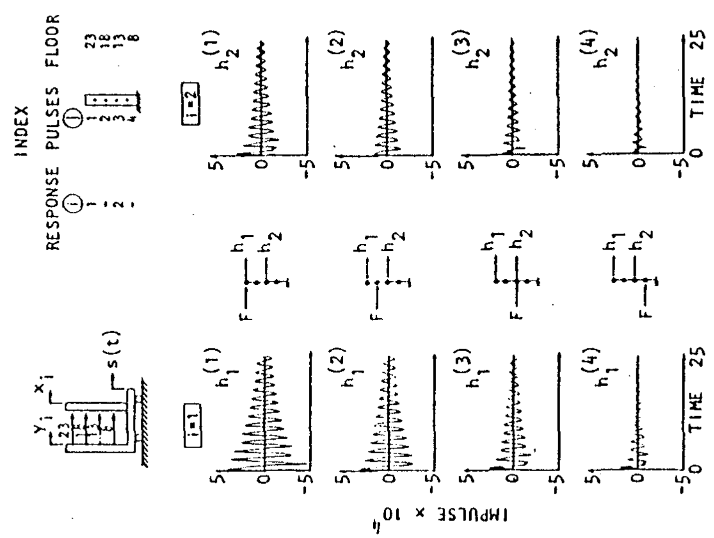

FIGURE 10. IMPULSIVE DISPLACEMENT RESPONSE TO 25 DOF SYSTEM

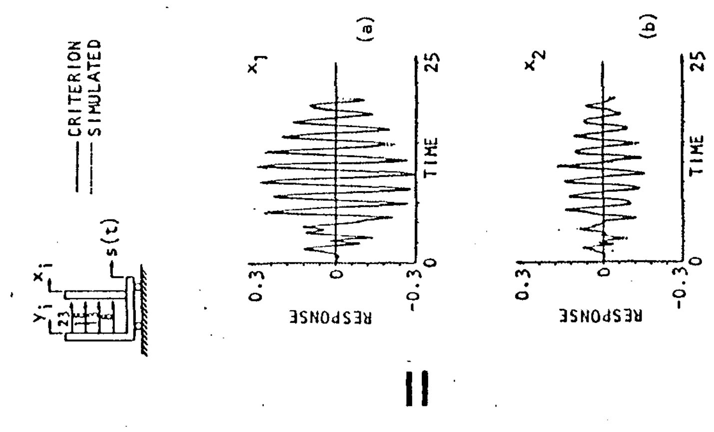

FIGURE 11. COMPARISON OF CRITERION AND SIMULATED RESPONSE OF 25 DOF SYSTEM

developed for pulse locations on Floors 8, 13, 18, and 23. The response motions induced by these pulsers are plotted on Figure 11 and are virtually identical to the motions caused by the El Centro Earthquake. Average force required is 50,000 lbf and the average impulse is 17 lbf-sec.

Figures 12 through 15 illustrate the application of pulse trains to induce a transient sine wave response. Other motions may also be generated, such as random and rapid sine sweeps (chirp). These motions are useful for measurement of transfer functions and for extraction of mode shapes. The structure of Figure 12, located at the University of California, Berkeley, has been extensively analyzed and tested on the Berkeley shake table[6]. This structure will be employed for pulse train studies to simulate earthquake motions[7] and to suppress earthquake motions[8]. In the latter case, the Berkeley shake table will be used to simulate earthquake motion while pulse generators will simultaneously be used to reduce the resultant structural motions.

PULSE GENERATING DEVICES

Pulse generating devices developed and now in development are composed of a class of metal cutting systems and a class of gas reactance systems. The metal cutting devices make use of the very high forces required to cut metal and are configured similar to broaching tools[9]. The shape of a metal projection controls pulse wave form (square, half-sine, etc.). The velocity of the cutting tool and the length of the metal projection govern the pulse duration[1]. For the metal removed, cutting coefficients typically range from 150,000 lbf/in^3 for aluminum to 300,000 lbf/in^3 for steel. Metal pulse generators producing up to 1,000,000 lbf have been proposed. Several varieties of metal cutting pulse generators are shown in Figures 16 through 19 and pictured in Figures 21 through 24.

The programmable gas pulse generator shown in Figure 20 is currently under construction; test stand calibrations will commence in the fall of 1980. Initial use provides for cold gas but the system is adaptable for both steam and chemically generated hot gas. Thrust amplitudes are controlled in the on-state by positioning the metering plug for flow control. Off-state for the pulse occurs by signaling the hydraulic actuator to move the metering plug to seal off gas flow at the nozzle. This device will be used for earthquake and anti-earthquake investigations on the structure shown in Figure 12 at the University of California, Berkeley.

TESTS WITH PULSE GENERATORS

A 20,000 lb shock isolated control room (50 ft x 50 ft) for a power plant was tested while functionally operating to induce motion-time histories expected from a specified base motion hazard[10]. One of the four pulse generators used is pictured in Figure 21. The specified pulse train and the four measured ones are presented in Figure 25. Typical measured transfer functions of the structure used to calculate the pulse train are presented in Figure 26 and include transfer function magnitude, phase, and impulse function. Magnitude units are the ratio of acceleration to force as function of frequency. The predicted control room

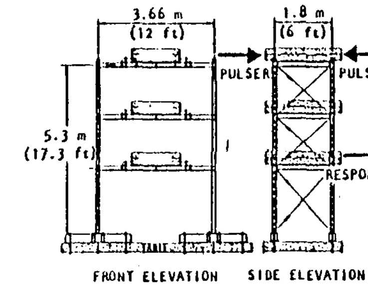

FIGURE 12. UCB TEST STRUCTURE

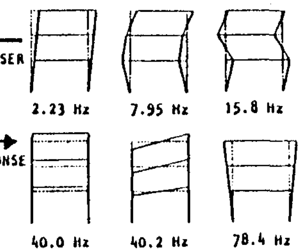

FIGURE 13. MODE SHAPES OF UCB FRAME DETERMINED BY SAP6

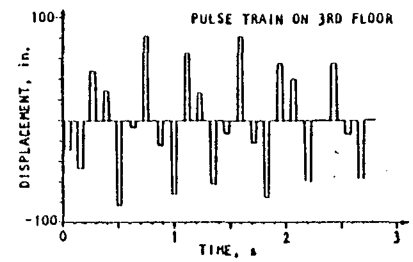

FIGURE 14. FORCE PULSE TRAIN LOCATED ON 3RD FLOOR OF UCB STRUCTURE TO INDUCE TRANSIENT SINUSOIDAL MOTION

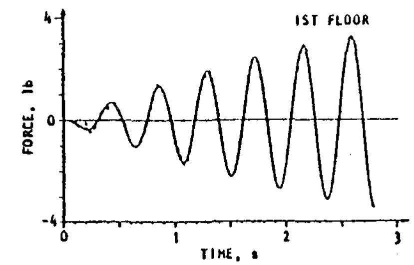

FIGURE 15. TRANSIENT SINUSOIDAL MOTION ON FIRST FLOOR OF UCB STRUCTURE INDUCED BY PULSE TRAIN AT 2.23 Hz OF FIG. 13

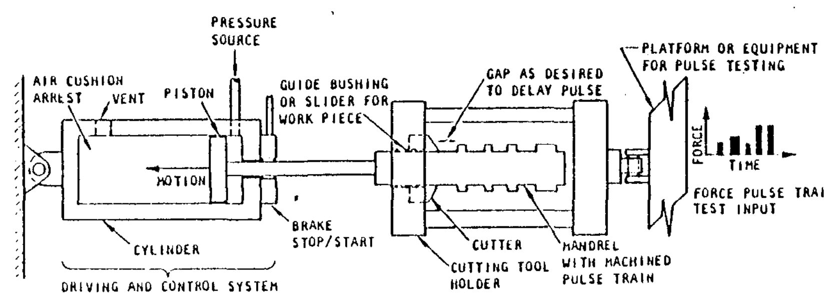

FIGURE 16. PULSE-FORMING DEVICE WITH DRIVING AND CONTROL SYSTEM MAXIMUM OUTPUT 8,000 lbf

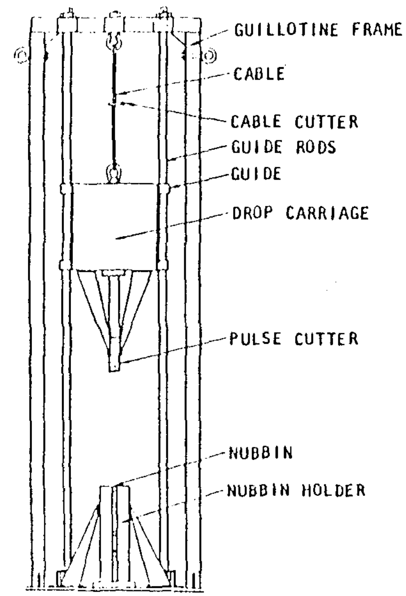

FIGURE 17. SKETCH OF MEDIUM-FORCE OUTPUT PULSE GENERATOR MAXIMUM OUTPUT 16,000 ft-lb AND 1,800 lbf-s

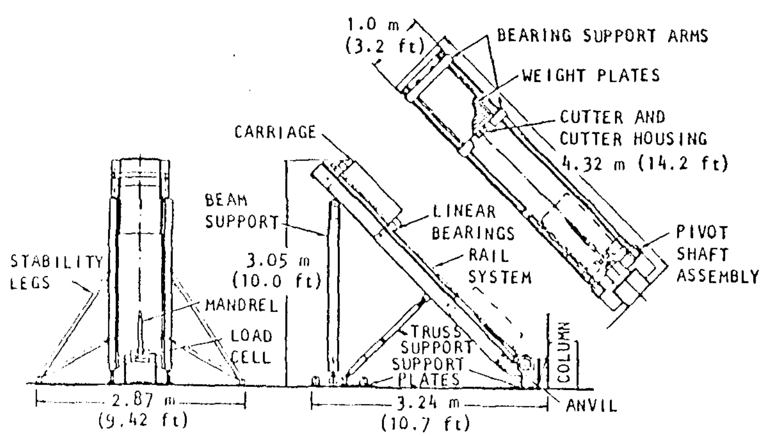

FIGURE 18. ASSEMBLY — IMPULSE TESTER MAXIMUM OUTPUT 54,000 ft-lb AND 4,700 lbf-s

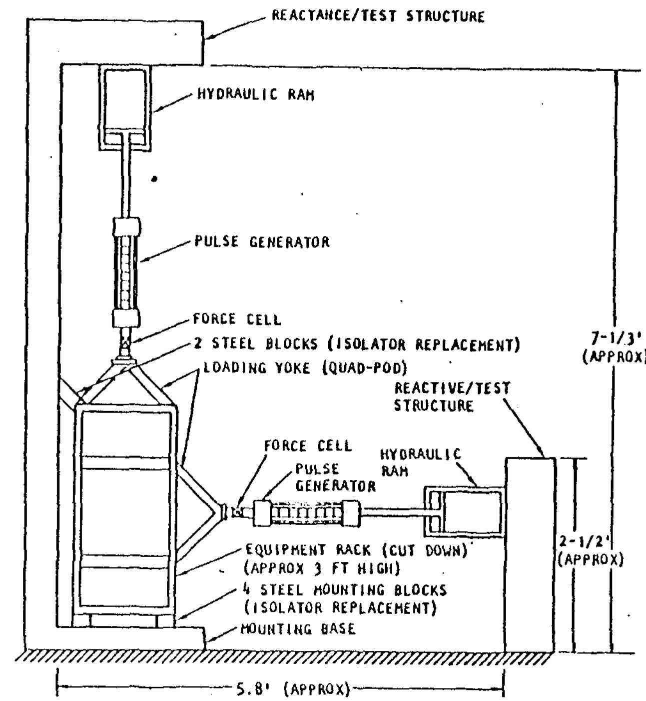

FIGURE 19. BIAXIAL TEST FACILITY CONFIGURATION MAXIMUM OUTPUT 15,000 lbf EACH AXIS

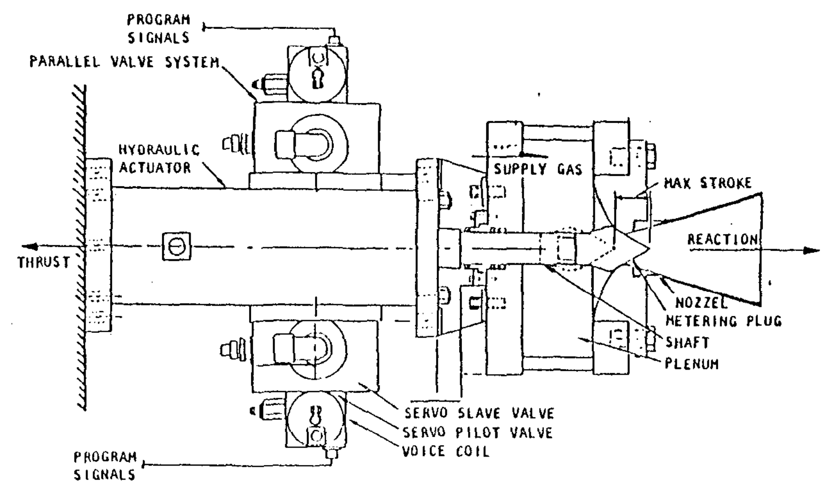

FIGURE 20. PROGRAMMABLE GAS PULSE GENERATOR COLD GAS SYSTEM — 500 TO 10,000 lbf

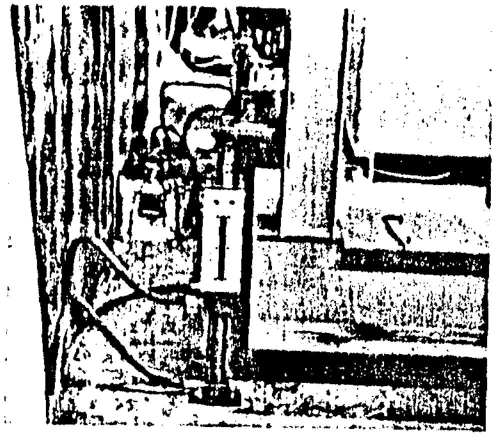

FIGURE 21. APPLICATION OF PULSE GENERATOR (SEE FIG. 16) FOR EQUIPMENT TEST ACCELERATION-TIME HISTORIES

FIGURE 22. PULSE GENERATOR (SEE FIG. 17) USED FOR TRANSFER FUNCTION AND MODE SHAPES OF STRUCTURE

FIGURE 23. LARGE PULSE GENERATOR (SEE FIG. 18) USED TO MEASURE TRANSFER FUNCTIONS AND MODE SHAPES OF LARGE STRUCTURES

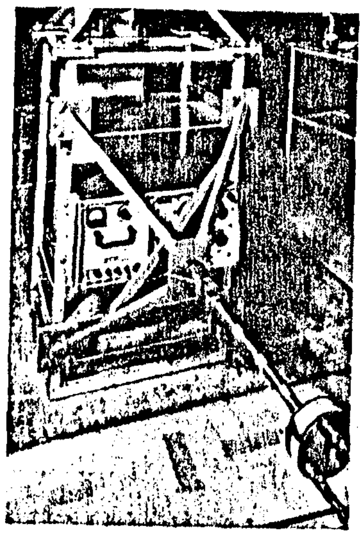

FIGURE 24. BI-AXIAL PULSE GENERATOR (SEE FIG. 19) FOR EQUIPMENT TESTS ACCELERATION-TIME HISTORIES

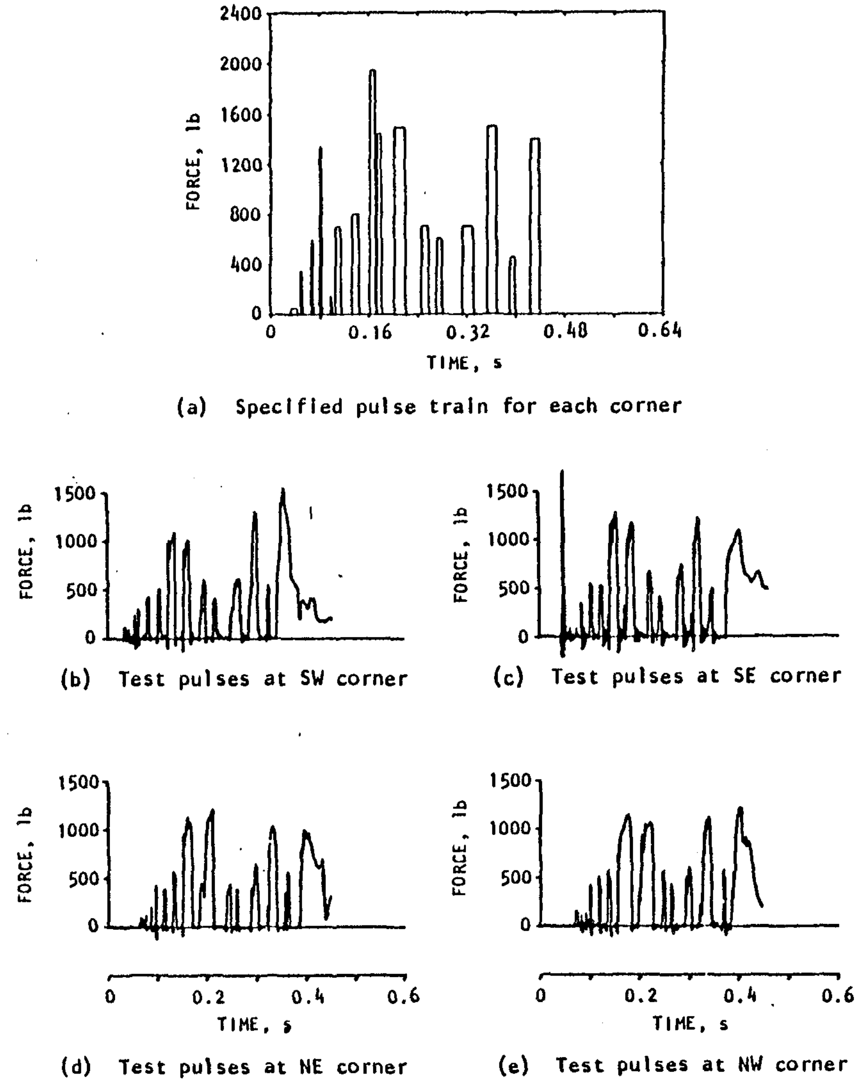

FIGURE 25. 200,000 LB SHOCK ISOLATED CONTROL ROOM PLATFORM: SPECIFIED AND ACTUAL TEST-INPUT PULSES USING FOUR PULSE GENERATORS SHOWN IN FIG. 21

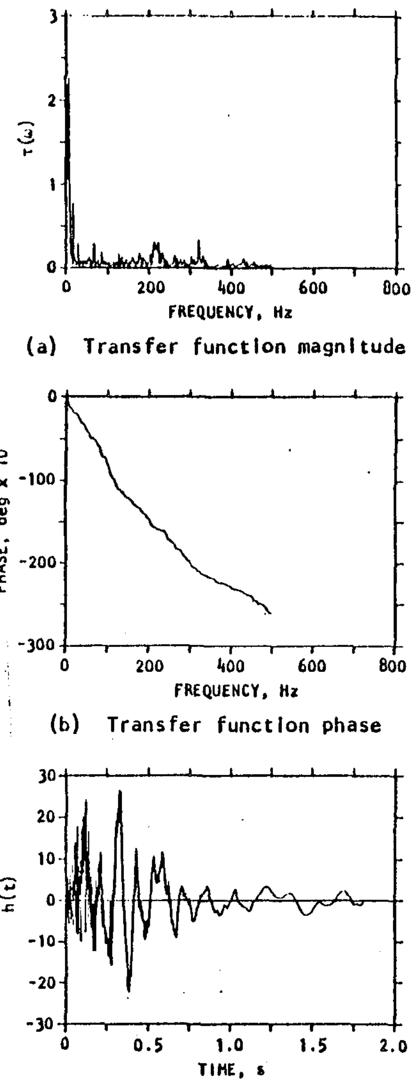

(a) Transfer function magnitude

(b) Transfer function phase

(c) Impulse function

FIGURE 26. CONTROL ROOM: MEASURED TRANSFER FUNCTION FOR 0.5 Hz TO 500 Hz

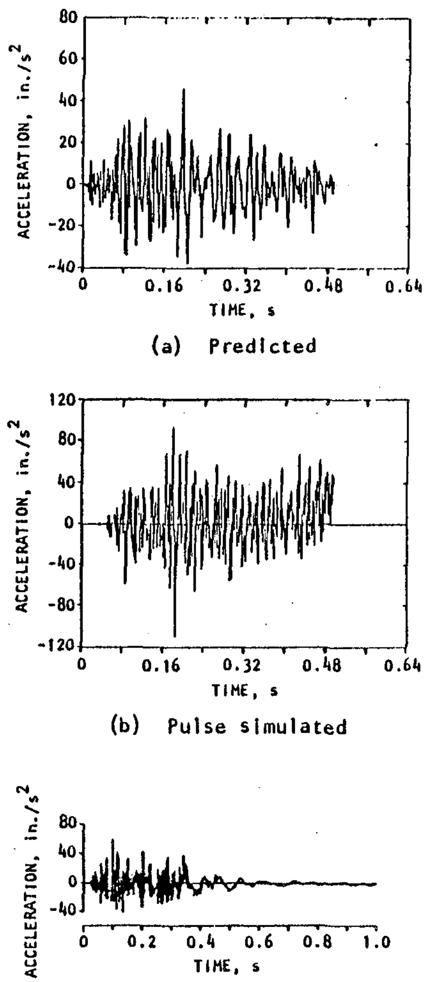

(a) Predicted

(b) Pulse simulated

(c) Pulse tested

FIGURE 27. CONTROL ROOM PLATFORM: ACCELERATION-TIME HISTORIES OF PREDICTED, PULSE-SIMULATED, AND PULSE-TESTED MOTIONS

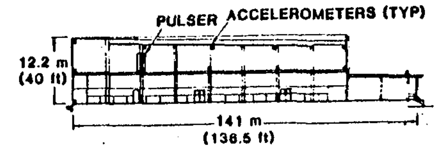

FIGURE 28. CROSS SECTION OF NUCLEAR PROCESSING PLANT SHOWING ACCELEROMETER AND PULSER LOCATIONS (PULSER EXCITATION NORMAL TO SECTION SHOWN)

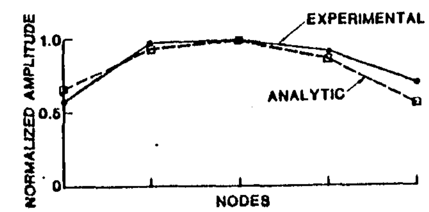

FIGURE 29. TYPICAL MODE SHAPE PLOT FROM EXPERIMENTAL AND ANALYTIC DATA (Frequency: 9.2 Hz)

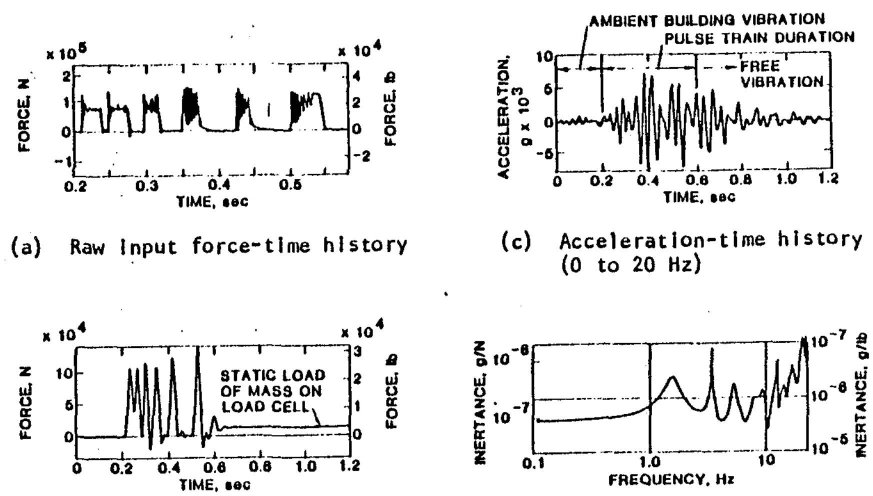

(a) Raw input force-time history

(b) Filtered input force-time history (0 to 20 Hz)

(c) Acceleration-time history (0 to 20 Hz)

(d) Transfer function (acceleration divided by force)

FIGURE 30. TYPICAL DATA RECORDS FROM PULSE TRAIN TESTS AND RESULTING TRANSFER (INERTANCE) FUNCTIONS COMPUTED FROM DATA — PULSE GENERATOR SHOWN IN FIGS. 18 AND 23

motion due to base motion hazard is given in Figure 27 together with computed pulse simulated motion and motions measured during tests with the pulse generators.

Tests of a large nuclear processing plant were performed to obtain transfer functions and to extract building modes and damping[11]. One of the buildings tested was a reinforced concrete structure 40 ft high, 136 ft wide, and 300 ft long. Figure 29 is a typical mode shape extracted from the pulse generated data given in Figure 30. The pulse generator used in these tests is shown in Figures 18 and 23.

ACKNOWLEDGMENTS

This study was supported in part by the United States National Science Foundation under Grant No. PFR77-15010. The assistance and guidance provided by Dr. John B. Scalzi is greatly appreciated.

REFERENCES

1. Safford, F.B. and Masri, S.F. "Analytical and Experimental Studies of a Mechanical Pulse Generator," Jnl of Eng. for Industry, ASME, Series B, 96:2, May 1974, pp. 459-470.

2. Masri, S.F.; Bekey, G.A.; and Safford, F.B. "An Adaptive Random Search Method for Identification of Large Scale Nonlinear Systems," 4th Symp. for Identification and System Parameter Estimation, Int. Federation of Automatic Control, Tbilisi, USSR, Sep 1976.

3. Masri, S.F. and Safford, F.B. "Dynamic Environment Simulation by Pulse Techniques," Proc. ASCE Eng. Mech. Div. 101:EM1, Feb 1976, pp. 151-169.

4. Masri, S.F. and Caughey, T.N. "A Nonparametric Identification Technique for Nonlinear Dynamic Problems," Jnl of Appl. Mech. ASME, 46:2, Jun 1979.

5. Masri, S.F. and Safford, F.B. "Earthquake Environment Simulation by Pulse Generators," Proc. 7th World Conf. on Earthquake Eng. Istanbul, Turkey, Sep 8-13, 1980.

6. Clough, R.W. and Tang, D.T. Earthquake Simulator Study of a Steel Frame Structure, Experimental Results, Vol. 1, EERC 756. Berkeley, CA: Univ. of Calif. Earthquake Engineering Center, 1975.

7. Safford, F.B. Validation of Pulse Techniques for the Environmental Simulation of Earthquake Motions in Civil Structures, U.S. National Science Foundation Grant No. PFR77-15010, Washington, D.C., 1978.

8. Masri, S.F.; Bekey, G.A.; Safford, F.B.; and Dehghanyar, T.J "Anti-Earthquake Application of Pulse Generators," Proc. Dynamic Response of Structures, Instrumentation, Testing Methods and System Identification, ASCE Specialty Conference, Atlanta, GA, Jan 1981.

9. Safford, F.B. "Mechanical Force Pulse Generator for Use in Structural Analysis," U.S. Patent Office No. 4,020,672, May 1977.

10. Safford, F.B. et al. "Air-Blast and Ground-Shock Simulation Testing of Massive Equipment by Pulse Techniques, 5th Int. Symp. on Military Application of Blast Simulation, Fortifikationsforvaltningen, Stockholm, Sweden, May 23-26, 1977.

11. Yates, D.G and Safford, F.B "Measurement of Dynamic Structural Characteristics of Massive Buildings by High-Level Multiple Techniques," Shock & Vibration Bull., 50, SVIC. Washington, DC: Naval Res. Lab, 1980.

Proceedings of the Second

Specialty Conference
on

Dynamic Response of Structures: Experimentation, Observation, Prediction and Control

Organized by the Engineering
Mechanics Division of the
American Society of Civil Engineers

CO-SPONSORED BY:
ASCE/EMD Technical Committee on Experimental
Analysis and Instrumentation
ASCE/EMD Technical Committee on Dynamics
ASCE/STD Technical Committee on Dynamic Effects
Earthquake Engineering Research Institute
National Science Foundation
Structural Engineers Association of California
Wind Engineering Research Council
Georgia Institute of Technology, School of Civil Engineering

Gary Hart, Editor

JANUARY 15-16, 1981
Sheraton, Atlanta
ATLANTA, GEORGIA

NSF Grant CEE-7715010

Published by the
American Society of Civil Engineers
345 East 47th Street
New York, New York 10017

ANTI-EARTHQUAKE APPLICATION OF PULSE GENERATORS

by

Sami F. Masri[1], George A. Bekey[2], Frederick B. Safford[3], Tejav J. Dehghanyar[4]

Abstract

This paper is concerned with a feasibility study into the use of servocontrolled gas pulse generators to mitigate the earthquake-induced motions of tall buildings. A simple yet reliable on-line active control algorithm is developed and applied, by means of numerical simulation studies, to a model of an existing steel frame structure. The control concept is shown to be effective in controlling the response of linear as well as nonlinear building systems under dynamic excitation.

Introduction

Analytical and experimental studies [1,2]* have shown that among the class of passive auxiliary mass dampers used for vibration control, the impact damper, which is a highly nonlinear version of such devices, has a superior performance record compared to the conventional dynamic vibration neutralizer when used under dynamic environments resembling earthquake excitations. However, due to the transient nature of earthquake ground motions, the impulsive forces imparted by the impact damper to the primary structure (see Fig. 1) do not always occur at the optimum time from the motion reduction point of view. Consequently, the efficiency of the impact damper, like that of other similar passive damping devices, is substantially reduced compared to its efficiency under periodic excitation.

A current research effort [3] is concerned with the validation of the concept of using pulse techniques [4] to simulate the response of structures to arbitrary dynamic environments [5]. In the course of this study, (1) an efficient algorithm has been devised for determining the optimum force pulse-train characteristics to be applied at different locations in the structure so as to match the criteria response [6], and (2) gas pulse generators, employing digital servocontrollers and hydraulic actuators in conjunction with a gas storage system and a nozzle with a metered flow to furnish the needed thrust, are being built.

---

[1] Professor, School of Engineering, University of Southern California

[2] Professor, School of Engineering, University of Southern California

[3] Associate, Agbabian Associates, El Segundo, California

[4] Graduate student, School of Engineering, University of Southern Calif.

* Numbers in brackets designate items in the reference list.

In view of the preceding discussion, this paper is concerned with a study of the feasibility of using servocontrolled gas pulse generators to mitigate the earthquake-induced oscillations of tall buildings or similar structures.

Control Algorithm

A recent study by the authors [7] presented a relatively simple on-line pulse control algorithm suitable for use with distributed parameter systems subjected to arbitrary nonstationary disturbances. The main idea of the algorithm is that resonance phenomena can be eliminated, or at least drastically reduced, by disorganizing the orderly and gradual buildup of the structural dynamic response by timed firing of a pulse of suitable magnitude applied in the proper direction. Furthermore, in order to minimize the amount of control energy utilized, the control force should be applied only when the structural response exceeds a certain threshold level related to the resistance of the structure.

Assume, as a first order approximation, that the structure to be controlled is modeled as an equivalent linear single-degree-of-freedom (SDOF) system as shown in Fig. 2. Suppose that at time $t = t_o$, the threshold barrier has been exceeded. Then the expected value of the response, under the assumption that the excitation is a zero-mean random process, is given by

$$E[y(t)] = y_o u(t - t_o) + \dot{y}_o v(t - t_o) + x_p(t) \quad (1)$$

where

$$u(t) = \exp(-\zeta\omega t)(\cos \omega_d t + \frac{\zeta\omega}{\omega_d} \sin \omega_d t) \quad (2)$$

$$v(t) = \frac{1}{\omega_d} \exp(-\zeta\omega t) \sin \omega_d t \quad (3)$$

$$x_p(t) = \int_{t_o}^{T_o} h(t - \tau)\, p(\tau) d\tau \quad (4)$$

$h(t)$ = Impulsive response of the system = $v(t)$ (5)

$p(t)$ = Impulsive control force of duration T_d and peak level P_o (6)

ω_d = $\omega\sqrt{1 - \zeta^2}$ (7)

ω = Fundamental frequency of the system (8)

ζ = Ratio of critical damping of the system (9)

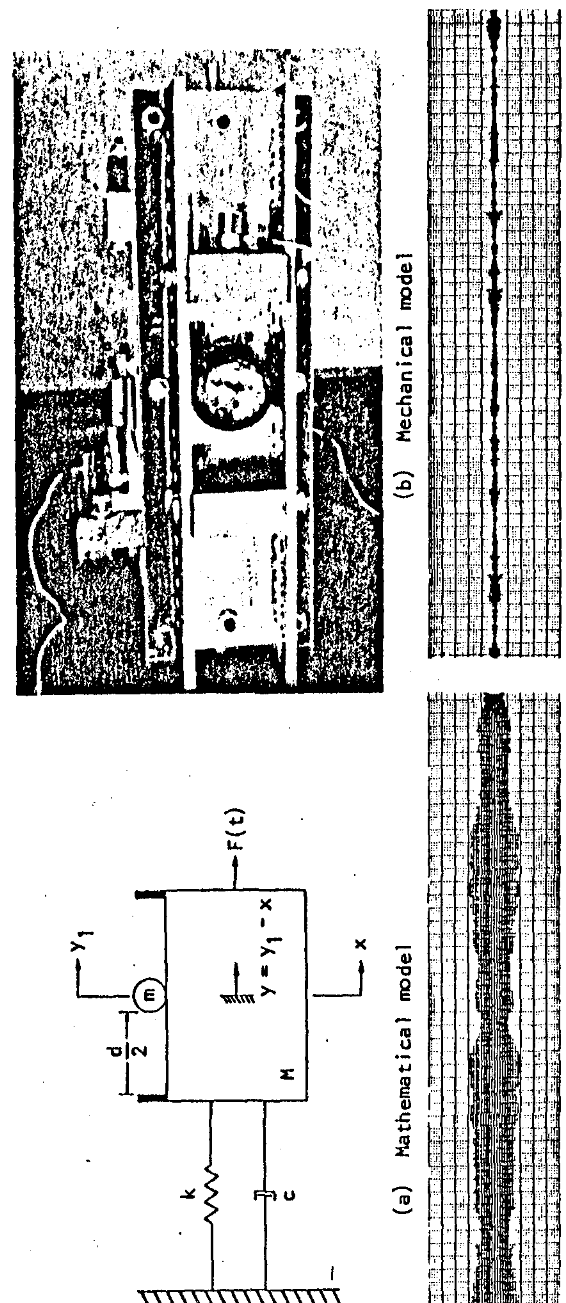

(a) Mathematical model (b) Mechanical model (c) Motion without damper (d) Motion with impact damper

FIGURE 1. IMPACT VIBRATION DAMPER WITH RANDOM EXCITATION

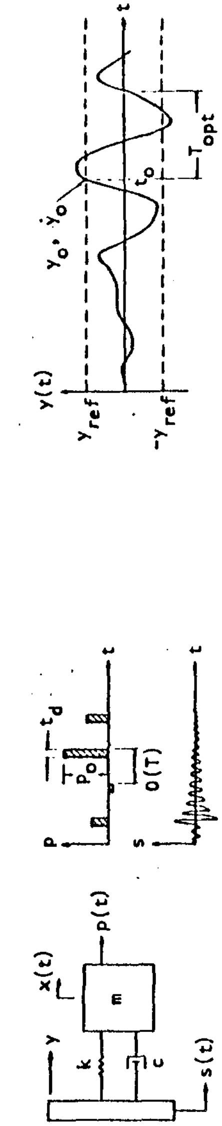

FIGURE 2. EQUIVALENT SDOF SYSTEM TO BE CONTROLLED

The cost function to be minimized will be selected as

$$J(P_o) = \int_{t_o}^{t_o+T_{opt}} (E[y(t)])^2 dt \tag{10}$$

where T_{opt} is the optimization period, chosen to be O(T), with T being the fundamental period of the system.

Due to the nature of the expressions for u, v, and x_p appearing in Eq. 1, Eq. 10 can be analytically evaluated and differentiated to yield the optimum pulse amplitude P_{opt} which will minimize $J(P_o)$. The resulting analytical expression for P_{opt} will involve simple algebraic expressions (which need to be evaluated only once for a given system) multiplying the "initial" displacement and velocity y_o and $\dot{y}_o$. Thus, once a control pulse is called for, virtually negligible computational effort (and hence, control lag time) is needed to determine the optimum pulse magnitude, direction, and timing. This useful feature of the proposed control algorithm is significant in assessing the feasibility of the method for on-line implementation.

Applications

The utility of the proposed method will now be demonstrated by applying it to a three-degree-of-freedom model of a three-story steel frame (Fig. 3) that has been extensively studied, both analytically and experimentally [8,9] at the University of California, Berkeley (UCB).

Assume that a single pulse controller is located at the first story of this structure and that the threshold levels for triggering the controller are y_{ref} = {0.64, 0.88, 1.0}. Using a rectangular pulse of duration T_d = 0.01 sec and an optimization period T_{opt} = 0.5 sec results in the controlled response shown in Fig. 6. Corresponding results for a single controller location at m_2 and at m_3 are shown in Figs. 7 and 8.

Comparing Figs. 6, 7, and 8, it is seen that regardless of the controller location, the response of each mass is kept nearly bounded by the selected threshold levels. However, from the control energy point of view, significant reduction in the required impulse can be achieved if the pulse generator is located at the top floor, rather than the lower floor of the structure. The optimum location of pulse generators is being studied as a refinement to conserve impulse requirements.

The relative velocity response of the structure with and without control is shown in Fig. 9. Note that in spite of the transients corresponding to the control pulses, substantial reduction in the velocity is obtained with a single controller.

The relative displacement response of the same structure, with the same controller parameters used in Figs. 6 through 9, under the action of the El Centro, 1940 earthquake ground motion, and under a stationary random ground motion, is shown in Figs 10 and 11, respectively. As in the case of artificial earthquake D1, the results shown in Figs. 10 and 11 show that a single controller acting at the top floor can effectively control the system motion to within any reasonable threshold level.

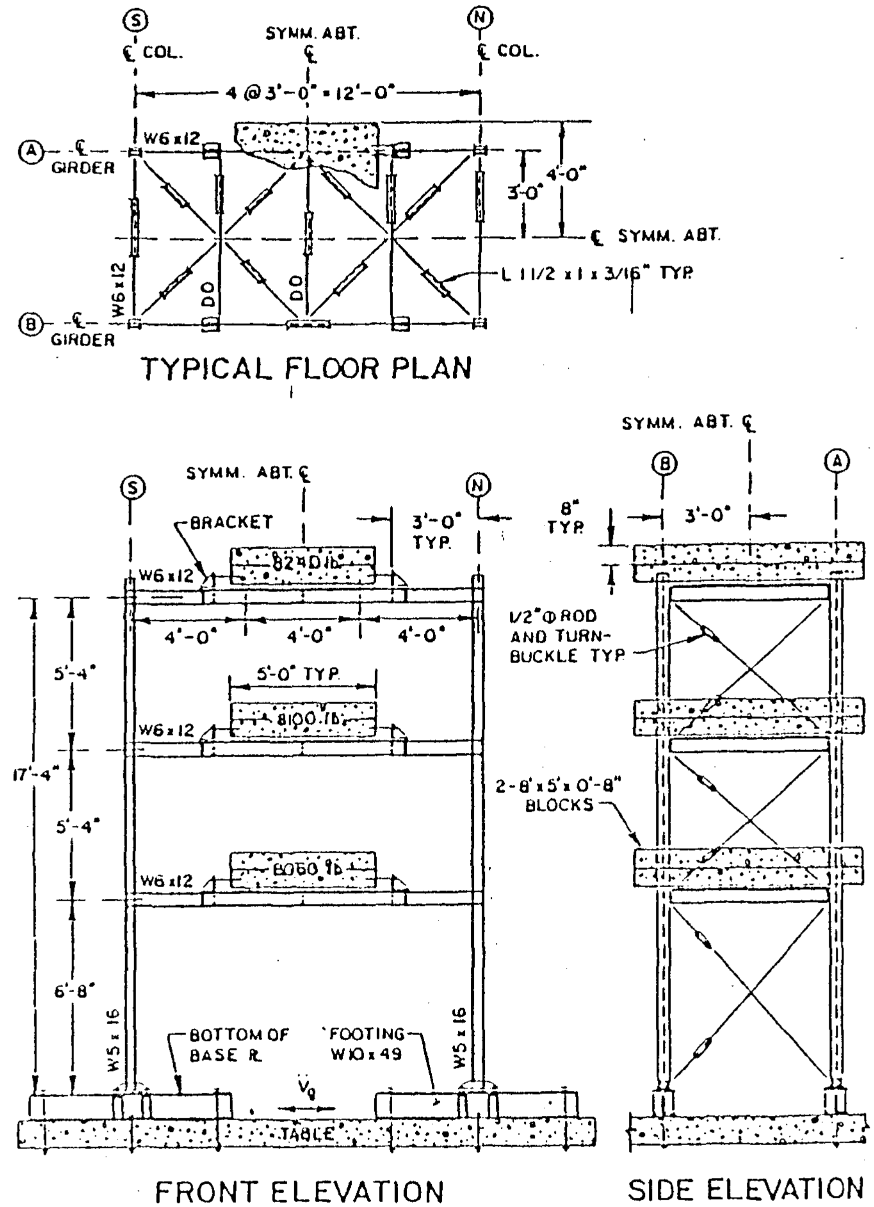

FIGURE 3. PLAN AND ELEVATIONS OF THE TEST STRUCTURE [8]

$\ddot{S}$ = E.Q. D1

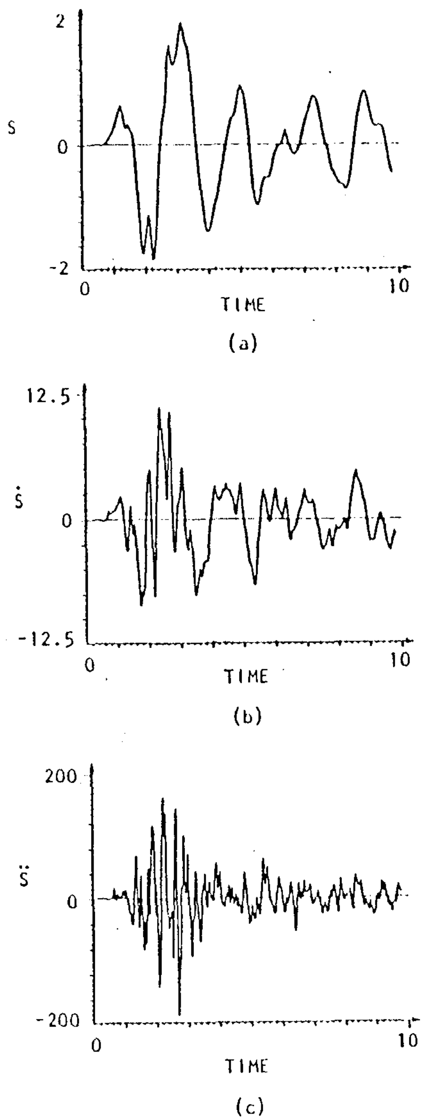

FIGURE 4. BASE MOTION CORRESPONDING TO E.Q. D1

$\ddot{S}$ = E.Q. D1 NO CONTROL

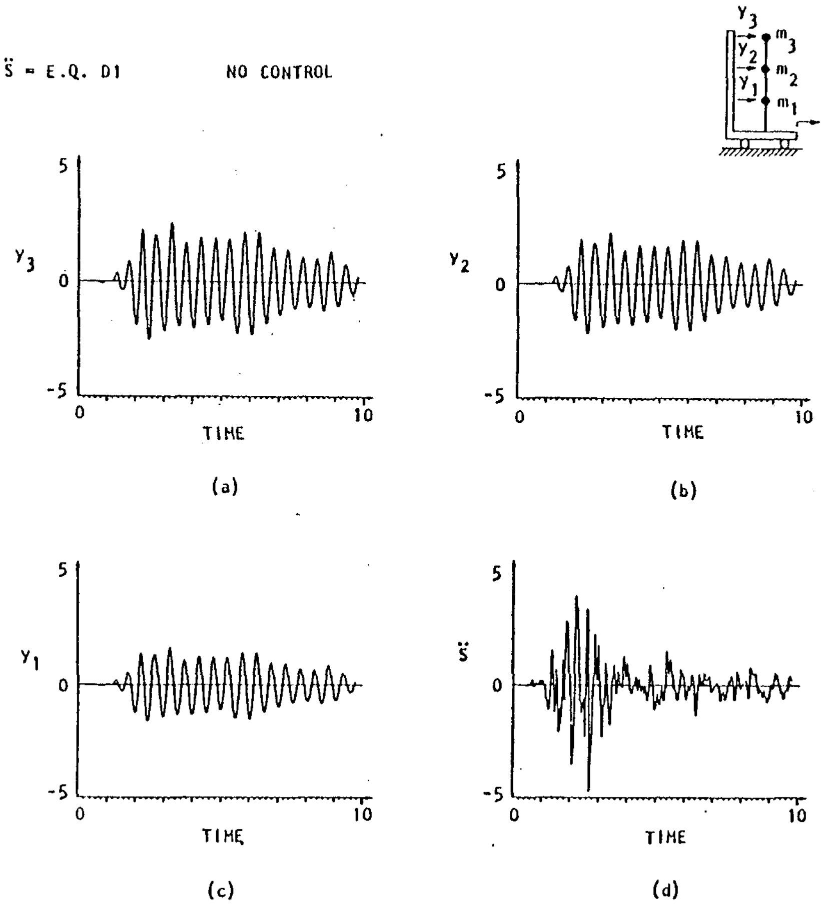

FIGURE 5. RESPONSE OF MODEL UCB-1 WITHOUT CONTROL UNDER EXCITATION E.Q. D1

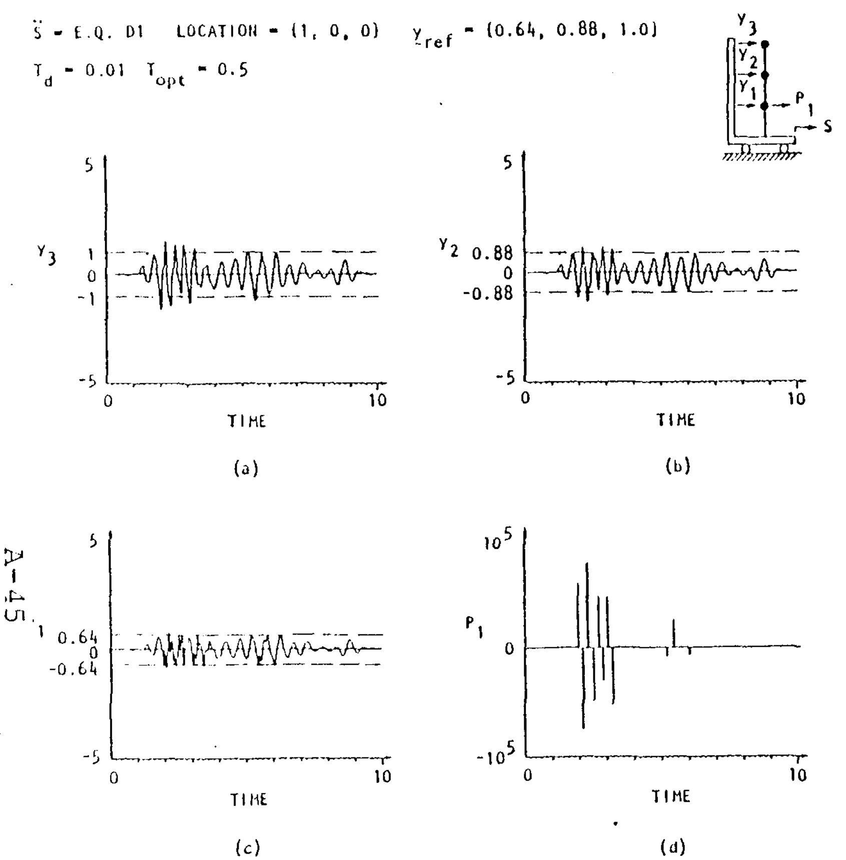

FIGURE 6. CONTROLLED RESPONSE OF MODEL UCB-1 UNDER EXCITATION E.Q. D1; CONTROLLER ACTING AT m_1

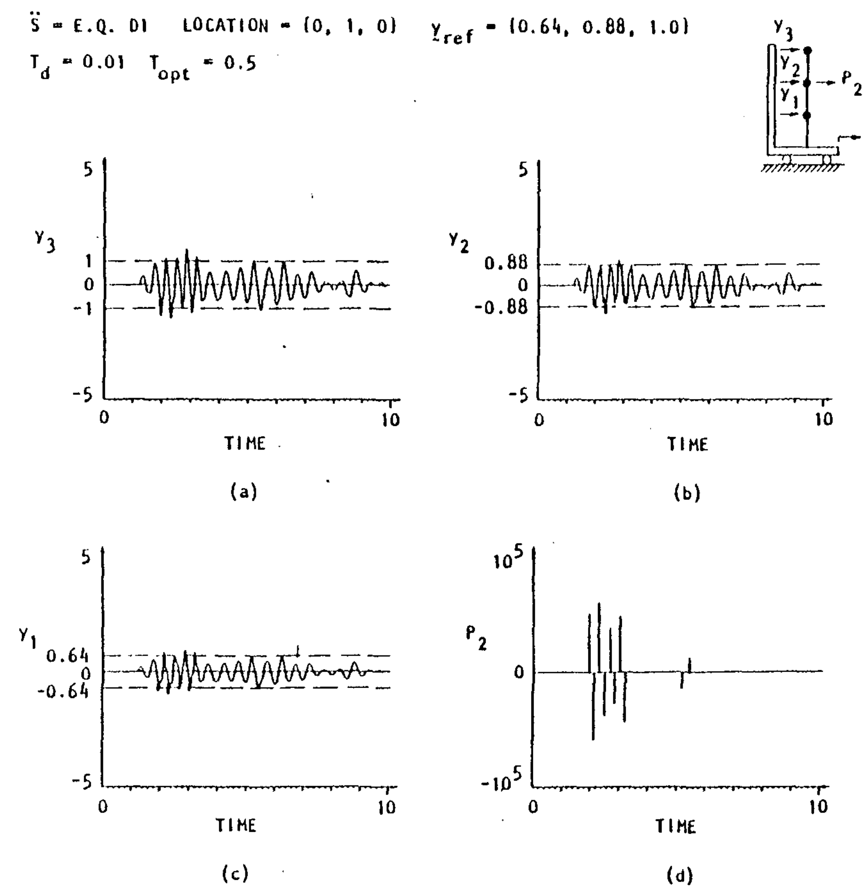

FIGURE 7. CONTROLLED RESPONSE OF MODEL UCB-1 UNDER EXCITATION E.Q. D1; CONTROLLER ACTING AT m_2

$\ddot{S}$ = E.Q. D1 LOCATION = (0, 0, 1) Y_{ref} = (0.64, 0.88, 1.0)

T_d = 0.01 T_{opt} = 0.5

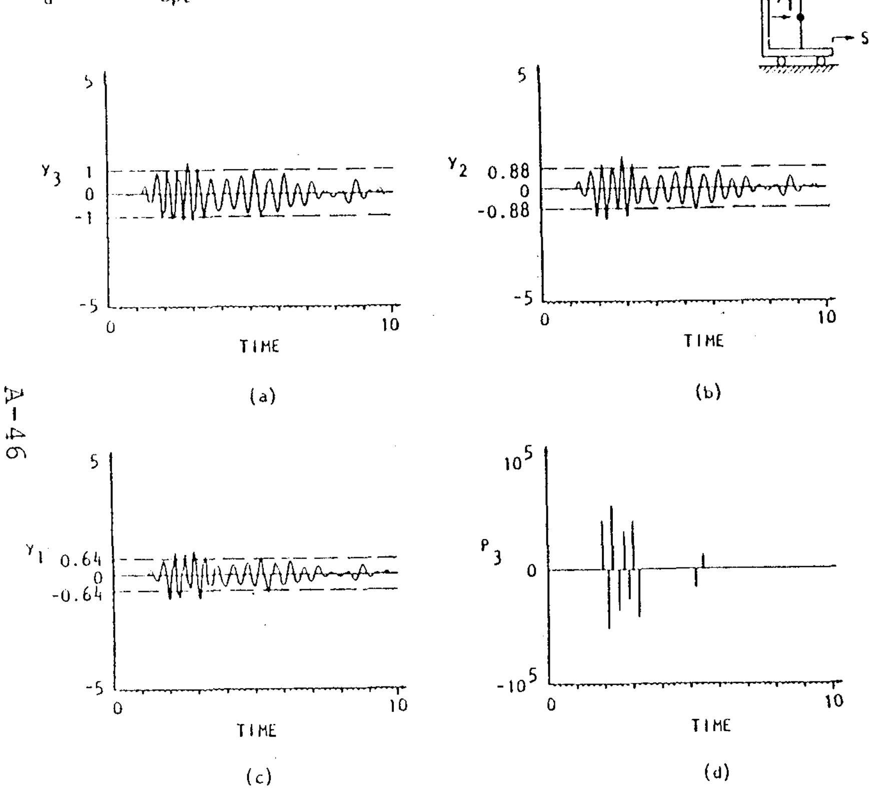

FIGURE 8. CONTROLLED RESPONSE OF MODEL UCB-1 UNDER EXCITATION E.Q. D1; CONTROLLER ACTING AT m_3

EXCITATION: E.Q. D1 LOCATION = (0, 0, 1)

Y_{ref} = (0.64, 0.88, 1.0) T_d = 0.01 T_{opt} = 0.5

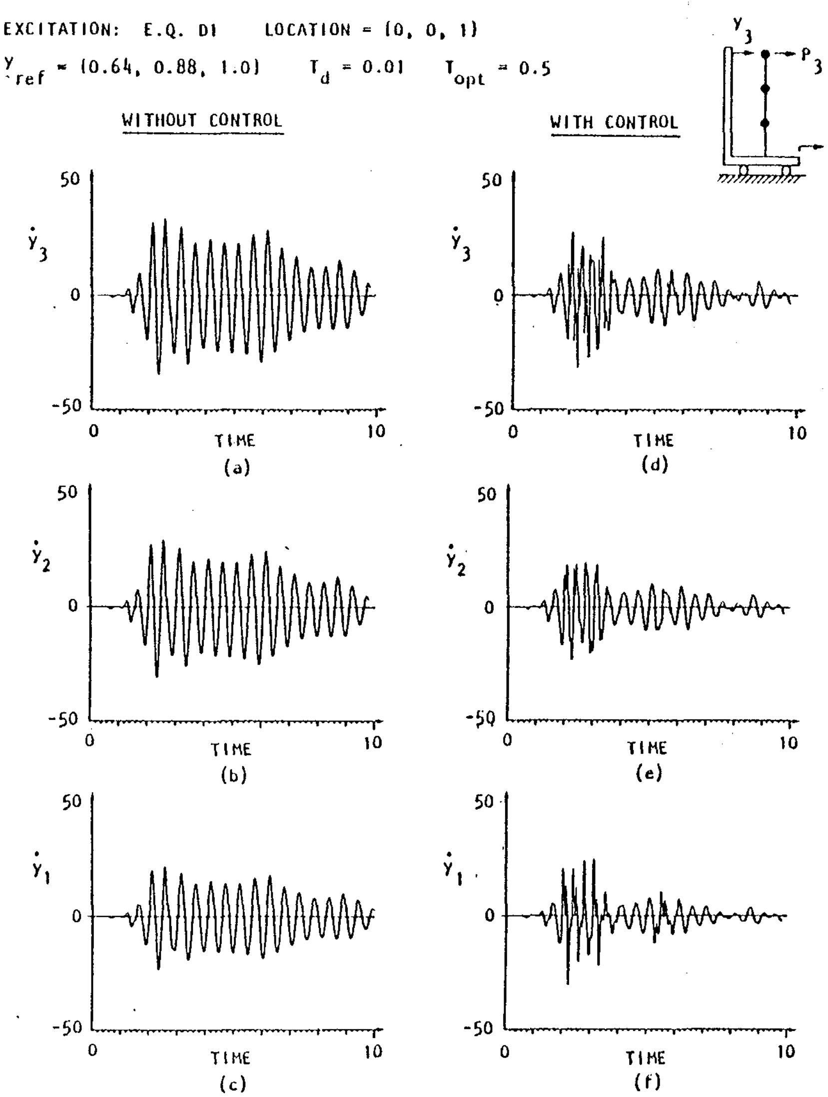

FIGURE 9. RELATIVE VELOCITY RESPONSE UNDER EXCITATION E.Q. D1; CONTROLLER AT m_3

$\ddot{S}$ = E.Q. ELC LOCATION = (0, 0, 1) Y_{ref} = (0.64, 0.88, 1.0)
T_d = 0.01 T_{opt} = 0.5

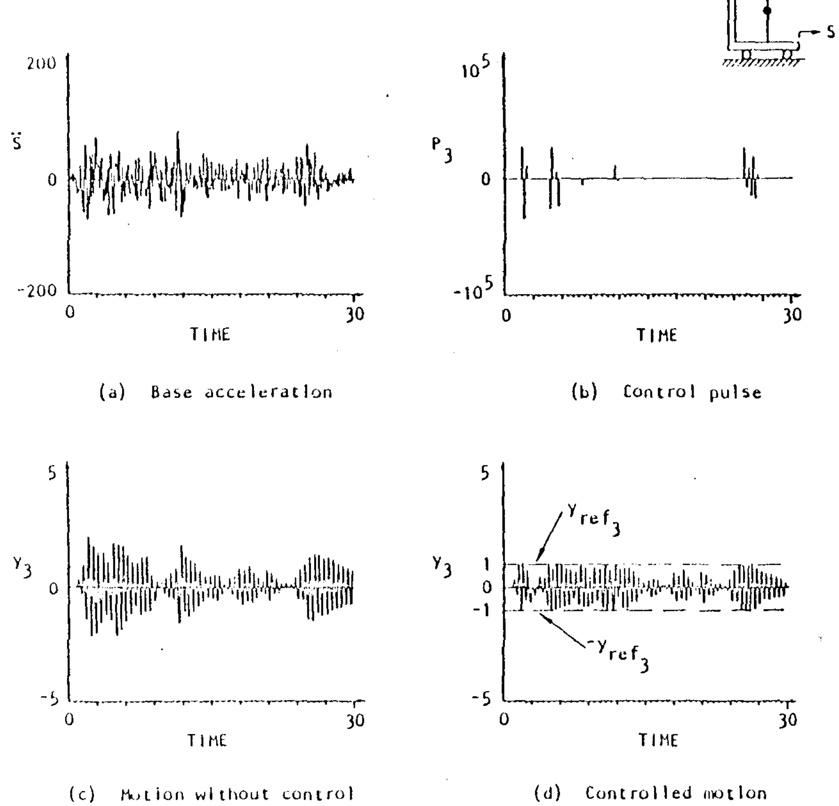

FIGURE 10. RELATIVE DISPLACEMENT RESPONSE UNDER EXCITATION E.Q. ELC; CONTROLLER AT m_3

$\ddot{S}$ = RANDOM σ = 100 LOCATION = (0, 0, 1)
Y_{ref} = (0.64, 0.88, 1.0) T_d = 0.01 T_{opt} = 0.5

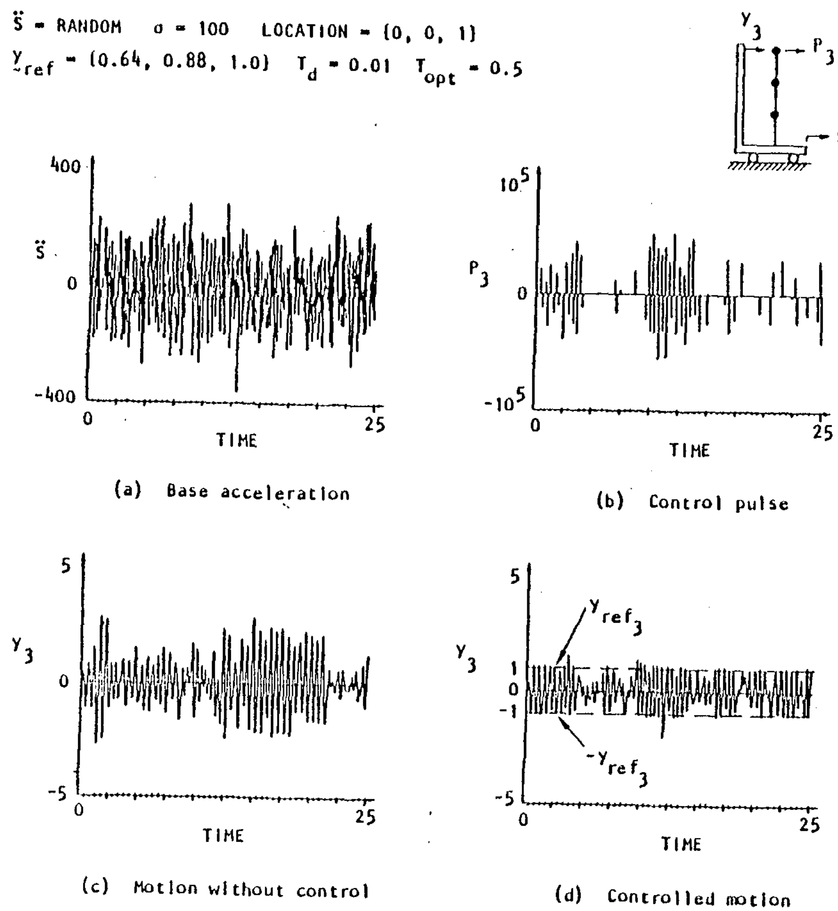

FIGURE 11. RESPONSE OF MODEL UCB-1 UNDER STATIONARY RANDOM EXCITATION; CONTROLLER AT m_3

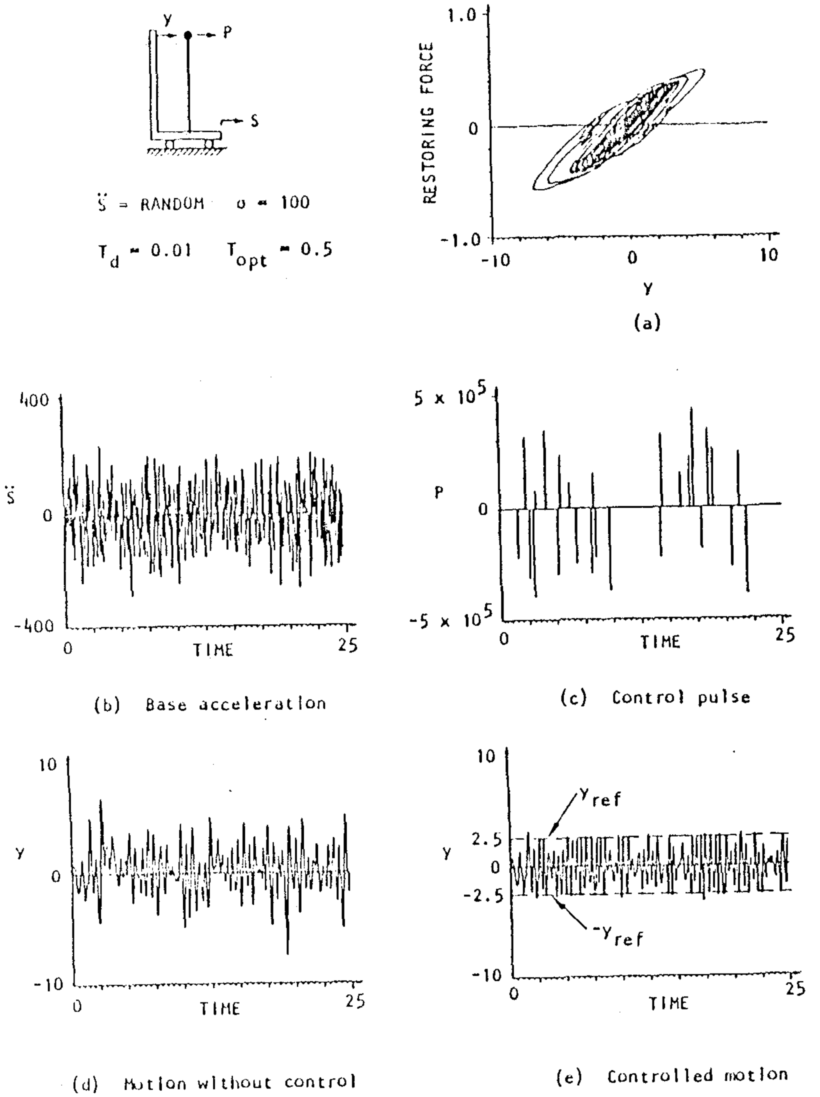

FIGURE 12. CONTROLLED RESPONSE OF A SDOF NONLINEAR SYSTEM UNDER STATIONARY RANDOM EXCITATION

To illustrate the performance of the proposed control algorithm when used in conjunction with nonlinear systems, consider a hypothetical SDOF system with the hysteretic characteristics shown in Fig. 12a. Under the action of stationary random excitation, the relative motion with and without control is shown in Fig. 12. As in the case of linear systems, it is clear that the control method is also successful in limiting the motion of this typical nonlinear system.

Conclusions

This paper shows the feasibility of using pulsed open-loop adaptive control for reducing the oscillations of tall buildings on similar distributed parameter systems subjected to strong ground shaking or arbitrary nonstationary disturbances.

The method is open-loop to reduce computing time, it is adaptive in order to take into account the varying nature of the system, and it uses pulse control to circumvent the problem of producing large control forces over sustained periods of time. Redundancy techniques using multiple microprocessors and motion sensors in parallel will ensure very high probability for amplitude and timing control of pulse generators.

Acknowledgment

This study was supported in part by a grant with the National Science Foundation.

References

1. Masri, S.F. "Steady-State Response of a Multidegree System with an Impact Damper," *J. Applied Mechanics*, Vol. 40, 1973, pp 127-132.

2. Masri, S.F. and Yang, L. "Earthquake Response Spectra of Systems Provided with Nonlinear Auxiliary Mass Dampers," *Proc. 5th World Conf. on Earthquake Engineering*, Rome, 1973.

3. National Science Foundation (NSF). *Feasibility of Force Pulse Generators for Earthquake Simulations*, NSF Grant PFR 77-15010. Washington, DC: NSF, 1979.

4. Safford, F.B. and Masri, S.F. "Analytical and Experimental Studies of a Mechanical Pulse Generator," *ASME J. Eng. Ind.*, Vol. 96, Series B, May 1974, pp 459-470.

5. Masri, S.F.; Bekey, G.A.; and Safford, F.B. "Optimum Response Simulation of Multidegree Systems by Pulse Excitation," *ASME J. Dynamic Systems, Measurement, and Control*, Vol. 97, Series G, No. 1, 1975, pp 46-53.

6. Masri, S.F. and Safford, F.B. "Earthquake Environment Simulation by Pulse Generators," *7th World Conf. on Earthquake Engineering*, Istanbul, 1980.

7. Masri, S.F.; Bekey, G.A.; and Udwadia, F.E. "On-Line Pulse Control of Tall Buildings," *Structural Control*, ed. H.H.E Leipholz. Amsterdam: North-Holland Publishing Co. and SM Publications, 1980.

8. Clough, R.W. and Tang, D.T. *Earthquake Simulated Study of a Steel Frame Structure, Vol. I: Experimental Results*, EERC 75-6, University of California, Berkeley, Apr 1975.

9. Tang, D.T. *Earthquake Simulated Study of a Steel Frame Structure, Vol. II: Analytical Results*, EERC 75-36, University of California, Berkeley, Oct 1975.

10. Jennings, P.C.; Housner, G.W; and Tsai, N.C. *Simulated Earthquake Motions*, California Institute of Technology Report, 1968.

NSF Grant CEE-7715010

Advances in Dynamic Analysis and Testing

SP-529

Published by:
Society of Automotive Engineers, Inc.
400 Commonwealth Drive
Warrendale, PA 15096
October 1982

821459

Pulse Excitation Techniques

F. B. Safford
Agbabian Associates
El Segundo, CA

ABSTRACT

A series of rectangular or other simple pulses can be convolved with the impulse functions of a structure to induce motions closely approximating those caused by natural and man-made events. Control of the excitation; portability to the site; ease of attachment to the structure; multiaxial excitation; low cost of excitation equipment; and the ability to excite structures from simple harmonic motion to expected multifrequency response-time histories are possible by the development of pulse techniques. Recent investigations have also disclosed the utility of pulse techniques to oppose structural motions as in earthquakes or in large antenna arrays in space.

RECENT ANALYTICAL AND EXPERIMENTAL STUDIES [1]* indicate that a rudimentary series of rectangular or other simple pulses could be convolved with the impulse functions of a structure to induce motions closely approximating those caused by natural and man-made events. This result greatly simplifies the control of high energy devices as the problem is reduced to three functions of on, off, and amplitude control. It was further determined that the excitation could also be placed directly on structures at one location or at multiple locations of test convenience and in single or multiple axes. When the structural excitation is caused by base motion, pulse simulation with generators attached to the same structure can duplicate the natural or man-made event with the exception of the rigid body modes.

Transient shock tests on in-place equipment and buildings to simulate the motions induced by a nuclear event or an earthquake are largely limited to single-axis test machines. Further limitations exist in the size and weight of structures that can be tested. Simulating multiaxis loading on large structures with many degrees of freedom represents a difficult problem as it is impractical to generate continuously varying forces of sufficient magnitude. On the other hand, short duration forces of large magnitudes over a wide frequency range can be generated by pulse generators. Since a discrete number of pulses superficially presents an appearance quite different from a continuous excitation signal, it becomes necessary to select the pulses in such a way that the resulting vibration of the structure matches as closely as possible the response (e.g., displacement, velocity, or acceleration) produced by the continuous force, as determined by an appropriate error criterion.

Several large energy devices may be adapted for pulse train excitation. These include point source explosives, chemical rockets, metal cutting, and reactance by gas, water, or projectiles. The development and applications of several metal cutting systems are discussed together with a pulse modulated gas reactance system.

The central issue in testing is to induce multiaxial motion-time histories on a structure comparable to those caused by natural or man-made hazards, since failures and malfunctions are essentially nonlinear. Force pulse trains provide practical methods in many applications to test structures and equipments to the thresholds of damage and malfunction by inducing realistic response waveforms.

PROCEDURE

The procedure to develop the required pulse trains is illustrated in Fig. 1 for a massive nuclear power containment structure or a small equipment rack. The computational methods are iterative to obtain the pulse train, and the procedure may be used for either linear [2] or nonlinear systems [3]. Various iteration methods may be used; an optimization algorithm [4]

*Numbers in brackets designate references at end of paper.

using a spherical random search with a partially automatic control of the variance has proved to be quite efficient. It has been found that the variance can range over ten orders of magnitude, which permits rapid convergence and avoidance of local minima.

It is important to note that the method of Fig. 1 requires that the criterion response to the continuous input be known, which would generally not be true in practice. To accomplish this objective, the approach proposed here assumes that: (1) a mathematical model of the system under study is known, and (2) the inputs of interest (e.g., earthquake or nuclear blast) are given. Under these conditions the "criterion response" can be calculated and used to obtain the pulse train for the simulated test. The structure also can be represented by empirical models derived from mechanical impedance measurements.

The basic criterion used is the integral squared error between the reference and simulated response (see Fig. 1), evaluated at a sufficient number of points within the multiple-degree-of-freedom system to characterize it as completely as possible. The error criterion is given, and then the pulse occurrence times, pulse widths, and the pulse amplitudes are selected by a systematic search algorithm such that the error is minimized.

While the expected motion-time-history response is stressed as above, the pulse units can also be programmed to generate sine and random motion responses. These latter motions are useful for measuring impedance and for extracting modal properties of the structure. Additionally, a recent study [5] presented a relatively simple on-line pulse control algorithm suitable for use with distributed parameter systems subjected to nonstationary disturbances. The main feature of the algorithm is that resonance phenomena can be eliminated, or at least drastically reduced, by disorganizing the orderly and gradual buildup of the structural dynamic response by timed firing of a pulse of suitable magnitude applied in the proper direction. Furthermore, in order to minimize the amount of control energy utilized, the control force should be applied only when the structural response exceeds a certain threshold level related to the resistance of the structure.

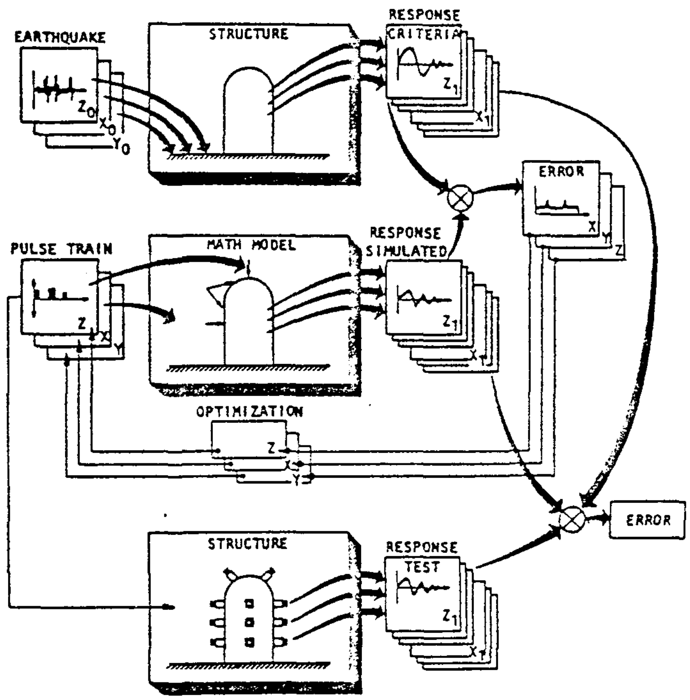

(a) Pulse test of nuclear reactor containment structure to simulate earthquake response

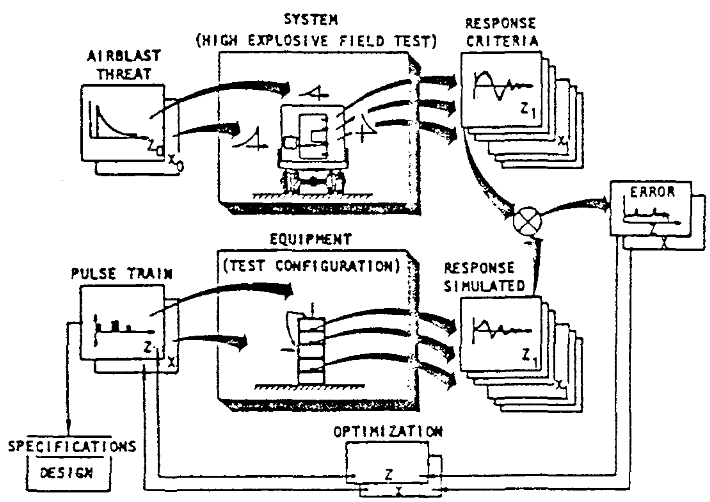

(b) Pulse test of communications equipment to match motions induced by air blast loads

FIGURE 1. PROCEDURE FOR PULSE TESTS FOR A WIDE RANGE OF STRUCTURES AND ENVIRONMENTS

APPLICATIONS

The 25-story building modeled as a linear system in Fig. 2, has the mode shapes shown in Fig. 3, and under base excitation by the El Centro Earthquake yields the motion time histories plotted in Fig. 6 (solid line) for the 13th and 23rd floors [6]. Figure 5 shows the driving point impulse functions for Floors 8, 13, 18, and 23 as well as the transfer impulse functions between floors and each excitation location. Using the procedures of Figs. 4, 5, and 6, the force pulse trains of Fig. 4 were developed for pulse locations on Floors 8, 13, 18, and 23. The response motions induced by these pulsers are plotted on Fig. 6 (dotted line) and are virtually identical to the motions caused by the El Centro earthquake. Average force required is 50,000 lbf and the average impulse is 17,000 lb-sec. Fifty-two pulses are required, having average pulse widths of 410 ms.

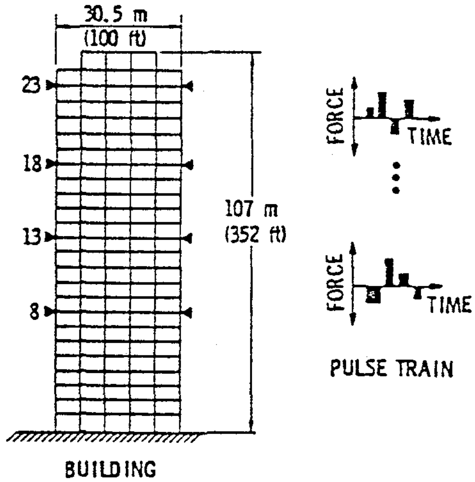

FIGURE 2. PULSERS ARRAYED FOR EARTHQUAKE SIMULATION TEST OF A MULTISTORY BUILDING

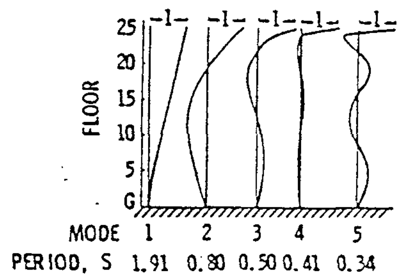

FIGURE 3. BUILDING NATURAL MODES OF VIBRATION

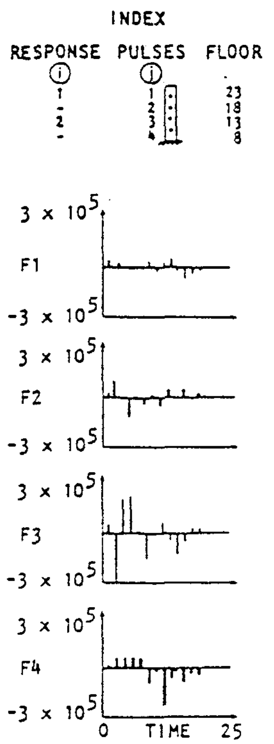

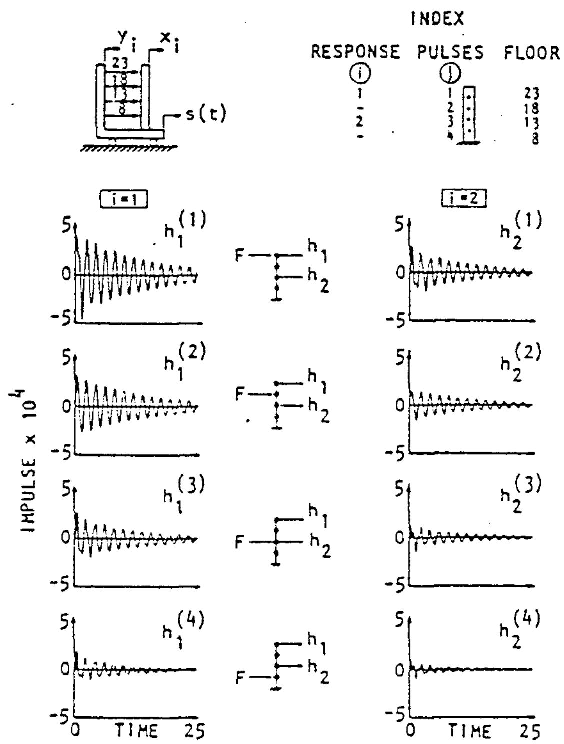

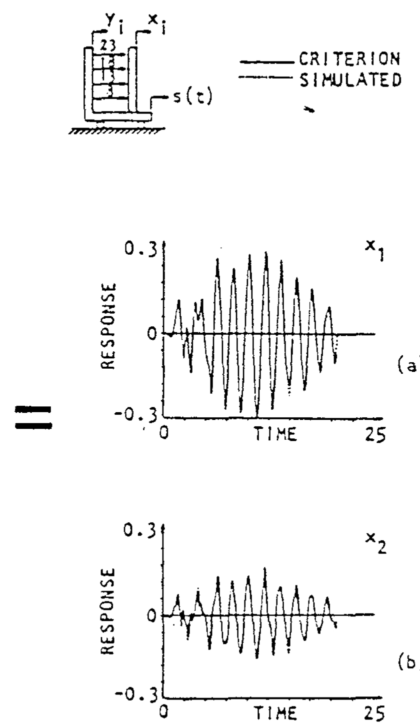

FIGURE 4. OPTIMUM PULSE TRAINS FOR 25 DOF SYSTEM

FIGURE 5. IMPULSIVE DISPLACEMENT RESPONSE TO 25 DOF SYSTEM

FIGURE 6. COMPARISON OF CRITERION AND SIMULATED RESPONSE OF 25 DOF SYSTEM

A 200,000 lb shock isolated control room (50 ft x 50 ft) for a power plant was tested while functionally operating to induce motion-time histories expected from a specified nuclear base motion threat [7]. One of the four pulse generators used is pictured in Fig. 21. The specified pulse train and the four measured ones are presented in Fig. 7. Typical measured transfer functions of the structure used to calculate the pulse train are presented in Fig. 8 and include transfer function magnitude, phase, and impulse function. The predicted control room motion due to base motion hazard is given in Fig. 9 together with computed pulse simulated motion and motions measured during tests with the pulse generators.

Tests of a large nuclear processing plant were performed to obtain transfer functions and to extract building modes and damping [8]. One of the buildings tested was a reinforced concrete structure 40 ft high, 136 ft wide, and 300 ft long (Fig. 10). Figure 11 is a typical

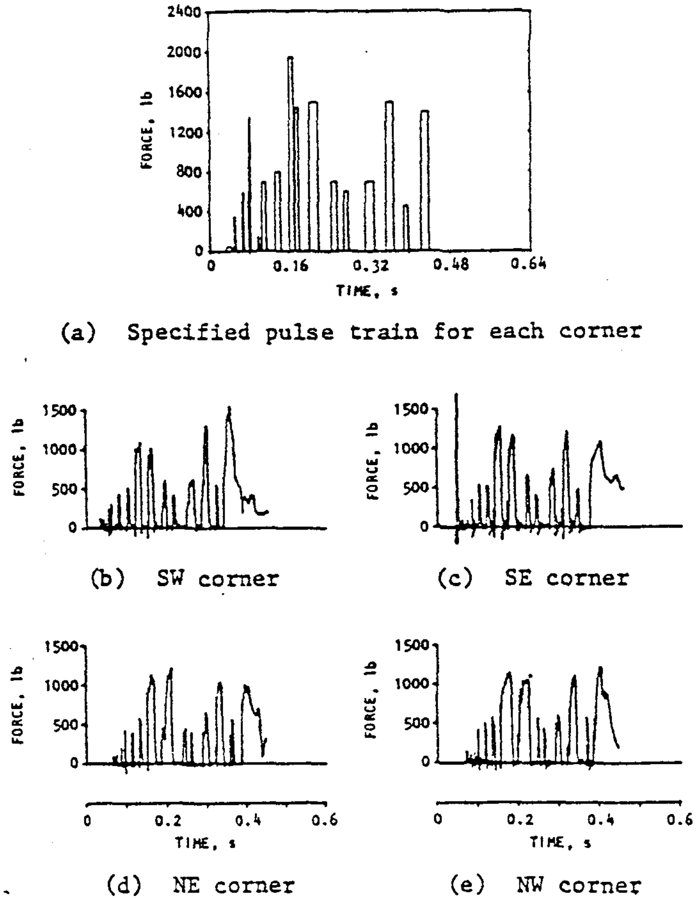

(a) Specified pulse train for each corner

(b) SW corner (c) SE corner

(d) NE corner (e) NW corner

FIGURE 7. 200,000 LB SHOCK ISOLATED CONTROL ROOM PLATFORM: SPECIFIED AND ACTUAL TEST-INPUT PULSES USING FOUR PULSE GENERATORS

mode shape extracted from the pulse generated data given in Fig. 12. The pulse generator used in these tests is shown in Fig. 23.

Figure 1(b) is a schematic for biaxial testing of command, control, and communication equipment subjected to battlefield high explosive and nuclear blast loads [9]. Data recorded on a communications equipment rack within the truck shelter during a 500-ton TNT (equivalent) test is given in Fig. 13. The pulse train required to induce motion in equipment to match the explosive field test data is covered in Fig. 14 with the computed equipment response using the pulse train shown in Fig. 15. The motion of Fig. 15 was obtained by convolving the pulse train with the impulse function of the equipment and rack. The impulse function was obtained by inverse transformation of measured impedance functions. This biaxial project is still in progress. Biaxial calibration and development trials of the system pictured in Fig. 24 are displayed in Fig. 16.

The utility of using pulse generators to reduce motions in structures as would be caused by an earthquake has been demonstrated by application to a model three-story steel frame (Fig. 17) that has been extensively studied, both analytically and experimentally [10, 11] at the University of California, Berkeley (UCB). A single pulse controller is located on the third floor, and the threshold levels for triggering the controller are set at 0.64 in. relative displacement for the first floor, 0.88 in. for the second floor, and 1 in. for the third floor. Results with and without control are given in Fig. 18. Corresponding results were obtained by locating the pulse controller on either the first or second floors as the response of each mass is kept nearly bounded by the selected threshold levels.

However, from the control energy point of view, significant reduction in the required impulse can be achieved if the pulse generator is located at the top floor, rather than the lower floor of the structure. The optimum location of pulse generators is being studied as a refinement to conserve impulse requirements. As in the case of El Centro Earthquake, artificial earthquake D1 [12] and stationary random ground motions show similar results that a single controller can effectively control system motion to within any reasonable threshold level.

PULSE GENERATING DEVICES

Pulse generating devices developed and now in development are composed of a class of metal cutting systems and a class of gas reactance systems. The metal cutting devices make use of the very high forces required to cut metal [1]. The velocity of the cutting tool and the length of the metal projection govern the pulse duration. For the metal removed, cutting coefficients typically range from 150,000 lbf/in^3 for aluminum to 300,000 lbf/in^3 for steel. Metal pulse generators producing up to 1,000,000 lbf have been proposed.

Force produced is directly proportional to the volume of metal removed or alternatively to the shear/fracture of chip removal. Waveform is obtained by varying the profile or contour of material to be sheared. Thus, variable force-time history results as the depth of cut varies with the profile of the metal workpiece. The most efficient means of force production is by use of circular cutting tools similar to broaching operations. Figure 19 provides a schematic of a force profile generator. The shaped nubbins may be spaced as shown or may be continuous over the entire stroke. Figures 21 through 24 show several machines that are now operable. The biaxial machine (Fig. 24) has been designed to accommodate a third independent test axis should the need arise.

The programmable gas pulse generator shown in Fig. 20 and again in Fig. 25 is undergoing test stand calibrations [13]. Two units have been constructed and will be mounted in opposition to provide opposing force direction (positive and negative pulse trains). Initial use provides for cold gas, but the system is adaptable for both steam and chemically generated hot gas. Thrust amplitudes are controlled in the on-state by positioning the metering plug for flow control. Off-state for the pulse

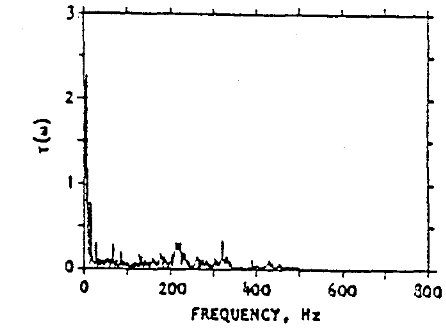

(a) Transfer function magnitude

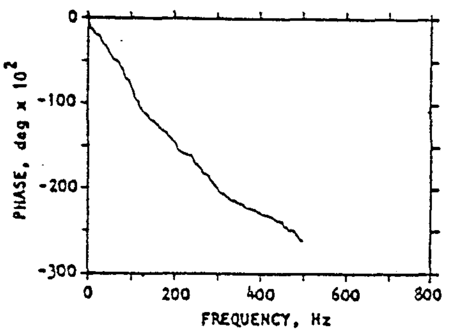

(b) Transfer function phase

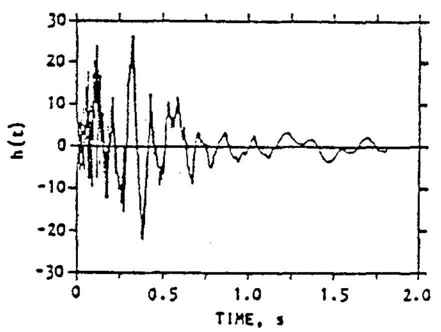

(c) Impulse function

FIGURE 8. CONTROL ROOM: MEASURED TRANSFER FUNCTION FOR 0.5 Hz TO 500 Hz

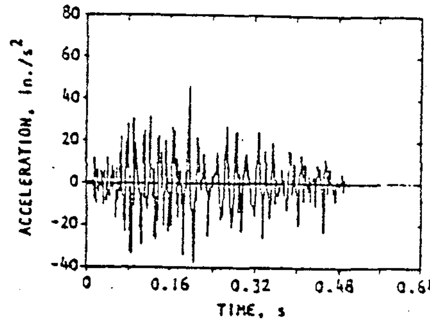

(a) Predicted

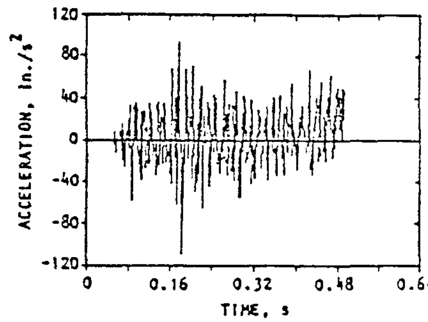

(b) Pulse simulated

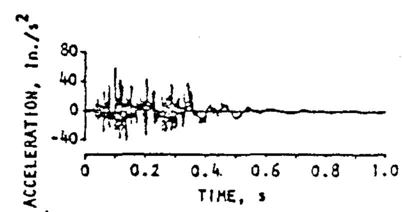

(c) Pulse tested

FIGURE 9. CONTROL ROOM PLATFORM: ACCELERATION- TIME HISTORIES OF PREDICTED, PULSE-SIMULATED, AND PULSE-TESTED MOTIONS

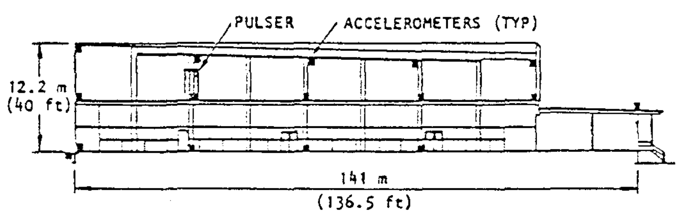

FIGURE 10. CROSS SECTION OF NUCLEAR PROCESSING PLANT SHOWING ACCELEROMETER AND PULSER LOCATIONS (PULSER EXCITATION NORMAL TO SECTION SHOWN)

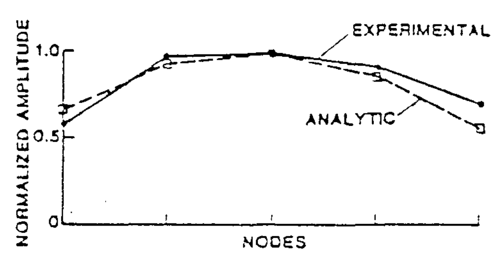

FIGURE 11. TYPICAL MODE SHAPE PLOT FROM EXPERIMENTAL AND ANALYTIC DATA (Frequency: 9.2 Hz)

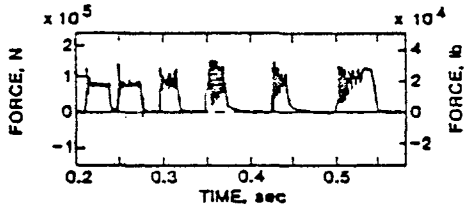

(a) Raw input force-time history

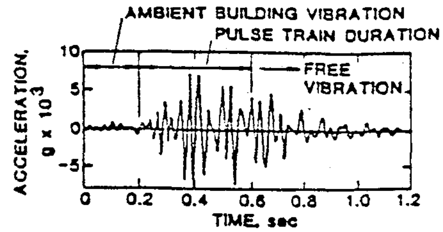

(c) Acceleration-time history (0 to 20 Hz)

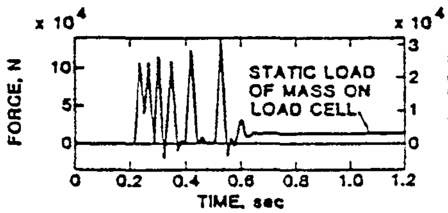

(b) Filtered input force-time history (0 to 20 Hz)

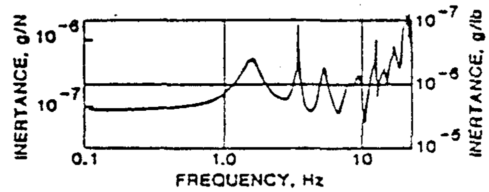

(d) Transfer function (acceleration divided by force)

FIGURE 12. TYPICAL DATA RECORDS FROM PULSE TRAIN TESTS AND RESULTING TRANSFER (INERTANCE) FUNCTIONS COMPUTED FROM DATA-PULSE GENERATOR

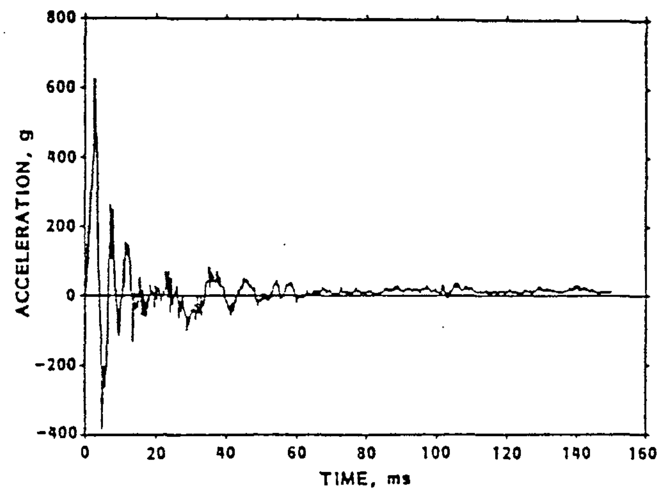

(a) Horizontal acceleration-time history

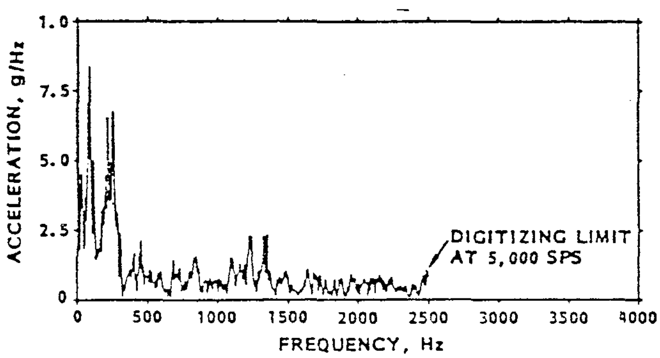

(b) Fourier modulus of horizontal acceleration response

FIGURE 13. HORIZONTAL RESPONSE OF COMMUNICATIONS EQUIPMENT FRAME INSIDE SHELTER TO AIR BLAST IN MISERS BLUFF II EVENT

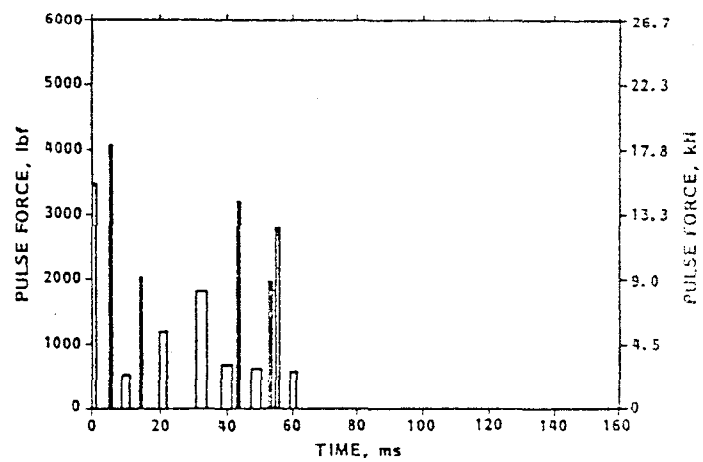

FIGURE 14. FORCE PULSE TRAIN REQUIRED TO INDUCE MOTION IN EQUIPMENT TO MATCH EXPLOSIVE FIELD TEST DATA OF FIG. 13(a)

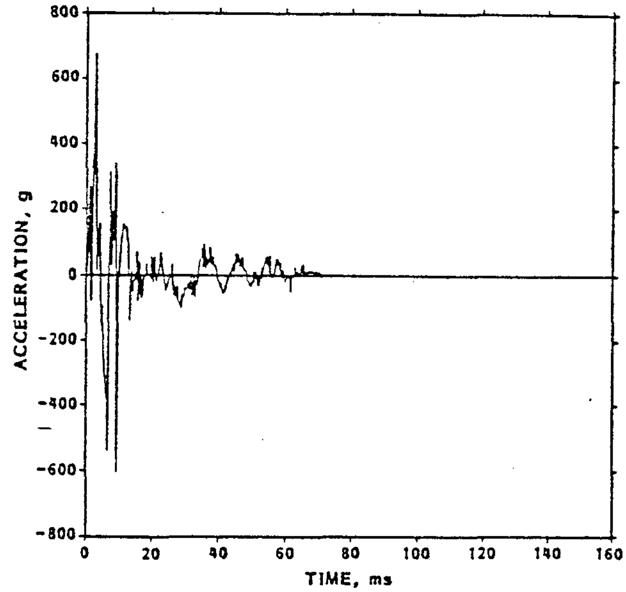

FIGURE 15. INITIAL COMPUTATION OF PULSE TRAIN GENERATED MOTION IN EQUIPMENT RACK TO MATCH THE OBJECTIVE FUNCTION OF FIG. 13(a)

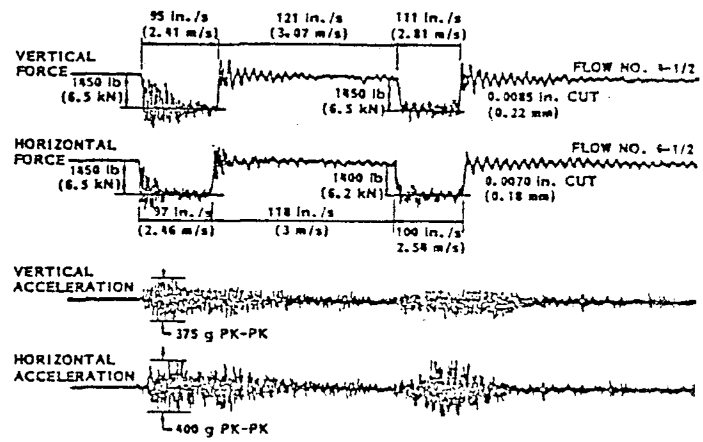

FIGURE 16. INPUT FORCE AND RACK ACCELERATION DATA FROM BIAXIAL TEST

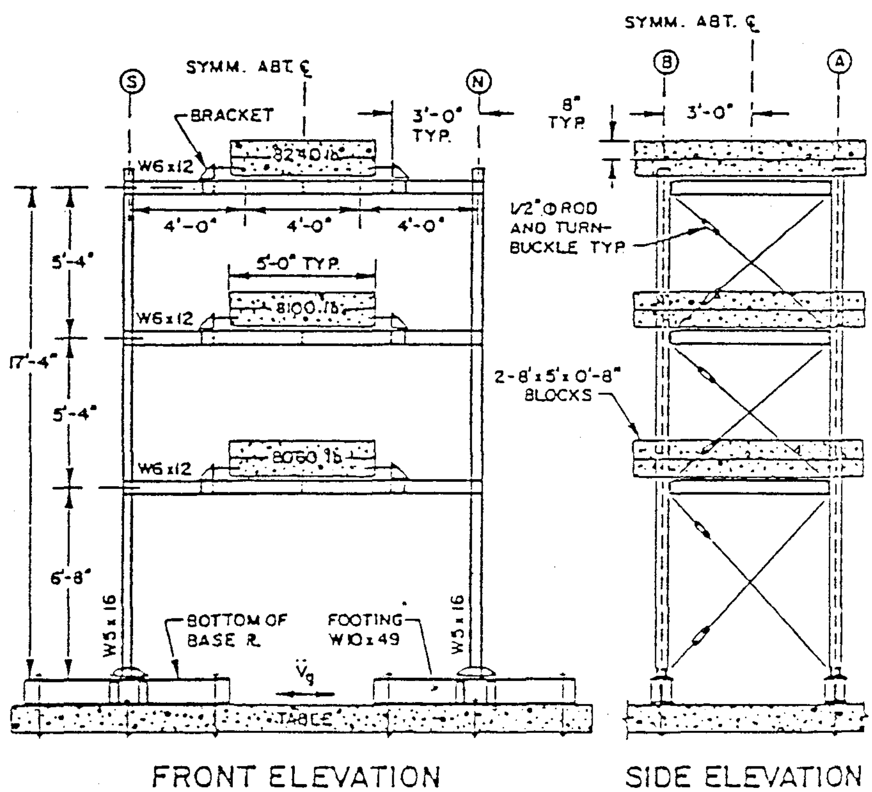

FIGURE 17. PLAN AND ELEVATIONS OF THE TEST STRUCTURE

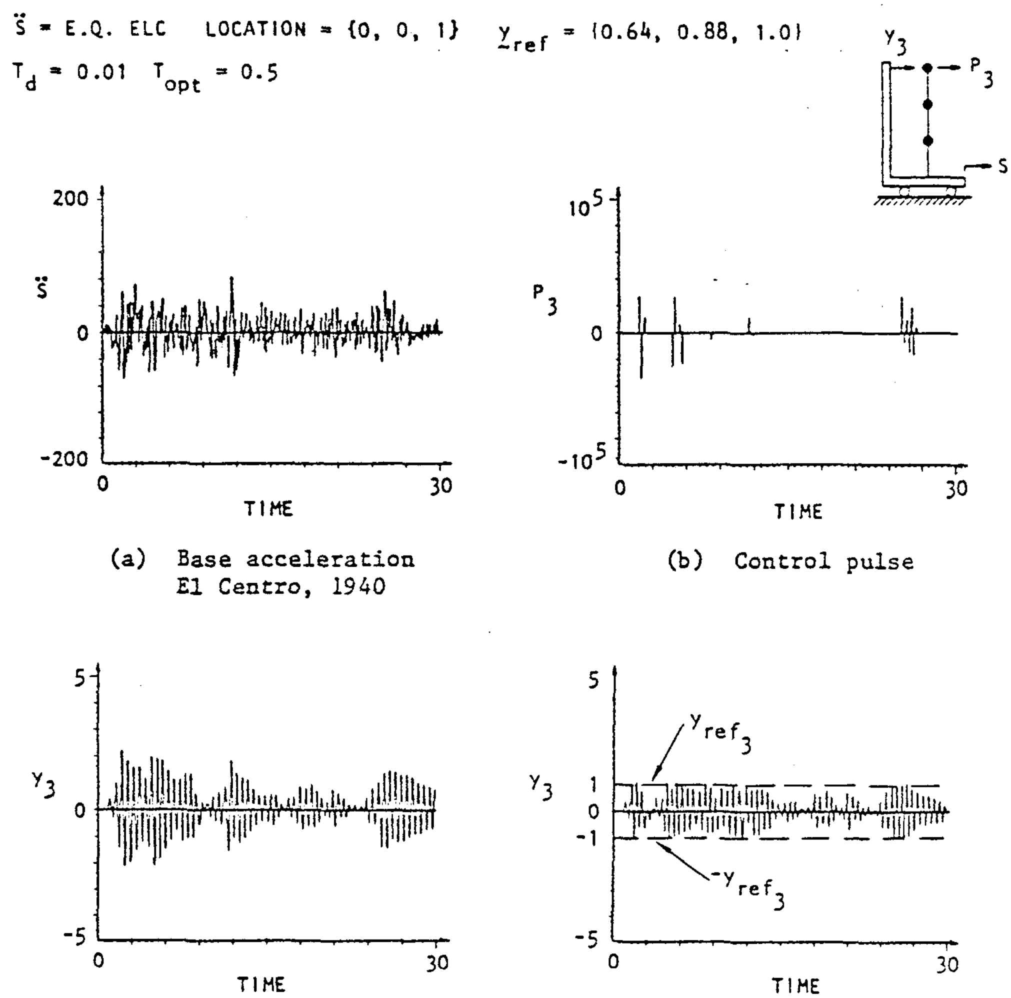

(a) Base acceleration El Centro, 1940

(b) Control pulse

(c) Displacement motion without control

(d) Displacement, controlled motion

FIGURE 18. RELATIVE DISPLACEMENT RESPONSE UNDER EXCITATION, EL CENTRO EARTHQUAKE PULSE CONTROLLER AT THIRD FLOOR

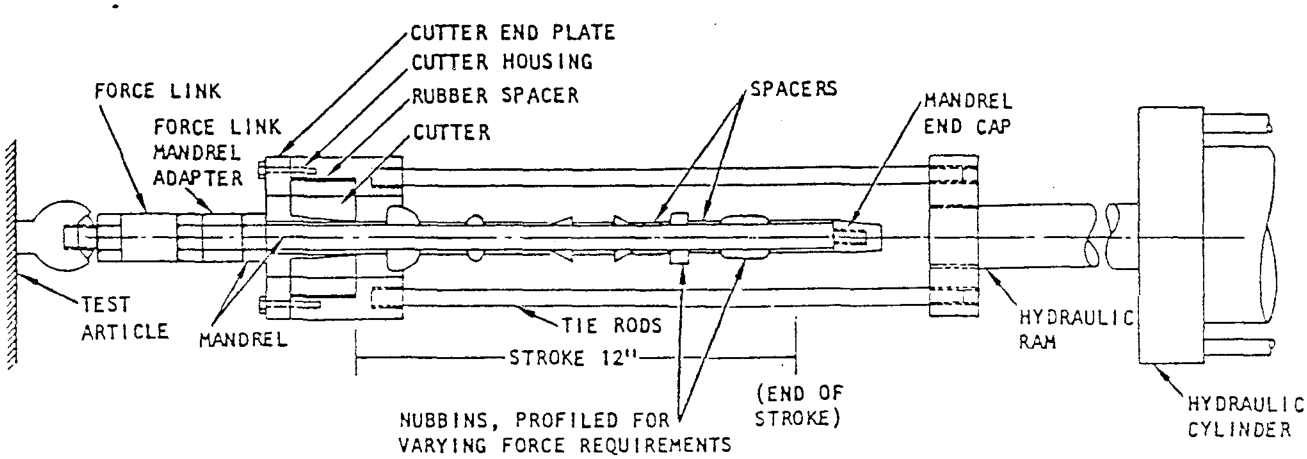

FIGURE 19. SCHEMATIC OF FORCE PROFILE GENERATION BY METAL CUTTING

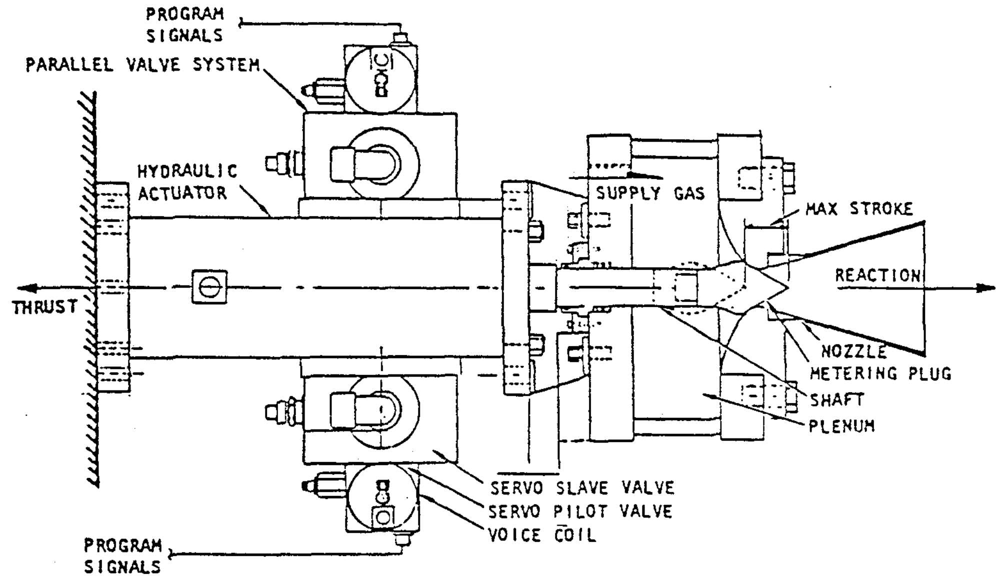

FIGURE 20. PROGRAMMABLE GAS PULSE GENERATOR COLD GAS SYSTEM — 500 TO 10,000 lbf

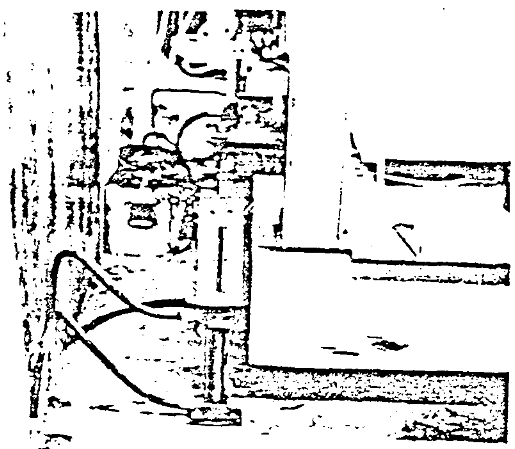

FIGURE 21. APPLICATION OF PULSE GENERATOR FOR EQUIPMENT TEST ACCELERATION-TIME HISTORIES (See Figs. 7-9) CAPACITY 8,000 lbf

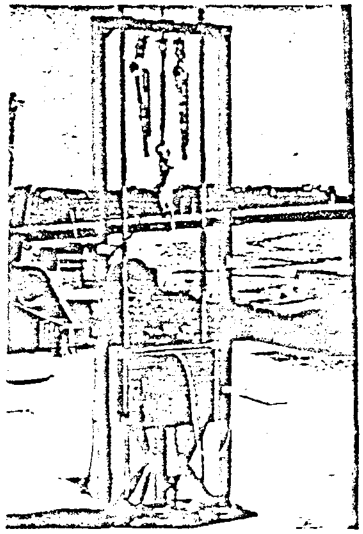

FIGURE 22. PULSE GENERATOR USED FOR TRANSFER FUNCTION AND MODE SHAPES OF STRUCTURE, CAPACITY 16,000 ft-lb

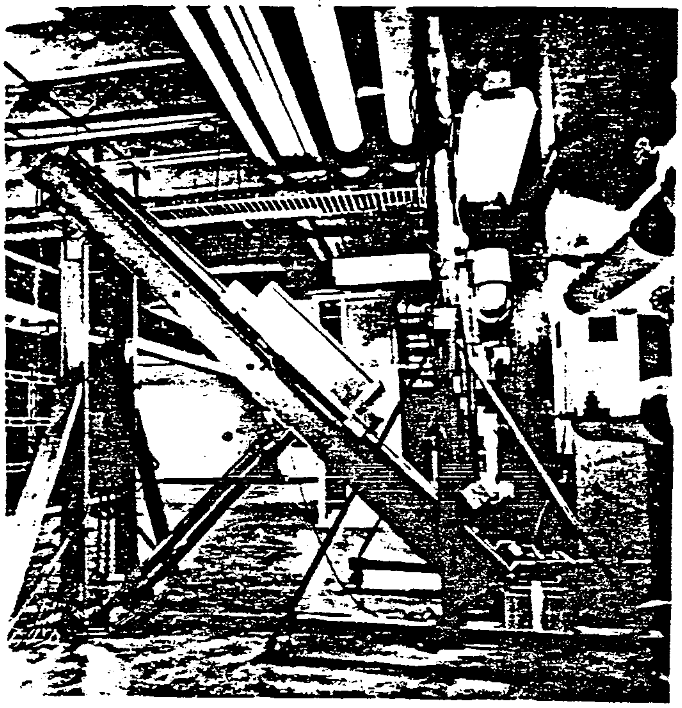

FIGURE 23. LARGE PULSE GENERATOR USED TO MEASURE TRANSFER FUNCTIONS AND MODE SHAPES OF LARGE STRUCTURES (See Figs. 10-12) CAPACITY 54,000 ft-lb

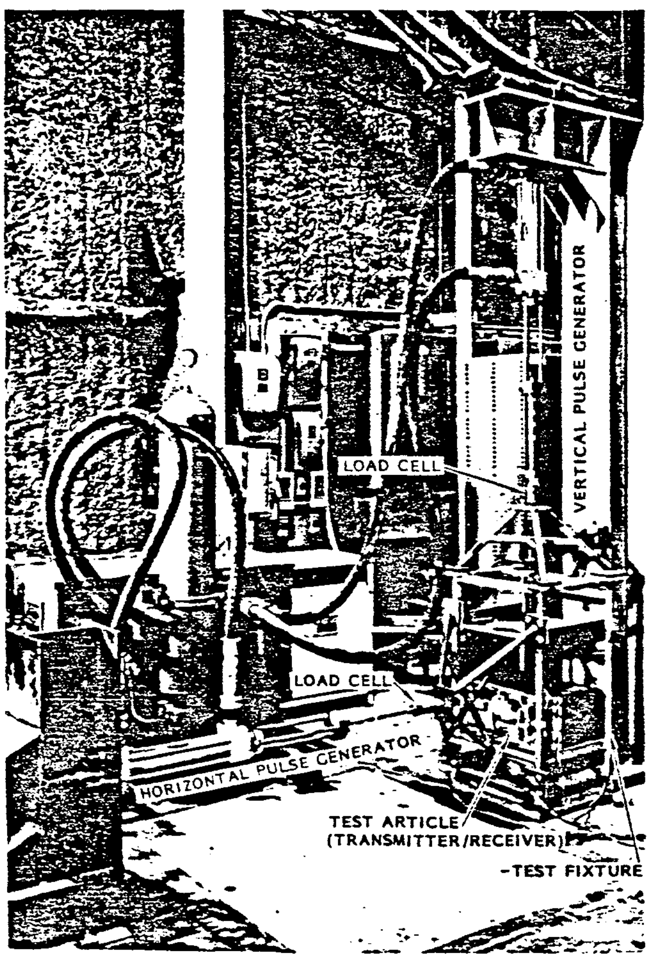

FIGURE 24. BIAXIAL PULSE GENERATOR TRANSIENT SHOCK TESTS OF EQUIPMENT DUPLICATING ENVIRONMENTAL ACCELERATION-TIME HISTORIES (See Figs. 13-16) CAPACITY 15,000 lbf EACH AXIS

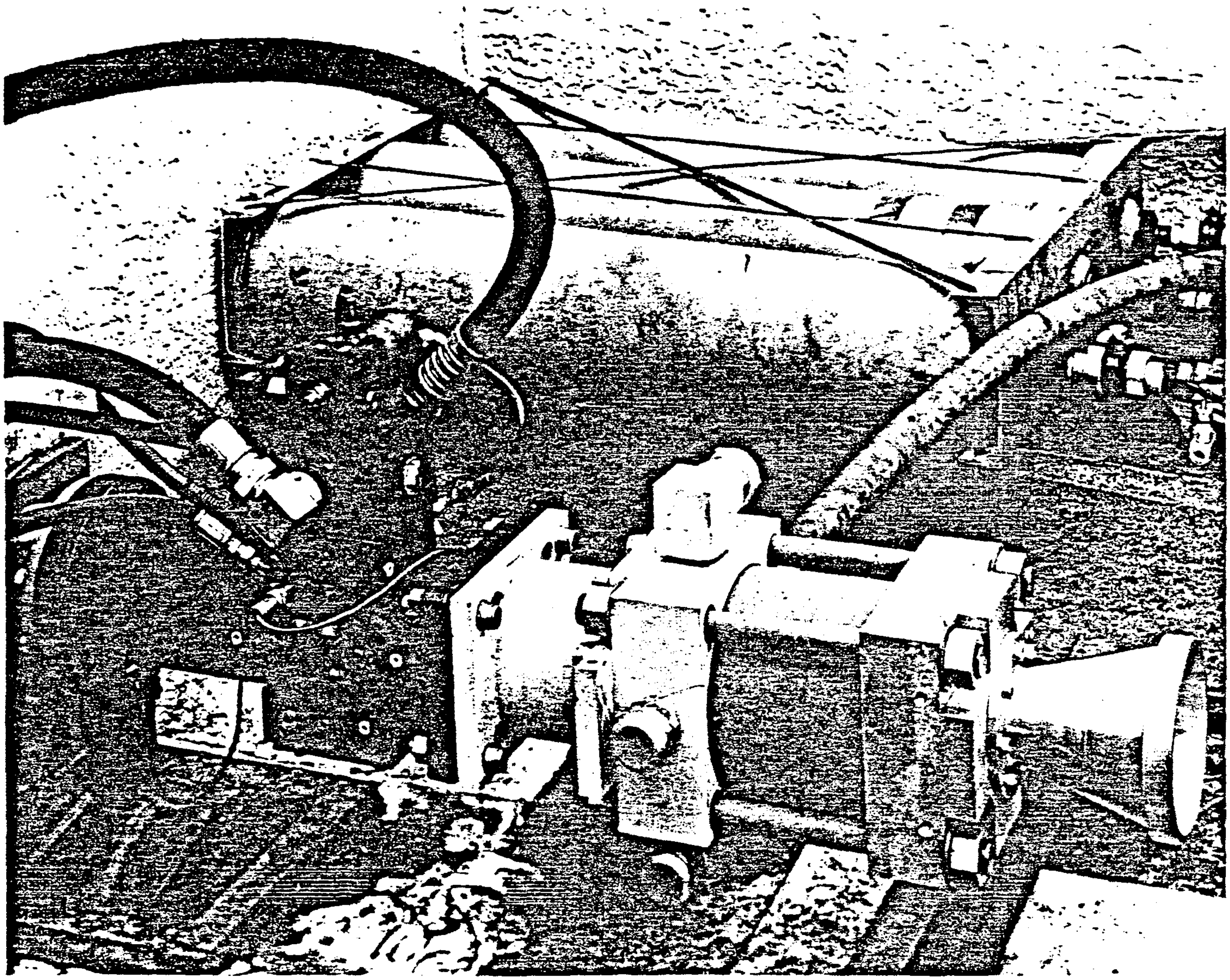

FIGURE 25. GAS PULSE GENERATOR USED FOR STRUCTURE TESTS ACCELERATION-TIME HISTORIES, FOR TRANSFER FUNCTIONS AND MODE SHAPES, AND FOR SUPPRESSION OF STRUCTURAL MOTIONS (See Figs. 17,18)

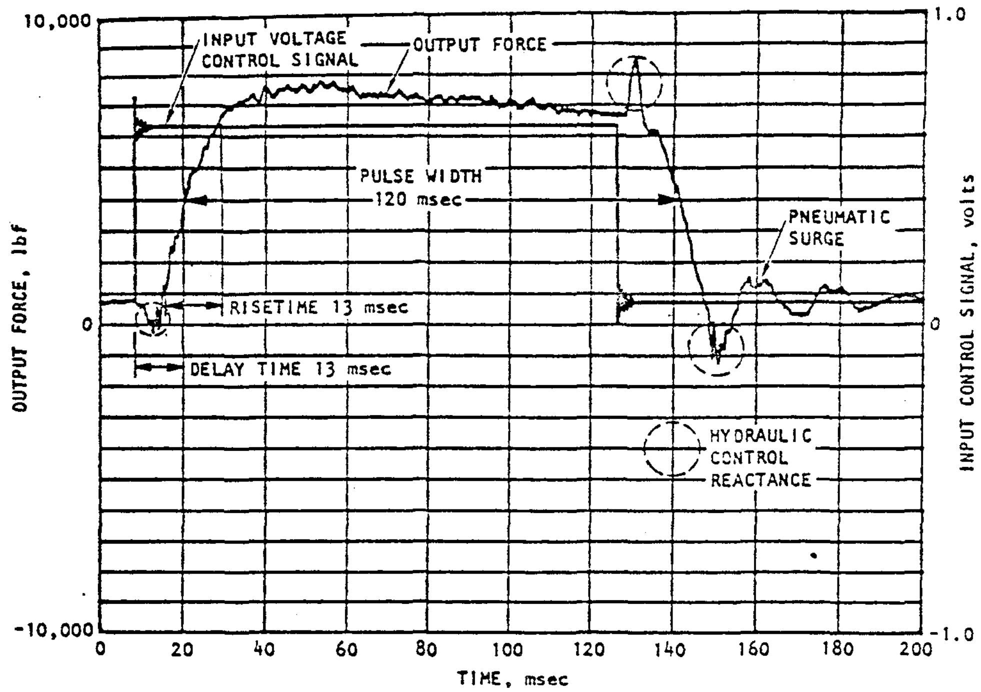

FIGURE 26. TYPICAL FORCE PROFILE OF GAS PULSE GENERATOR

occurs by signaling the hydraulic actuator to move the metering plug to seal off gas flow at the nozzle. Two devices will be used for earthquake and anti-earthquake investigations on the structure at the University of California, Berkeley (Fig. 17). Typical performance characteristics of the gas pulser is shown in Fig. 26. Using peaking methods superimposed on the control signal input, rise times of 11 ms have been obtained. The system has also been designed to accommodate two 90 gpm valves for parallel operation. This configuration will yield rise times of 7 ms.

CONCLUSIONS

The use of force pulse trains to induce structural motions simulating the effects of natural and man-made events has been introduced to circumvent the problem of producing large control forces over sustained periods of time. Additionally, the use of pulsed adaptive control for reducing oscillations of large structures to unknown disturbances has been shown to be feasible.

A number of metal cutting pulse generators have been produced and placed in operation to induce large structural motions of transient shock characteristics and also to measure the modal characteristic and impedance of structures. These devices are attractive due to low cost, portability, and ease of control. Pulse forces from a few hundred pounds to a million pounds are possible with frequency content variable up to recorded motions of 5000 Hz.

Programmable gas pulsers have also been developed and are now under test. Gas, hydraulic, and explosive source pulsers are being investigated for applications requiring inertial references.

ACKNOWLEDGEMENTS

The gas pulse system and the on-line motion suppression study was supported in part by a grant from the National Science Foundation under the direction of Dr. John B. Scalzi. The mechanical pulse generators were developed through the support of Mr. C.C. Huang, Corps of Engineers, Mr. R.E. Walker, Waterways Experiment Station, and Dr. William Schuman, Ballistic Research Laboratory. In addition to the staff of Agbabian Associates, Professors S.F. Masri and G.A. Bekey of the University of Southern California provided major contributions in control algorithms.

REFERENCES

1. Safford, F.B. and Masri, S.F. "Analytical and Experimental Studies of a Mechanical Pulse Generator," Jnl of Eng. for Industry, ASME, Series B, 96:2, May 1974, pp. 459-470

2. Masri, S.F. and Safford, F.B. "Dynamic Environment Simulation by Pulse Techniques," Proc. ASCE Eng. Mech. Div. 101:EM1, Feb 1976, pp. 151-169.

3. Masri, S.F. and Caughey, T.N. "A Nonparametric Identification Technique for Nonlinear Dynamic Problems," Jnl of Appl. Mech. ASME, 46:2, Jun 1979.

4. Masri, S.F.; Bekey, G.A.; and Safford, F.B. "An Adaptive Random Search Method for Identification of Large Scale Nonlinear Systems," 4th Symp. for Identification and System Parameter Estimation, Int. Federation of Automatic Control, Tbilisi, USSR, Sep 1976.

5. Masri, S.F.; Bekey, G.A.; Safford, F.B.; and Dehghanyar, T.J. "Anti-Earthquake Application of Pulse Generators," Proc. Dynamic Response of Structures, Instrumentation, Testing Methods and System Identification, ASCE Specialty Conference, Atlanta, GA, Jan 1981.

6. Masri, S.F. and Safford, F.B. "Earthquake Environment Simulation by Pulse Generators," Proc. 7th World Conf. on Earthquake Eng. Istanbul, Turkey, Sep 8-13, 1980.

7. Safford, F.B. et al. "Air-Blast and Ground Shock Simulation Testing of Massive Equipment by Pulse Techniques, 5th Int. Symp. on Military Application of Blast Simulation, Fortifikationsforvaltningen, Stockholm, Sweden, May 23-26, 1977.

8. Yates, D.G. and Safford, F.B. "Measurement of Dynamic Structural Characteristics of Massive Buildings by High-Level Multiple Techniques," Shock & Vibration Bull., 50, SVIC. Washington, DC: Naval Res. Lab, 1980.

9. Safford, F.B. et al. "Biaxial Accelleration Simulation Test Machine," Proc. 7th Int. Symp. on Military Application of Blast Simulation, Medicine Hat, Alberta, Canada, Jul 1981.

10. Cough, R.W. and Tang, D.T. "Earthquake Simulated Study of a Steel Frame Structure, Vol. I: Experimental Results," EERC 75-6, Univ. of California, Berkeley, Apr 1975.

11. Tang, D.T. "Earthquake Simulated Study of a Steel Frame Structure, Vol. II: Analytical Results," EERC 75-36, Univ. of California, Berkeley, Oct 1975.

12. Jennings, P.C.; Housner, G.W.; and Tsai, N.C. "Simulated Earthquake Motions," California Institute of Technology Report, 1968.

13. Safford, F.B. Validation of Pulse Techniques for the Environmental Simulation of Earthquake Motions in Civil Structures, U.S. National Science Foundation Grant No. PFR77-15010, Washington, D.C., 1978.